50 Jahre 1956 - 2006

GKSS FORSCHUNGSZENTRUM in der HELMHOLTZ-GEMEINSCHAFT

Investigation of correlations between radar deduced bathymetries due to the outer impact of a storm in the area "Salzsand"

(Vom Coastal Research Laboratory, Forschungs- und Technologiezentrum Westküste BÜSUM, der Christian-Albrechts-Universität zu Kiel als Diplomarbeit angenommen)

Author:
S. Flampouris

ISSN 0344-9629

HELMHOLTZ | GEMEINSCHAFT

wissen schafft nutzen

GKSS 2006/16

GKSS 2006/16

Investigation of correlations between radar deduced bathymetries due to the outer impact of a storm in the area "Salzsand"

(Vom Coastal Research Laboratory, Forschungs- und Technologiezentrum Westküste BÜSUM, der Christian-Albrechts-Universität zu Kiel als Diplomarbeit angenommen)

Author:

S. Flampouris

(Institute for Coastal Research)

GKSS-Forschungszentrum Geesthacht GmbH • Geesthacht • 2006

Die Berichte der GKSS werden kostenlos abgegeben.
The delivery of the GKSS reports is free of charge.

Anforderungen/Requests:

GKSS-Forschungszentrum Geesthacht GmbH
Bibliothek/Library
Postfach 11 60
D-21494 Geesthacht
Germany

Fax.: (49) 04152/871717

Als Manuskript vervielfältigt.

ISSN 0344-9629

GKSS-Forschungszentrum Geesthacht GmbH · Telefon (04152)87-0
Max-Planck-Straße 1 · D-21502 Geesthacht / Postfach 11 60 · D-21494 Geesthacht

GKSS 2006/16

Investigation of correlations between radar deduced bathymetries due to the outer impact of a storm in the area “Salzsand”

(Vom Coastal Research Laboratory, Forschungs- und Technologiezentrum Westküste BÜSUM, der Christian-Albrechts-Universität zu Kiel als Diplomarbeit angenommen)

Stylianos Flampouris

127 pages with 34 figures and 7 tables

Abstract

The basic requirement for all the coastal and marine activities is the knowledge of the bathymetry. In this thesis the concrete subject of interest is the determination of local depths by analyzing radar image sequences by the Dispersive Surface Classificator (DISC), a method to determine local maps of the hydrographic parameters, water depths and surface current. The analyzed radar data have been acquired by the Department of Radar Hydrography of GKSS research center, at the coastal area of the List West, Sylt Island, during a severe storm. The DiSC is based on the linear dispersion relation of the sea-surface wave and on the way that the waves interact with the seabed, as the sea state and tides are inhomogeneous in areas dose to the coast due to the spatial variations in the sea-bottom´s bathymetry. The commercial software DiSC is used in the current investigation. For the implementation of the objective, a concrete approach has been established. As this is one of the first times that the software used, all the parameters of the DiSC have been analyzed, tested and optimized. Due to the results of the optimization four new modules have been added for the quality control of the process. The significance of all the parameters of the method has been determined and the steering parameters of the analysis have been identified. The results (instantaneous sea level, mean depth over a tidal cycle and determination of sediment equilibrium) of the investigation are satisfactory and under specific assumptions their accuracy is comparable with most expensive or time consuming methods. This approach of the DiSC exposed the possibilities and the limitations of the method and the prospective extensions.

Zusammenfassung

Die Voraussetzung für viele küstennahen maritimen Aktivitäten bildet die Information über die Wassertiefe. In dieser Diplomarbeit liegt der Schwerpunkt auf Gewinnung der lokalen Tiefeninformationen aus der Analyse von Radarbildsequenzen unter Verwendung von Dispersive Surface Classificator (DiSC), einer Methode zur Berechnung von Karten mit hydrographischen Parametern wie Wassertiefe und Oberflächenströmung. Die analysierten Radardaten wurden

während eines starken Sturmes an der Messstation List West auf der Insel Sylt durch die Abteilung „Radarhydrographie“ am Institut für Küstenforschung/GKSS erhoben. DiSC basiert auf der linearen Dispersionsrelation der Wellen und ihrer Wechselwirkung mit dem Meeresboden. Der Seegang und die Wassertiefe sind inhomogen in küstennahen Gebieten mit zeitlichen Veränderungen der Bathymetrie. Für die aktuelle Forschung wird das kommerzielle Programm DiSC genutzt. Weil diese Software zum ersten Mal von einem Nichtentwickler eingesetzt worden ist, wurden alle Parameter von DiSC analysiert, getestet und optimiert. Infolge dieser Optimierung wurden vier neue Module entwickelt, die die Qualität der Prozesse überwachen. Die Signifikanz aller Parameter wurde ermittelt und die wesentlichen Parameter für die Analyse bestimmt. Die Ergebnisse (der momentane Wasserstand, mittlere Tiefe für einen Tidezyklus sowie die Bestimmung des Sedimentbudgets dieser Untersuchung sind zufrieden stellend unter der Annahme, dass ihre Genauigkeit mit viel teureren und zeitintensiveren Methoden vergleichbar ist. Dieser Test von DiSC zeigt die Möglichkeiten und Grenzen dieser Methode sowie die möglichen Erweiterungen.

Manuscript received / Manuskripteingang in TDB: 1. November 2006

Table of Contents

Tables and Figures

Acknowledgement

For the implementation of the thesis, I collaborated with Dr. F. Ziemer, who, in this short period, became my companion at the knowledge, a scientific leader, and a true teacher. He offered me the opportunity to work at the Department of Radar Hydrography at GKSS-Forschungzentrum Geesthacht GmbH and guided me during my whole effort. The chance working next to him and share some of his time with me, make me feel much more than lucky. The minimum that I can offer him back is a frank “thank you, Friedwart”.

I would like to thank Dr. J. Seemann and Dr. C. Senet (Vision 2 Techology GmbH, GITZ) for the honour to share with me their scientific creation, the Dispersive Surface Classificator and for our long and interesting conversations.

I want also to thank the rest of the employees at the Radar Hydrography Department, M. Cycewski and G. Schymura, for their help in practical problems and the guidance at my first steps at GKSS.

I feel thankfulness to Prof. R. Mayerle that as Director of the Master Course Coastal Geosciences and Engineering, University of Kiel, permitted and encouraged me to implement my thesis at GKSS and he contributes as supervisor.

At the end, I would like to thank my parents, who are my permanent supporters at my desires and actions.

Notations

∂	partial derivation operator
$\vec{k}$	2D wavenumber vector of sea-surface waves (rad m^{-1}, rad m^{-1})
$\vec{r}$	spatial vector
$\vec{u}_c$	2D near-surface current vector (ms^{-1}, ms^{-1})
C_G	group velocity of sea-surface waves (ms^{-1}, ms^{-1})
C_p	phase velocity of a sea-surface wave (ms^{-1}, ms^{-1})
d	water depth (m)
f	frequency (s^{-1})
ω	circular frequency (s^{-1})
g	gravitational acceleration
k	wavenumber (rad m^{-1}), magnitude
k_x, k_y, k_z	Cartesian wavenumber components (rad m^{-1})
t	time (s)
x,y,z	spatial coordinates (m)
Θ	3D spatio-temporal domain (m, m, s)
Ω	3D wavenumber-frequency domain (rad m^{-1}, rad m^{-1} rad s^{-1})
λ	wavelength (m)
θ	incidence angle
τ	waveperiod
ζ	sea-surface elevation (m)
ς	intrinsic dispersion of sea-surface waves (rad s^{-1})
ς^+, ς^-	positive and negative solution of dispersion (rad s^{-1})
P_r	received signal power
P_t	power
G_t	gain
R	distance
A_e	effective aperture area
λ_s	scattering wave length
λ_r	electromagnetic wave

1 Introduction

The observation and understanding of the environment is crucial for the effective use and sustainable development of the earth. More than 80% of the world population lives in a distance of 200km from the coast (VALEJO 2000).The spatial and temporal fluctuations of oceans on all scales, from hours to centuries, from meters to thousands of kilometers, affect environments and lives significantly. Since the antiquity, the ocean, by covering about the two thirds of the earth, has a vital role and influences on the human activities, as place of residence, source of commodities, trade routes, and recreation areas. To fulfill all those requirements, in a safe way, the study of the marine and coastal environment, the monitoring of oceanographic phenomena, the protection, the development, even the reclamation, of the coastal zones are unavoidable, especially in areas of socio-economical interest.

The changes, in the bathymetry or the shape of the coasts, have direct impact on the human activities, so the systematic monitoring is essential. Since the first trips of exploration the bathymetric data is a requirement, from rope and plummet to sonar and echo sounding and nowadays by the development of the remote sensing and a concrete wave theory, the acquisition of spatial and temporal bathymetries becomes part of the oceanographic routine.

1.1 Aim

The aim of the thesis is the extraction of the local water depth from the radar time series at the near shore coastal zone of List West at the north Sylt Island, Sylter Ellenbogen, during the period of a storm, by using the Dispersive Surface Classificator, DiSC. It is the first time that the DiSC is tested as part of an effort to be operationalized, for this reason it is essential, some objectives to be implemented, the first is the elaboration one specific and detailed methodology, the second is the optimization of the software and the amelioration of the software routines and interface and the third is the evaluation of the algorithm by an independent user.

1.2 Background

The survey of the sea surface by coastal microwave radar flourishes the last 30 years, the first civil system was the CODAR of NOAA (BARRICK 1977) and since then there are several around the world; it concerns mainly the measurement of ocean waves and surface currents. It is based on the spatial and temporal structure analysis of radar images of the sea surface. These radar images are generated by the interaction of electromagnetic waves with the sea surface ripples at grazing incidence. The spatial and temporal variability of the sea clutter information is analyzed in order to extract the wave spectrum and further sea state parameters, such as significant wave height and peak period, and it has been commercialised by at least two companies: the Wave MOnitoring System (WaMoS), developed by GKSS research center in Germany (ZIEMER 1991), (ZIEMER & DITTMER 1994), (NIETO 1999) and the Marine Radar Wave Extractor (WAVEX), developed by the MIROS AS Company in Norway (GRONLIE, 1995), (GANGESKAR and GRONLIE, 2000).

From the acquired image sequences, hydrographic parameters, such as the near-surface current-velocity vector, (SEEMANN et al. 1997), (SENET et al. 2001), the water depth, (OUTZEN 1998) and the calibrated full-directional wave spectra (SEEMANN et al. 1997), are determined. The method used up to now, here called the 'global method', is based on the analysis of radar backscatter signal variance spectra calculated by the squared modulus of a 3D Fast-Fourier Transformation performed on the image sequences. The 3D FFT in terms of image processing is a global operator. Therefore stationarity and homogeneity of the wave field must be fulfilled.

The recently developed DiSC, consists an algorithm, that analyses image sequences for the determination of physical parameters on a local spatial grid. The local analysis method, which allows the analysis of image sequences of an inhomogeneous, dynamic and dispersive surface. Till now the developers and the programmers of the specific method, were also the valuators and there are few publications about the use of the DiSC, (SENET 2004), (SENET et al. 2003), (SENET et al. 2001), (SEEMANN et al. 2000), (SEEMANN et al. 2000), (SEEMANN et al. 2000). The

thesis concerned the independent evaluation of the algorithm and the use of the software under real circumstances.

1.3 Area of research

The area of research is the West List, north-west side of the Sylt Island, laying in the German Bight. The Island of Sylt is situated on the West coast of Schleswig-Holstein at the North Sea coast of Germany and it is the most northern sandy barrier island of the Frisian chain of the Wadden Sea coast, for the map of the area see the figure 4-1. It has a length of 35 km and a width up to 13 km, its surface is 99 km^2. There are several scientific, economical and social criteria for the choice of this specific area. The common belief, “It’s the Sylt”, is the main sponsoring reason of the research.

Since the half of the 20^{th} century, the high and rapid erosion of the west coasts of the island and the social-economic aspects, transformed it into an experimental field about the coastal protection. The island started taken the current shape about the 17^{th} century and in general the northern and southern spit, is under continuous development. The tide, in area of Sylt is semi-diurnal and the tidal ranges reach around 2 m, which causes cross shore transport through the gaps between barrier islands of German Bight. The long shore transport along the coast is mainly wave-induced and therefore also alternates in direction, this is obvious at Sylt; the island grows northward as well as southward by spit prolongation in both directions. Tidal currents are dominant seaward of the longshore bar, with resulting sediment transport to the North. It is proved by measurements of sediment transport (SISTERMANS & NIEUWENHIUS 2004), that the sediment dynamic of the island is that at the southern part of Sylt, the net long shore transport is directed southward and at the northern part of Sylt, the net long shore transport is directed northward. The coast is eroding along the entire western coast. The island loses the majority of this sand through storm surges. The base of the island rises gradually from the foreshore, where a sandy reef is located. Shore and reef together function as a transportation mean. Waves and tides continuously erode and move away material from the sandy shore and foreshore area, causing structural erosion.

The vulnerable island of Sylt has a multi-functional, socio-economic character and is covered by a mixture of natural and cultural territories; the permanent population of Sylt is about 21.000 persons and more than the double during the summer, (AHRENDT 2001). Besides high level standards in living and recreation facilities, Sylt provides unique aspects of a biotope. In 1985, the region was designated as national park in recognition of the high ecological significance of the Wadden Sea. The Sylt Island also provides many recreational opportunities. The long west coast with its sandy beaches attracts many tourists and has considerable economic importance not only for the island but also for the federal state. Fisheries and aquacultures and urbanisation, care about safety of people and investments.

The conclusion of the above analysis is that the island of Sylt is an island of high activities, where there are several problems to be confronted for the unhindered evolution of the island. The initial concrete constructions for the protection against the erosion, dramatically fast were proved an engineering error, therefore since 1960's and more intensively since 1980's (APPENDIX I), beach nourishments take place very often that makes Sylt, a deeply investigated island under permanent monitoring. The need of continuous and precise as well as assessment data is necessary against the erosion, sediment transport for the port operations, engineering constructions and disaster prevention. The crucial contribution of the Radar Hydrography is to provide a tool for the assessment of spatial changes in the sand regime, with the special quality to be applied under heavy weather conditions, as "there is no excuse for not considering the remote sensing methods in any monitoring system" (VOGELZANG 2000).

1.4 Outline

The extraction of the depth from a sequence of radar images is an indirect process, at which remote sensing techniques are combined with the linear gravity wave theory and through a multi-step arithmetic method the local current vectors and the depth are calculated. Therefore, at the Chapter 2, the basics about the radar technology and the imaging of the sea surface are described. The linear sea-surface wave theory, by concentrating the Dispersion concept, is presented at the Chapter 3.

The methodology (Chapter 4) of the thesis is separated into three sections, the Pro-DiSC, which includes all the preprocessing before the image processing by using the Dispersion Surface Classificator, section DiSC, and the Post-DiSC where all the post processing of the results of the main algorithm are described.

The central part of this thesis (chapters 5-8) compromises the achievements. The chapter 5 describes the optimization of the DiSC by discussing all the parameters of the algorithm. The results of the present effort are presented at the Chapter 6 and are analytically discussed at the Chapter 7 and Chapter 8, where there is the geophysical interpretation of them and the general conclusions of the thesis and the outlook for further investigation.

2 Radar imaging

The current chapter presents the basics about the remote sensing, the technology of the nautical radars and the modulations mechanisms of the radar images. It is based mainly on publications of (SKOLNIK 1990), (LONG 1975) and (DOONG 2003).

“Remote sensing is the science, and to some extent, art, of acquiring information about the Earth's surface without actually being in contact with it. This is done by sensing and recording reflected or emitted energy and processing, analyzing, and applying that information”, as it is defined by (CANADA CENTER FOR REMOTE SENSING 2003).

Recently, high level technologies originally developed for military purposes have been converted for scientific and civil applications. A number of earth observation missions have been successfully undertaken providing some useful information. Oceanography, geology, hydrology, forestry and agriculture have been targeted for such applications as hazardous events prevention and territory management. Many of the sea-state parameters for coastal and oceanographic researches can now be observed by remote sensing techniques, including wave heights, currents, surface wind fields, ocean color and sea surface temperature. Ocean wave remote sensing techniques can be performed from coastal ground, ship, aircraft or satellite. The sensor types include infrared sensor, optical sensor and radar. In this case, the used sensor is radar.

2.1 Introduction to the microwave remote sensing

Among the set of remote sensing devices, we focus here to the RADAR, RAdio Detection And Ranging. Passive radar measures the electromagnetic radiation emitted by any radiating source, while active radar possesses its own radiation source and receives echoes from the sea surface. Thus the active radars do not require solar illumination and may be operated at night. Radars with different frequency bands have their own functions and limitations. Microwave radars, with wavelengths ranging from 0.1 cm to 100 cm, are noted for their ability to penetrate rain, fog and clouds. The spatial resolution of a radar system depends on the transmitted signal in range and on the antenna pattern in direction. The range resolution of a pulsed microwave

radar is dependent on the fine duration of the transmitted pulse and the incidence angle (LILLESAMD & KIEFER 1994). The azimuth resolution is dependent on the microwave wavelength and the antenna length; the ratio antenna length to microwave length is called real aperture. It may be improved by either decreasing the wavelength of electromagnetic wave or by increasing the antenna length. However, the shorter wavelength radars are affected by the sea spray or the rain drops.

Recently, remote-sensing techniques at the coastal zone applied to wave and current measurement with coastal radar have become more important.

Applications like coastal management and ship guidance require increasing data density as opposed to single point measurements. Remote sensing techniques are also advantageous in that; there is no need to install a mooring in the open sea, which could potentially be damaged by bad weather conditions or approaching ships. Coastal radar used nowadays the microwave radar (Frequency ranges from 3 to 30 GHz) and High-Frequency (HF) radar (Frequency ranges from 3 to 30 MHz). Both use electromagnetic waves to remotely sense ocean surface currents and sea states over extended areas. Microwave radars have the advantage of simpler installation, but do not cover areas as large as it is possible to cover with HF radars. Microwave marine radars originally used for navigation have been developed to measure the ocean waves, such as the WaMoS system (REICHERT et al. 1999). HF radars with wavelengths of 100 m to 10 m are mostly operated at the coast, based on groundwave or skywave propagation.

Although the observation range of coastal radars is not as extensive as satellites, the superiority of wave measurement by land-based radar lies in its capability to observe 3D images of the sea state by routine operation, as opposed to 2D observation made from satellite or aircraft. In addition, the wave monitoring systems by coastal radars are relative easy to install and operate. Thus it would appear that coastal radars are the potential instruments for the remote sensing activities of waves in the future.

2.2 Sea Clutter

For a navigational radar, backscatter of the transmitted signal by elements of the sea surface often places severe limits on the detectability of returns from ships, aircraft and missiles, navigation buoys, and other targets sharing the radar resolution cell

with the sea. These interfering signals are commonly referred to as sea clutter or sea echo. Since the sea presents a dynamic, endlessly variable face to the radar, an understanding of sea clutter will depend not only on finding suitable models to describe the surface scattering but on knowledge of the complex behavior of the sea as well. Fortunately, a close relationship between radar and oceanography has grown up in the remote-sensing community, leading to the accumulation of a large amount of useful information about scattering from the sea and how this scattering relates to oceanographic variables.

It would seem a simple matter to characterize sea clutter empirically by direct measurement of radar returns for a wide variety of both the radar and environmental parameters that appear to affect it. Parameters relating to the radar or its operating configuration, such as frequency, polarization, cell size, and grazing angle, may be specified by the experimenter, but the environmental parameters are quite another matter-for two reasons. First, it has not always been clear which environmental variables are important. For example, wind speed certainly seems to affect clutter levels, but correlation of clutter with, say, ships' anemometer readings has not been entirely satisfactory. The state of agitation of the surface (sea state) appears to have a strong effect, but it is a subjective measure, and its relation to the prevailing local winds is often uncertain. Moreover, it has been found that the stability within the lower most layers above the sea, steered among others by the temperatures of the air and the sea surface. This affects the way in which the measured wind speed is related to the generation of clutter-producing waves, yet the importance of these effects were unappreciated over most of the history of sea clutter measurements; so air and sea temperatures were seldom recorded. Even if the importance of an environmental parameter has been recognized, it is often difficult to measure it with accuracy under real-sea conditions, and there are practical and budgetary limits to obtaining open-ocean measurements in sufficient variety to develop any really meaningful statistica1 models of clutter. Little wonder that many aspects of sea clutter remain frustratingly unidentified.

It is commonly noted that the appearance of sea clutter depends strongly on the size of the resolution cell or radar footprint. For large cells it appears distributed in range and may be characterized by a surface- averaged cross section with relatively modest

fluctuations about a mean value. As the size of the resolution cell is reduced, clutter takes on the appearance of isolated target like, or discrete, returns that vary in time. At these higher resolutions, the distributed clutter is often seen to consist of a dense sequence of discrete returns. When the discrete returns stand well out of the background, as they are seen to do for any polarization but most clearly with horizontal polarization at small grazing angles, they are called sea spikes and are a common clutter contaminant in this radar operating regime.

In 1956, however it is observed that at high-frequency (HF) wavelengths (tens of meters) scattering appeared to arise from a resonant interaction with sea waves of one-half of the incident wavelength (CROMBIE 1956), i.e., to be of the Bragg type. Reinforced by the theoretical implications of various small waveheight approximations and wave tank measurements under idealized conditions, the Bragg model was introduced into the microwave regime by many workers. This produced a revolution in thinking about the origins of sea clutter because it involved the sea wave spectrum, thus forging a link between clutter physics and oceanography in what became the field of radio oceanography. However, fundamental conceptual problems in applying the Bragg hypothesis in microwave scattering, along with recent questions about the validity of its predictions and the possibility of alternative scattering hypotheses, have reopened inquiry into the physical origins of sea scatter and how best to model it. This being the case, speculation about physical models will be kept to a minimum in the sections on the empirical behavior of sea clutter.

2.2.1 Radar equation

The easiest way to describe the radars is the mathematical formulation, as the single most useful description of the factors influencing radar performance is the radar equation which gives the range of radar in terms of the radar characteristics. One form of this equation gives the received signal power P_r as:

$$P_r = \frac{P_t G_t}{4\pi R^2} \times \frac{\sigma}{4\pi R^2} \times A_e \qquad (2.1)$$

The right side has been written as the product of three factors to represent the physical processes taking place. The first factor is the power density at a distance *R* meters from a radar that radiates a power of P_t watts from an antenna of gain G_t. The nu-

merator of the second factor is the target cross section σ in square meters. The denominator accounts for the divergence on the return path of the electromagnetic radiation with range and is the same as the denominator of the first factor, which accounts for the divergence on the outward path. The product of the first two terms represents the power per square meter returned to the radar. The antenna of effective aperture area A_e intercepts a portion of this power in an amount given by the product of the three factors.

2.2.2 Backscatter mechanisms

There are various measuring techniques based on the backscatter theories of radar signal. Some are based on the analysis of the backscatter intensity of the return radar signal. Others use both the backscatter intensity and the Doppler spectrum. The mechanism that leads to a scattering of the electromagnetic waves from the sea surface is dependent on the incidence angle. At small incidence angles with respect to the vertical (less than about 15-20°), the main scattering mechanism is quasi-specular, and the roughness scales which govern the backscattering intensity cover all scales from about 3 times the electromagnetic wavelength. At moderate incidence angles (from about 20° to 70°), the main process is the so-called "Bragg resonant process", which is generated by the waves on the surface which are of the same order as the electromagnetic wavelength. At larger incidence angles (grazing angles above 70°), the backscattering is more complex, including shadowing effects and other complex mechanisms. In some cases (HF radar) the backscattered signal provides "direct" information on the wavelengths of interest, because the Bragg wavelength is of the same order. In other case, marine radars, airborne or spaceborne real or synthetic aperture radars, the backscatter is related to short wavelengths, but its modulations are related to the wavelengths of interest. For systems that use the Doppler information of the backscattered signal, the principle is in the relationship between the Doppler information and the wave orbital velocity that is in turn related to the wavelength.

2.2.2.1 Bragg backscattering

The Bragg backscattering consists the main theory broadly used for the backscattering of radars, e.g. ground based or naval radars, ERS SAR and at the present paragraph there is the description of the mechanism.

As the incidence angle of the radar is oblique to the local mean angle of the ocean surface, there is almost no direct specular reflection except at very high sea states. Therefore it is assumed that at first approximation Bragg resonance is the primary mechanism for backscattering radar pulses. The Bragg equation defines the ocean wavelengths for Bragg scattering as a function of radar wavelength and incidence angle:

$$\lambda_s = \frac{\lambda_r}{2\sin\theta} \tag{2.2}$$

where λ_s is the sea surface wavelength, λ_r is the radar wavelength and θ is the incidence angle.

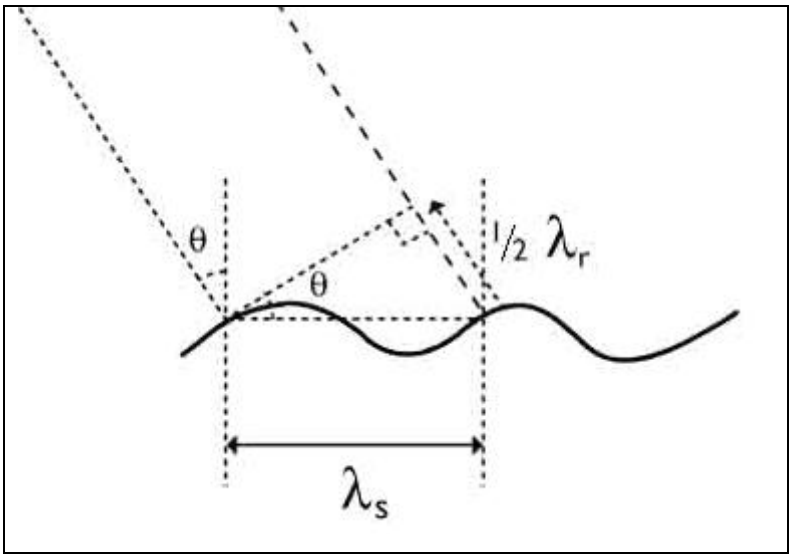

Figure 2-1. Scheme to visualize the relation between the scattering wave with the length λ_s and the electromagnetic wave with the length λ_r. The relation between those two is observed by (CROMBIE 1956) and consist the basic principle of the radar systems.

The short Bragg-scale waves are formed in response to wind stress. If the sea surface is rippled by a light breeze with no long waves present, the radar backscatter is due to the component of the wave spectrum which resonates with the radar wavelength. The Bragg resonant wave has its crest nominally at right angles to the range direction.

For surface waves with crests at an angle ϕ to the radar line-of-sight, as shown at the figure, 2.2.2.1.1, the Bragg scattering criterion is:

$$\lambda_s' = \frac{\lambda_r \sin\phi}{2\sin\theta} = \lambda_s \sin\phi \qquad (2.3)$$

where: λ_s' is the wavelength of the surface waves propagating at angle ϕ to the radar line of sight.

The radars directly image the spatial distribution of the Bragg-scale waves. The spatial distribution may be effected by longer gravity waves, through tilt modulation, hydrodynamic modulation and velocity bunching.

Moreover, variable wind speed, changes in stratification in the atmospheric boundary layer, and variable currents associated with upper ocean circulation features such as fronts, eddies, internal waves and bottom topography effect the Bragg waves.

2.2.3 Modulation mechanisms

There are several modulation mechanisms that effects the measurements by the radar, the integrated effect of the processes are described in the next three paragraphs is that one image of long wave field is impressed to the radar signal that is related to the instantaneous sea surface by a Modulation Transfer Function (MTF). For the study discussed within this thesis, it is only necessary to localize the position of the moving wave crests and not the retrieve the real shape of the surface. The linear scaled imaging of the wave crests within the radar backscatter fields is not affected by the MTF, thus the intense about it is not real strong.

2.2.3.1 Tilt

At the sea-surface wave theoretical formulation the sea surface consists of large swells on which short gravity and capillary waves are superimposed. From the electromagnetic viewpoint, the smaller waves are treated by previously developed theories for slightly rough surfaces (WRIGHT 1966). Effects of the macrostructure, sea and swell, are included by considering changes in scattering caused by the tilting of the small structure (short gravity and capillary waves) by the dielectric background (sea and swell).

2.2.3.2 Hydrodynamics

The sea clutter depends on the hydrodynamic conditions of the area of investigation; the effect of the currents on the signal is the most investigated. The most obvious effect of a current on sea clutter would be a shift in the peak of the Doppler spectrum. Another effect is related to the fact that the excitation of the surface-wave system depends on the *apparent* wind; so there can be significant differences in wave-height according as the wind is blowing with or against the current. It is proved that the waveheight is proportional to the square of the wind speed. Even with no wind the presence of strong current shears can produce highly agitated surfaces.
Shipboard observers have reported bands of roaring breakers passing by on an otherwise smooth surface, presumably produced by powerful surface-current shears associated with large-amplitude internal waves. The general effect of the current is a change in the surface roughness, which can be expected to give rise to a change in sea clutter cross section (LONG 1990).

2.2.3.3 Shadowing

The shadowing effect at the image sequences of the coastal radar caused by the shape of the waves. The waves are characterized by bright signals from the near slopes and the absence, not illuminated by the radar, of signals from the far slopes. For the sea, it is likely that effects of shadowing become appreciable for angles of incidence closer to horizontal than the crest height and the sea wavelength. The shadowing of troughs by crests cause the reduction in expected scattered power. At near grazing incidence angles, when shadowing is appreciable, it is expected that the top of the crests contribute significantly to creating the effective reflecting surface. Therefore, the magnitude of the reflected field will depend in the incidence angle, and the location of the effective reflecting surface will also be a function of that angle.

3 Wave theory

For the complete approach of the subject, it is essential to present the basic principles of the wave theory on which the whole effort is based. Under the general title, wave theory, is covered a broad approach of physical phenomena, that they present the same or similar physical behavior. The approach is the same for the sound or the light waves or even for the sea-surface waves. The physical parameters of the matter, density, elasticity, plasticity and surface tension, are described by relation between the spatial and temporal wave parameters: the wavelength, λ, and the waveperiod, τ are common in any of the phenomena that are described by the wave theory. The function describing the relation between the λ and the τ depending on the free physical parameters is a dispersion relation. The dispersion relation consists the mathematical solution of the equations of motion describing free plane wave propagation on a surface (MARSDEN & CHORIN 2004)

The Chapter 3 consists an effort to approach the fundamental principles of the wave theory though the sea-surface waves, the theory is written in many publications, in this case, as reference are used the publications of (SOUKISSIAN 2003), (TOMCZAK 2005) and mainly (SENET 2004), as he described in his PhD dissertation, for the development and implementation of the method.

3.1 Sea-Surface Waves

The ocean surface waves are defined as "the manifestation of the exchange of kinetic energy between the atmosphere and ocean and, as such, is a vital and highly complex factor in coastal and ocean applications" (TOMCZAK 2005). Of course there are many definitions about the sea-waves. The common classifications of the sea waves are according to the driving forces, meteorological forcing, earthquakes, tides and the restoring forces, surface tension, gravity.

The figure 3-1 compresses all the information about the energy distribution of the waves versus the frequency, the classification of the surface-sea waves and the generating force of each of them.

Within the bandwidth of this thesis we considered the wind generated waves and as balancing force mainly the earth gravity. The general concept of the mechanism of

wind sea-surface waves generation: If wind skims along the water surface, small perturbations of the near- boundary atmospheric pressure field lead to small perturbations of the water surface. The distorted surface allows viscous or turbulent energy transport, leading to the growth of waves. Several theories have been developed for the detailed explanation of the phenomenon (MILES 1957), (PHILLIPS 1966), (HASSELMANN 1962) but still it has not totally been clarified.

3.2 Modelling of the Sea-Surface waves

The sea-surface waves belong to the first physical phenomena that have been mathematical modeled. The mathematical approach of the waves is deterministic, stochastic (LONGUET-HIGGINS 1952), (GODA 1970) and chaotic, (MOON 1992). In this case, the approach is deterministic and consists of the classical sinusoidal modelling of the phenomenon.

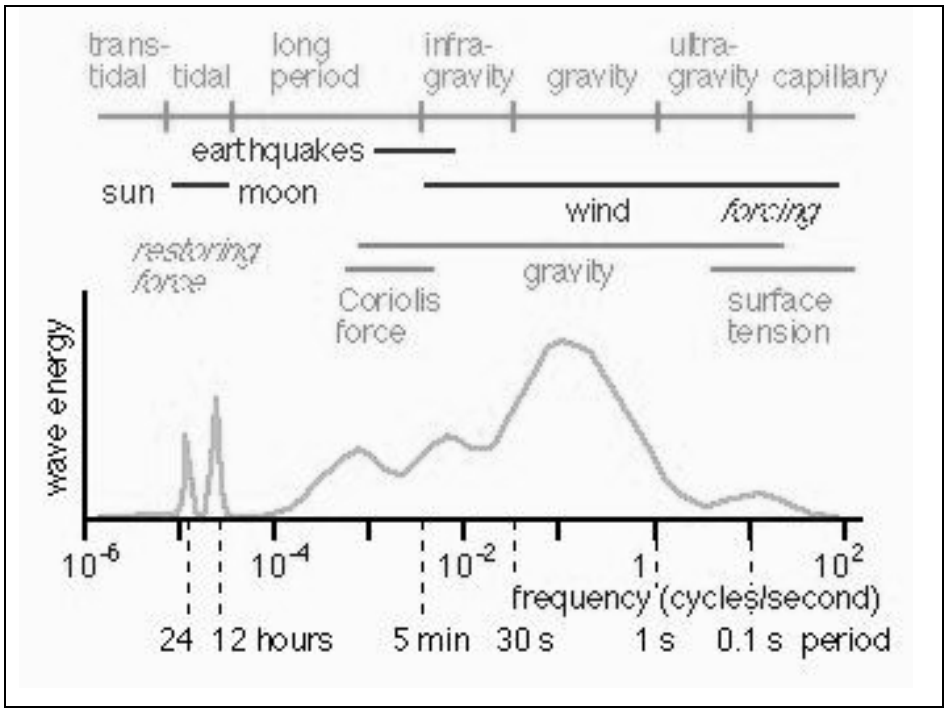

Figure 3-1. Hypothetical energy spectrum compromising the most important periodic processes in the ocean and their driving and balancing forces (TOMCZAK 2005).

3.2.1 Sinusoidal approach

The more common and easy understandable approach of the sea-waves is the concept of a wave as a harmonic oscillation. It is characterized by the wavelength λ or the

wavenumber $k = 2\pi\lambda^{-1}$, the period τ or the angular frequency $\omega = 2\pi\tau^{-1}$, the amplitude η and the direction of propagation θ.

A sea-surface wave is a plane wave and therefore k and θ can be expressed in Cartesian coordinates as a two-component wavenumber vector, $k = (k_x, k_y)$. A linear sea-surface wave is of sinusoidal shape. Deviations from this shape are expressed as nonlinearities. A single sinusoidal plane wave has the form

$$\zeta(\Theta) = \hat{S}e^{i(\vec{k}\cdot\vec{r}-\omega t)} + \hat{S}_* e^{-i(\vec{k}\cdot\vec{r}-\omega t)} \qquad (3.1)$$

where ζ is the sea-surface elevation in the spatio-temporal domain $\Theta = \Theta(x, y, t)$, $\hat{S} = \zeta_0 e^{i\phi_0}$ is the spectral Fourier coefficient, where ϕ_0 is the initial phase, $\hat{S}_*$ is the complex conjugated of $\hat{S}$ and $\vec{k}$ is the wavenumber vector and $\vec{r}$ is the spatial vector. The expression: $\phi = \phi_0 + \vec{k}\cdot\vec{r} - \omega t$ descibes the phase, ϕ.

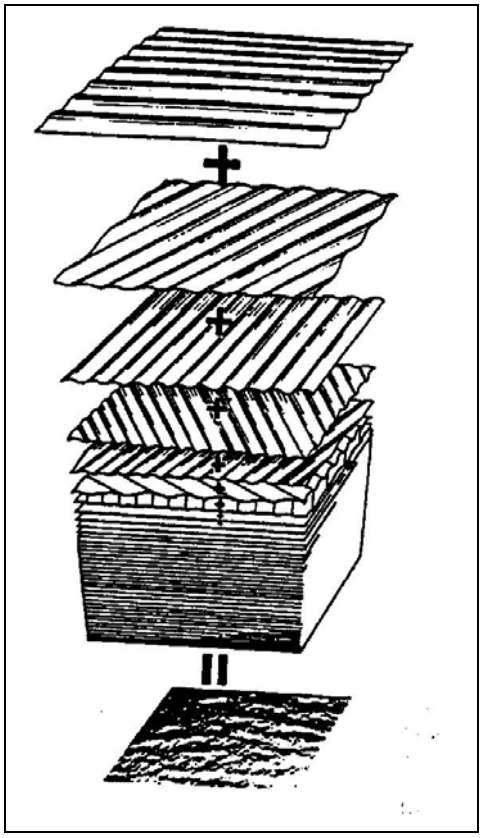

Figure 3-2. Schematic superposition of different singles waves (GODA 1970).

By generalizing the above concept, a wave field is defined as the superposition of single waves and its shape is the sum of n single waves.

$$\zeta(\Theta) = \sum_{n=1}^{\infty} \hat{S}_n e^{i(\vec{k}_n\cdot\vec{r}-\omega_n t)} + \sum_{n=1}^{\infty} \hat{S}_{*n} e^{-i(\vec{k}_n\cdot\vec{r}-\omega_n t)} \qquad (3.2)$$

where $\vec{k}_n$ is the nth wavenumber vector, ω_n is the nth frequency and $\hat{S}_n = \zeta_n \cdot e^{i\phi_{0,n}}$ is the nth Fourier coefficient for the nth wave.

3.2.2 Stationarity of Wave fields

In the mathematical science, a stationary process is a stochastic process in which the probability density function of one random variable *X* does not change over time or position. As a result, parameters such as the mean and variance also do not change over time or position, experimental proved for at least short periods (PRINS 1996).
Therefore, the general definition of the stationarity makes clear that for a wave field two conditions must hold to fulfill the criterion of stationarity: the local temporal phase gradient, $\partial\phi_i/\partial t$, have to be invariant in time for a considered time period:

$$\frac{\partial\phi_i}{\partial t} = \omega_i \text{ and } \frac{\partial\zeta_{0,i}}{\partial t} = 0 \qquad (3.3)$$

where ϕ_i is the temporally local phase, $\zeta_{0,i}$ is the temporally local amplitude and ω_i is the temporally local frequency, which is constant. If one of the above criteria does not hold for at least one wave of the wave field for the period of the observation, the wave field is instationary.

3.2.3 Homogeneity of Wave fields

A stochastic process is defined homogeneous in space if the transition probability between any two state values at two given times depends only on the difference between those state values (PRINS 1996).
For a wave field in an oceanic box two conditions must hold to fulfill the criterion of homogeneity: the spatially local phase gradients, $\frac{\partial\phi_i}{\partial x}$, $\frac{\partial\phi_i}{\partial y}$, and the local amplitude, *y*, have to be invariant in space. Defined for the Cartesian coordinates *(x, y)*, the criteria of homogeneity are

$$\frac{\partial\phi_i}{\partial x} = k_{x,i} \text{ and } \frac{\partial\zeta_{0,i}}{\partial x} = 0 \qquad (3.4)$$

and

$$\frac{\partial\phi_i}{\partial y} = k_{y,i} \text{ and } \frac{\partial\zeta_{0,i}}{\partial y} = 0 \qquad (3.5)$$

where ϕ_i is the spatially local phase, $\zeta_{0,i}$ the spatially local amplitude, and k_i are the spatially local wavenumber vector, which are constant. If one of the above criteria does not hold in the considered ocean box for at least one wave of the wave field, the wave field is inhomogeneous. The above-mentioned processes are inhomogeneous processes. The spectral effects due to inhomogeneous and instationary processes are illustrated in figure 3.3.

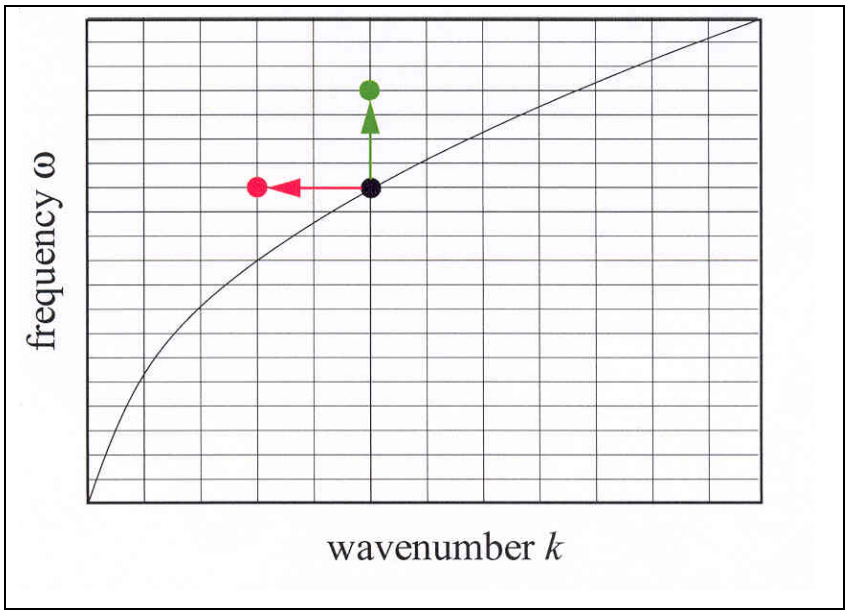

Figure 3-3. Spectral instationarity and inhomogeneity illustrated in a 2D $k-\omega$ section: if a wave field is instationarity, the global spectral signal is smeared to other frequencies (green dot); if a wave field is inhomogeneous, the global spectral signal is smeared to other wavenumbers (red dot), (SENET 2004).

3.2.4 Dispersion relation

Assuming a non-viscous, incompressible and homogenous liquid, e.g. water, the dispersion relation of sea surface waves is derived from the Eulerian equation of motion, the continuity equation and the dynamic and kinematic boundary conditions of the dispersion relation is given in (WINKEL 1994).

The phase speed C_p and the group speed C_g are given by

$$C_P = \frac{\omega}{k} \text{ or } C_P = \frac{\lambda}{\tau} \tag{3.6}$$

and

$$C_G = \frac{d\lambda}{d\tau} \text{ or } C_P = \frac{d\omega}{dk} \tag{3.7}$$

The phase speed C_p determines the speed of propagation of a single wave component, and the group speed determines the propagation of the wave field's energy. In extremely shallow water (wavelength $\lambda > 0.1 \cdot d$) $C_G = C_P$; in deep water ($\lambda < \frac{d}{2}$) the condition $C_G = \frac{C_P}{2}$ holds.

The dispersion relation describes the dynamic relation between wavenumber k and angular frequency ω and determines the phase speed, speed of propagation) of a wave. The term "normal" dispersion implies that longer waves have a higher phase speed than shorter waves. This performance holds for capillary waves. The linear dispersion relation for free gravity sea surface waves, if the surface is ignored is given by

$$\tilde{\omega}(\vec{k}) = \sqrt{gk \tanh(kd)} + \vec{k} \cdot u_c \tag{3.8}$$

Where g is the gravitational acceleration, d is the water depth, $\vec{u}_c$ is the near surface current.

In (3.8) the first term is called the intrinsic frequency, $\varsigma^{\pm} = \pm\sqrt{gk \tanh(kd)}$, and the second term is called the Doppler frequency, $\omega_D = \vec{k} \cdot u_c$, indicates the effect of the near surface current. Following (3.8), the accelerations which force an elevated particle to move back to the initial position, $\vec{\zeta}$ is $\vec{g}$, this happens to waves longer than 0.1 m. When the waves $\lambda < 0.1m$, only the surface tension of water has a significant effect on small waves, those waves are called capillary-gravity waves and the relation which describes them take account also the surface tension, in this case they are ignored. The water depth d and the near surface current vector $\vec{u}_c$, are free parameters which influence the shape of the dispersion shell in the wavenumber frequency domain, Ω . Therefore the shape of the dispersion shell can be used to inversely determine these free parameters.

The dispersion relation generates a shell in the 3D Ω domain. The intrinsic dispersion shell is symmetric about the rotational axis, figure 3-4. The intrinsic dispersion

relation has two solutions, ς^+ and ς^-. These two solutions are redundant, a consequence of the symmetrical attributes $\varsigma^+ = -\varsigma^-$ of the Fourrier transformation.

Because of the redundancy of the dispersion shells $\varsigma^+(\vec{k})$ and $\varsigma^-(\vec{k})$ are hermetic and only one of the shells is needed to describe the energy of wave fields in the Ω domain.

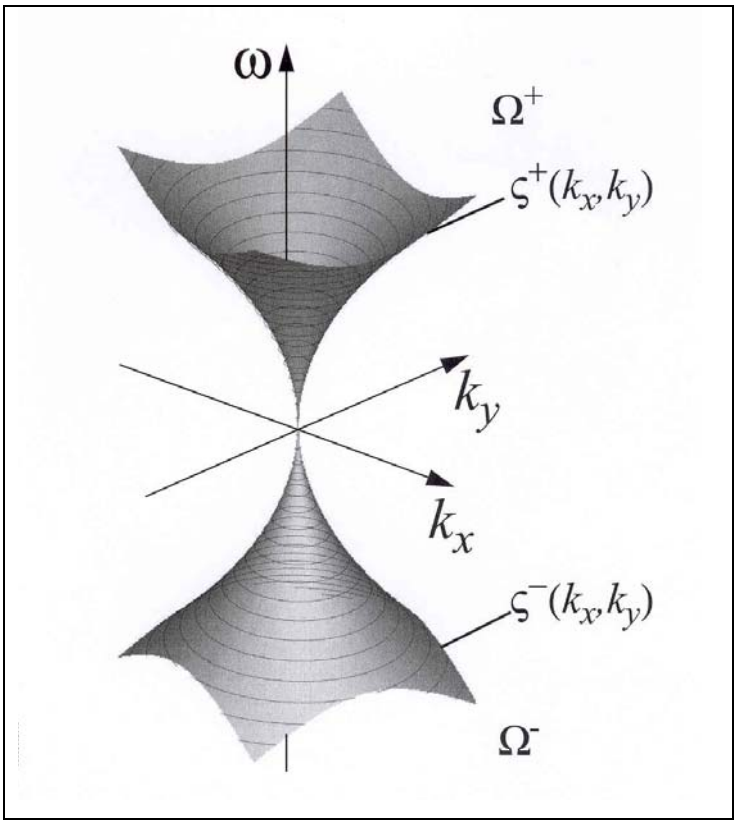

Figure 3-4. Positive and negative intrinsic dispersion relation, ς^+ and ς^- of linear deep-water surface-gravity waves in the 3D Ω domain (with positive and negative hemisphere, Ω^+ and Ω^-), (SENET 2004).

3.2.5 Near-Surface Current and Water Depth

At the current section is given a brief description of the influence of the near surface currents and the water depth.

If a near-surface current, $\vec{u}_c$ is present, waves are Doppler shifted. The Doppler shift, ω_D leads to a frequency shift of ω. If a current is directed in a direction opposite to that a wave, the wave's absolute, in the inertial coordinate system of the ob-

server, frequency is increased and vice versa. The deformation of the dispersion relation due to the Doppler effect is illustrated in Figure 3-5c.

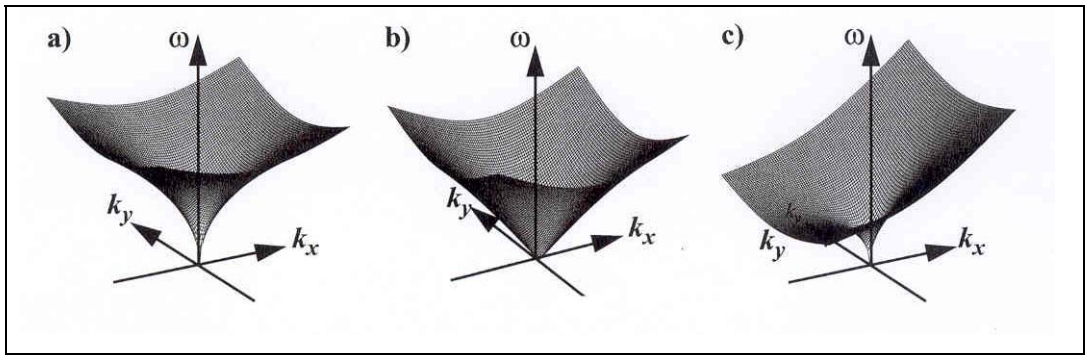

Figure 3-5. Dispersion relation of linear surface-gravity waves in the 3D Ω domain: a) intrinsic deep water dispersion shell, b) intrinsic shallow-water dispersion shell and c) Doppler shifted deep-water dispersion shell influenced by a near- surface current, (SENET 2004).

For deep-water waves, defined by the condition $d \gg \lambda$, the approximation $\tanh(kd) \approx 1$ holds and can be substituted into (3.8). By assuming $\vec{u}_c = 0$, the deep-water wave solution is as follows:

$$\varsigma^+(k) = \sqrt{gk} \tag{3.9}$$

In shallow waters, where d is small compared to λ, the shallow-water dispersion relation is:

$$\varsigma^+(k) = k\sqrt{gd} \tag{3.10}$$

obtained when the approximations $\tanh(kd) \approx kd$ and $\vec{u}_c = 0$ are substituted into (3.8).

4 Methodology

The complete methodology of the present investigation is described analytically in this chapter. The methodology is divided into three sections, Pro-DiSC (sec. 4.1), DiSC (sec. 4.2) and Post-DiSC (sec. 4.3). The main process is the use of the Dispersive Surface Classificator, Pro-DiSC includes the necessary preparations for the exertion of the DiSC and at the Post-DiSC the post process analysis and investigation of the results of DiSC. The flow chart of the methodology, Appendix II, (because of the size of the flow chart at every section is presented the corresponding part of the flow chart) is the axis of implementation of the whole effort.

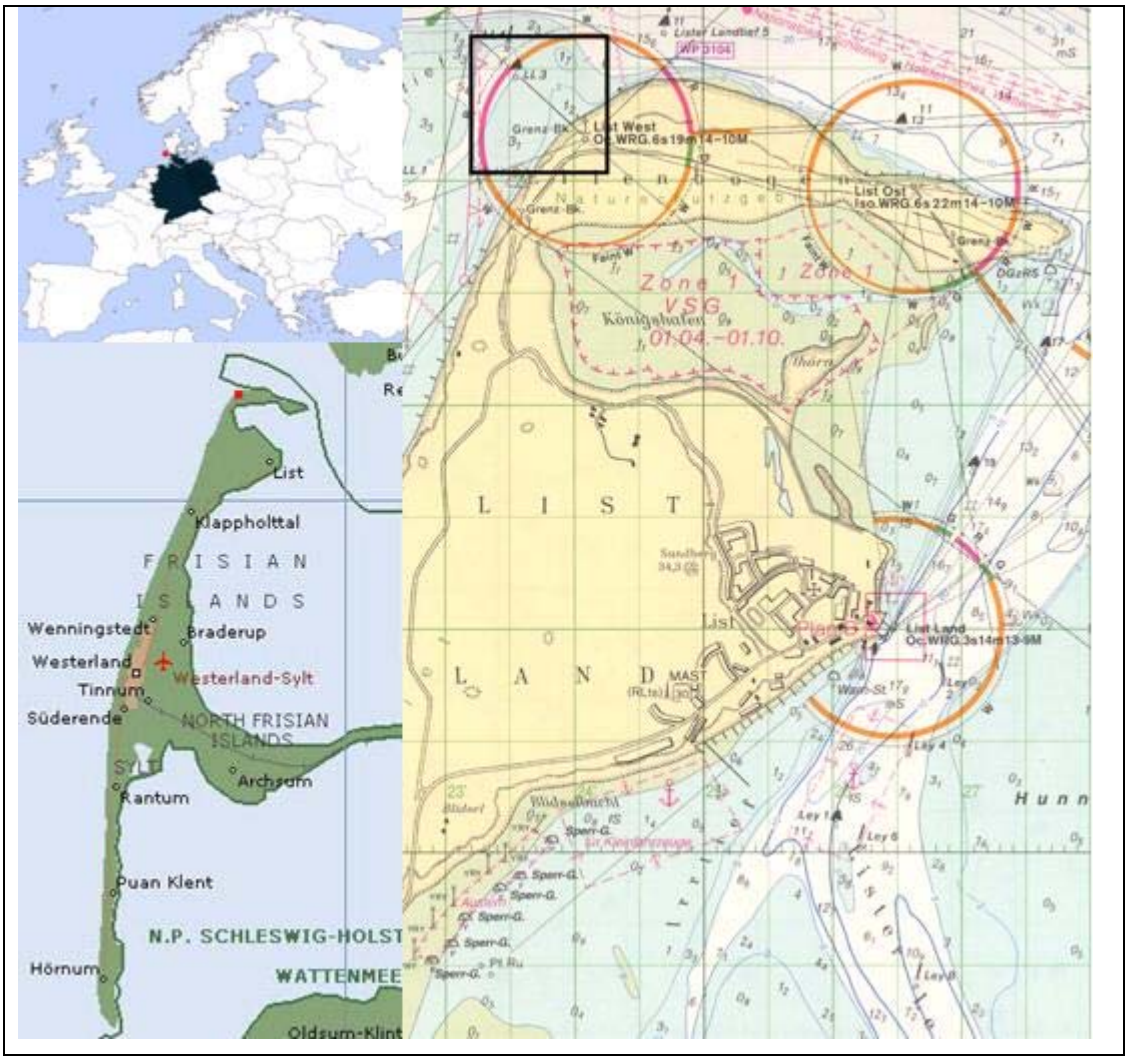

Figure 4-1. Maps for the localization of the research area position, in the black frame on the right map, (Microsoft Encarta © and BSH 2002).

4.1 Pro-Disc

In the section 4.1 of the thesis, there are a brief introduction to the radar station of List West, for the deeper comprehension of the experimental setup, the reasons about the period of the investigation, the description and the preprocessing of the wind and radar data.

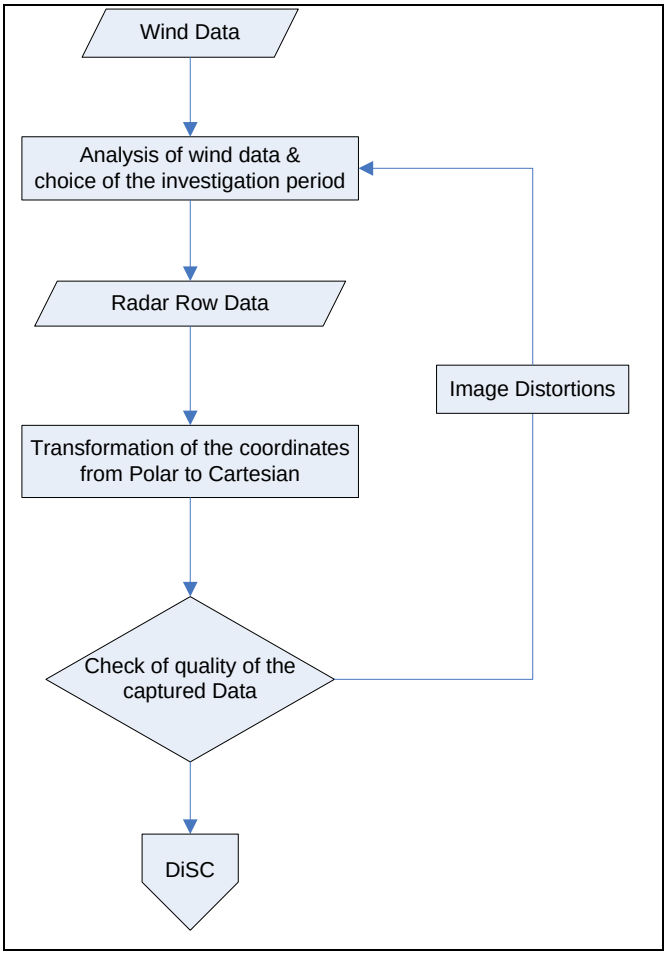

Figure 4-2. Flow chart of the Pro-DiSC data processing, the first step is the analysis of the meteorological data for the choice of the investigation period; the second step is the transformation of the image sequence coordinates from Polar to Cartesian and the quality control of them.

4.1.1 Experimental Setup: Sylt

The monitoring station was mounted near the lighthouse List West on the island of Sylt in the German Bight, see figure 4-1. The area covered by the radar images show List West, the Lister Landtief, and parts of the Lister Tief. The used instrument for

the acquisition of the sea-surface is a software-hardware combination, figure 4-3, presented by (NIETO et al. 1999) as part of the Wave Monitoring System (WaMoS), consisting of a Furuno FR 1201 (FURUNO MANUAL 1989) nautical radar, a WaMoS II analog-digital converter and a WaMoS II software package for the acquisition of the radar images. The used instrument for the observation is a ground-based nautical X-band radar with horizontal polarization, mounted 25m above the NN. The radar was mounted for about six years, but the period of the present investigation is the last week of February of 2002.

In addition to the acquisition system, there is a meteorological station, Meteorological Weather Station by Siggelkow Geraetbau GmbH (SIGGELKOW MANUAL 2000) at the same mast with the radar, approximately 23m over the NN.

Figure 4-3. The left image presents the radar of List West station, next to the lighthouse of the List West, and on the right the mast of the radar Furuno FR 1201, on the top and the meteorological station few meters lower (Image source: KOR, GKSS).

The monitored parameters are, the minimum, maximum and mean of wind velocity (m/s), wind direction (degrees), air pressure (hPa), light intensity, radiation, temperature (Celsius grad), humidity for a period of six seconds and every six seconds, the data are stored immediately.

4.1.2 Wind Data

The first query was the choice of the analysis period, the available row radar data are about for six years, 1999 till 2005, with gaps, so it was essential to define a criterion about the choice of the period. As long as the aim of the thesis is the investigation of the bathymetric changes during one storm by using radar measurements, it was obligatory to define the storm. It is important to be underlined here that the intensity of the backscattering depends on the wave conditions, which means that the wind as wave generation force is important; therefore the wind data are necessary for the present investigation to define enough long periods of strong wind.

To define the storm, two different wind data sets were used. The first one is from the meteorological station of the radar station and the second is from the Seewetteramt of Hamburg, taken at port of the List.

The weather station of the radar, already mentioned, records eighteen different values every six seconds. The format of each recording is a string like the following: A1111222233334444…18181818CR

Where A is the starting character and CR the Carriage Return and each number represents one digit of the monitored parameter.

Therefore, for the choice of the analysis period, it was necessary the development of a set of routines for the extraction of the useful data and the creation of one text file with the interesting parameters, wind velocity and direction, and the plot of the time series every 10 minutes the threshold of the wind velocity was 34knots, the estimated storm is 8 Beaufort (www.noaa.gov). The basic concept of the program is: the line by line reading of the data file the identification of the position of the A and CR; and according to them the selection of the desired parameters.

The second weather data set is from the Seewetteramt of Hamburg. The weather station is laying on Sylt, 55°00'48"N and 8°24'47"E, 10m above ground and 26 m over NN. In the data files, year, month, day, the wind direction in degrees and the 10-min

means of the wind velocity in nautical miles per hour, were recorded. In this case also, a commercial package for the data analysis was used to filter the values that are less than 34knots and visualize the results.

Table 4-1. Overview of wind events with available radar data. The first quarter of 2002 shows the highest number of events.

Year		2000	2001	2002	2003	2004	2005
Quarter of the year	1st		1	**3**		2	2
	2nd		1			1	
	3rd					1	
	4th	1	1	1	1		

The above analysis of different wind data sets had similar results, Appendix III. The number of the storms which satisfied the criterion of 34 knots is about thirty for the 6 years, but there were not available radar data for all of these storms. Hence the dates of the storm are compared with the dates of the available radar data (see section 4.1.3) and the result is presented at the table 4-1. The result of the above process is ten radar data sets during the storm surges. Finally, the storm at the end of February 2002, 20th to 28th, was chosen for several reasons. The specific storm was the longest and the wind velocity the highest, so the observation of full developed sea is possible, important for the measurements. In addition to that, the length of the storm was enough for the movement of the sediment, fact that permits the hope of obvious results.

4.1.3 Radar Data

During the storm surge from 20th to 28th of February 2002, sequences which consisted of 256 single images were acquired with a time interval of 1.8 s, which is equal to the antenna rotation time. Thus, the total sampling time was approximately 8 minutes. The polar images cover a radius of approximately half mile, were interpolated to a Cartesian grid with a cell size of 7m x 7m, corresponding to the spatial resolution of the radar. The number of pixels for one image is 288 x 288. The image sequence, presented here as an example (figure 4-5), was acquired on 22 February 2002 at 18.00, the exact specifications of the Cartesian grid of the nautical radar im-

age sequences are listed at the table 4-2. The antenna rotation time varies from sampling to sampling but lays near the 1.8s, the reason of the variance is the wind impact to the antenna.

For the complete approach of the subject, it is essential to mention the reasons that there are not available radar data during all the period of the six years, even though the radar was on function.

Table 4-2. Specification of the Cartesian grid of the nautical radar image sequences.

Number of pixel in x-direction (west-east) N_x	288
Cartesian-grid pixel resolution in x-direction (west-east) Δx	6.82m
Spatial length in x-direction (west-east) X	982m
Number of pixel in y-direction (south-north) N_y	288
Cartesian-grid pixel resolution in y-direction (south-north) Δy	6.82m
Spatial length in y-direction (south-north) Y	982m
Number of images per image sequence N_t	256
Temporal resolution (antenna-rotation time) Δt	1.8s
Temporal length of an image sequence T	460s

First of all, it is known and commonly accepted that the most difficult part of the marine sciences is the collection of the data, the rough and many times unforeseen circumstances influence or destroy the equipment, i.e. the lightning consists one of the most common factors of the radar destruction. A second reason is the huge storage capacity that it is necessary for the row radar data, every sampling needs about 90Mb and only lately the technology permits in small volume high storage capacity which is useful in the field. Also the archiving of all these terabytes of row data confronts several problems, mostly at the hardware; enough data were corrupted by hardware malfunctions.

The transformation of the coordinates of the radar data from polar to Cartesian was released by the use of an already developed software in PV-Wave, (SENET & SEEMANN 1999). The algorithm of the software is the Nearest Neighbor interpolation method. For each cell of the polar coordinates, the distance between the cell and the center of the image and the angle between the line which connects each cell with the

center and the y-axis are calculated, so for each cell there is a pair of coordinates, (distance, angle). By using the nearest neighbor algorithm all these pairs are matched to the Cartesian grid. All the images that are used in the thesis are oriented northward and the coordinates of the lower left corner is (3459945, 6102539) in GK. The reason that the coordinates are not presented at all the figures is that there is not this possibility at the software.

4.2 DiSC

In the current section is presented the main part of the methodology of the thesis. By using the commercial software DiSC, the radar data were analyzed. As it is shown at the flowchart (figure 4-4), this is the longest and sorest point of the analysis, the total processing time exceeds the 600 hours and the volume of the calculations is estimated about one terabyte. The DiSC, Dispersive Surface Classificator, is a recently developed algorithm (SENET 2004), which analyses image sequences for the determination of physical parameters on a local spatial scale, it consists a local analysis method, which allows the analysis of inhomogeneous image sequences of a dynamic and dispersive surface. The basic idea of the method is that in shallow waters wave fields become inhomogeneous due to spatially variable bathymetries. Local changes of the wave field, containing the local bathymetry information, therefore must be taken into account.

The DiSC is complicated and multi step method which was developed at the Radar Hydrography Department of the GKSS and now it is a commercial product by Vision 2 Technology GmbH, partner of the Geesthachter Innovations- und Technologie-Zentrum (GITZ).

The basic parts of the DiSC are the following:

- Transformation of the image sequence to the spectral domain by 3D FFT,
- Decomposition of the complex-valued image spectrum for the separation of the wave signal from the noise, by using filtering techniques
- Directional and dispersion separation of the complex-valued spectrum into spectral bins at 2D wavenumber planes of constant frequency,

- 2D inverse Fast Fourier Transformation (2D FFT^{-1}) of the spectral bins, yielding complex-valued, one-component spatial maps in the spatio-frequency domain,
- Calculation of spatial maps of local wavenumbers from the one-component images of constant frequency,
- Composition of the one-component local wavenumber maps of constant frequency to local 3D spectra and
- Use of the spatial maps of local wave number vectors and power for the calculation of spatial hydrographic-parameter maps.

The exertion of the DiSC that is presented at the section 4.2 follows the sequence of the software that includes in some cases two steps of the above process.

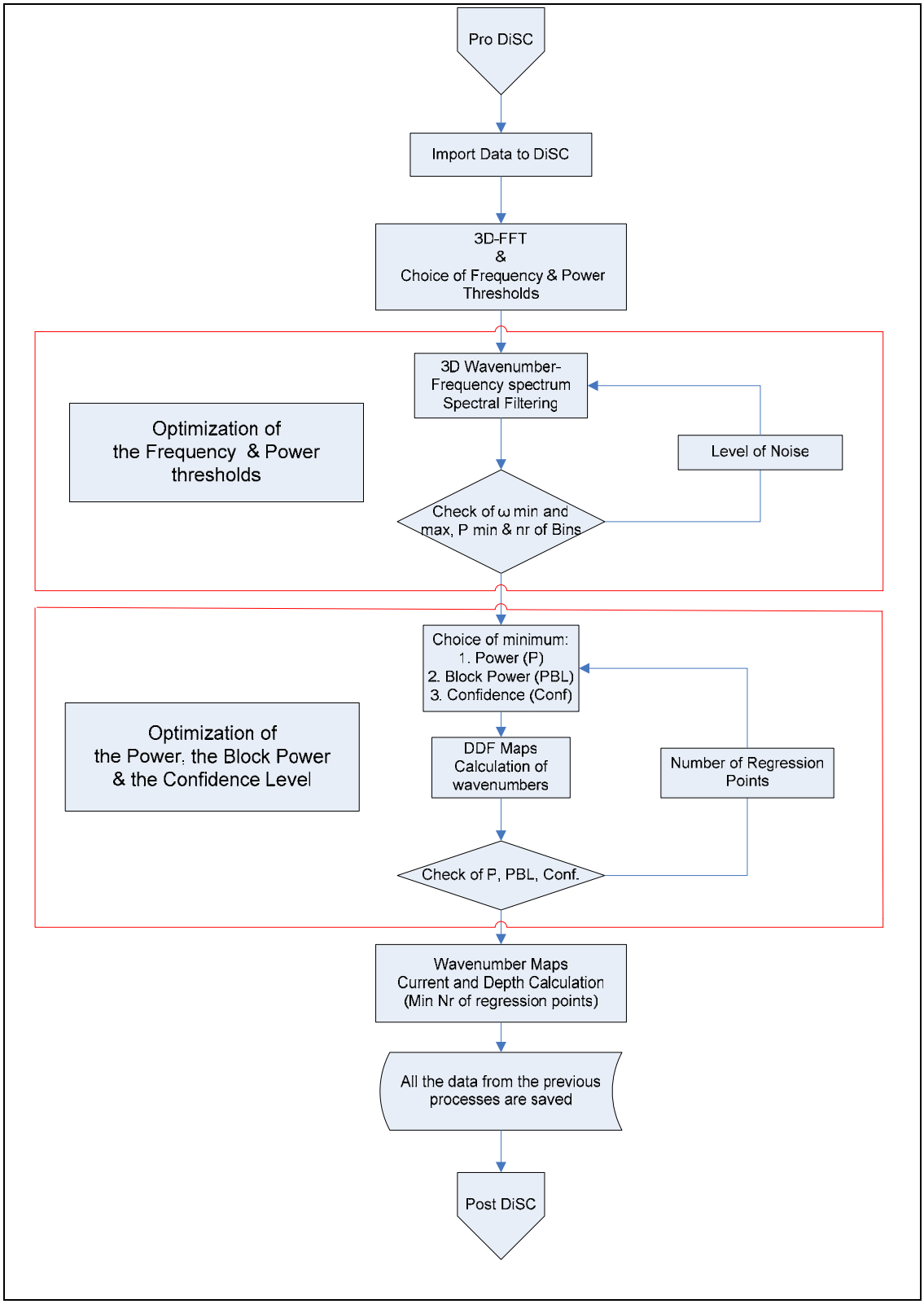

Figure 4-4. Flow chart of the DiSC processing. The first steps are the import of the data in the software and the calculation of the 3D-FFT. The next step is the choice of Frequencies bins and the inverse 2D-FFT, the third step is the choice of the regression for the calculation of the local wavenumbers and their calculation and the last step is the calculation of the area depth.

4.2.1 Assumptions of DiSC

The use of DiSC has two basic assumptions, stationarity and validity of the multi-component AM-FM image model, (SENET et al. 2003).

Stationarity: The imaged process analyzed by DiSC has to be stationary. Stationarity implies the temporal invariance of a signal. Assuming stationarity, DiSC can treat the spatial Fourier decomposition of the distinct frequency components independently, with the complex-valued spatial image at a constant frequency,

Validity of the multi-component AM-FM image model: For inhomogeneous images the amplitudes or the spatial phase gradients (i.e. the local-wavenumber vectors) vary. This information is only implicitly included in the coefficients of the Fourier decomposition. To enable explicit analysis, the spatial Fourier decomposition is transformed to an image representation, composed of a superposition of 2D jointly amplitude-frequency-modulated, locally coherent, analytic signals, multi-component AM-FM image model.

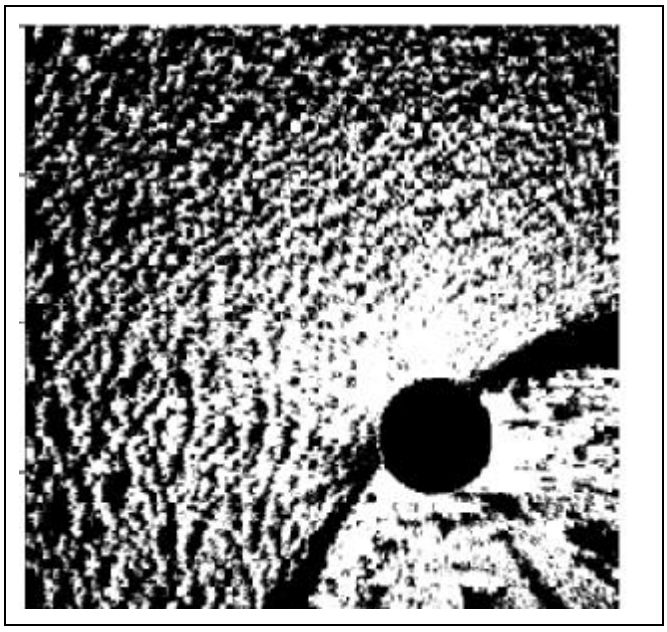

Figure 4-5. One of the 256 individual radar images, the acquisition time of each of these images is 1,8 s (see table 4-2). The coordinates of the lower left corner is (3459945, 6102539) in GK, the image covers an area of 982x982 m^2 and it is oriented towards north and east. In the lower part a clear wave crest is visible. It is mainly in that part where DiSC results are reliable.

4.2.2 Input parameters

The input data set of the DiSC is the 3D image sequence that has to be analyzed, each of the radar image sequence, has three dimensions, the x (easting), the y (northing) and the time t (as number of images), these information are imported at the beginning of the process to the DiSC. In addition to them, the number of pixels at x- and y-axis, the real size of each pixel and the rotation period of the antenna are imported (Appendix IV). An example nautical radar image of a sequence is given in figure 4-5.

During the process, the user has to define, from the sequence of the calculated spectrum, the anchor positions for the spectral filter bank in the 3D spectrum domain, which is used for the spectral separation. The demanded parameters are the minimum and maximum bin, the power where these bins are minimum and maximum and the number of bins. For the calculation of the wavenumbers are necessary the spatial parameters, power, block power, confidence limits and also the size of the cell, more analytical presentation in the next section. The processed image sequences and the parameter are tabulated at the Appendix V.

4.2.3 The algorithm and the exertion of DiSC

The next step of the analysis is the core of the DiSC algorithm. Till the development of the theory and the software of DiSC the common method was the global analysis which is based on spectral filtering and the analysis of the real-valued 3D gray-variance spectra. The spectral phase, which contains information on the local image structure (OPPENHEIM and LIM 1981), was not used. The DiSC, for the determination of the physical parameters on a local spatial scale, recovers the spatial structure of the image sequence from the complex-valued 3D spectrum, which calculated in the previous step. The main idea of the local-analysis method is the decomposition of the complex-valued 3D image spectrum, followed by a 2D FFT^{-1} into the spatio-frequency domain. The basic parts of the method includes algorithm steps described briefly and without mathematical explanations in the succeeding sections.

4.2.3.1 3D Fast Fourier Transformation

The first step is the transformation of the data. A discrete 3D Fourier Transformation, 3D FFT, can be obtained by the decomposition into 1D FFTs. A 3D FFT using the world and spectral coordinates and the result of this process is a discrete complex-valued image spectrum of the 3D domain. The discrete grid resolution of the 3D spectrum is calculated the spatio-temporal extension of the initial image sequence. More details about the above technique at (SENET 2004). By the 3D-FFT, the initial dimensions (x, y, t) are transformed to (k_x, k_y, ω), the result of the x-dimension is the x-component of the global wavenumber, of the y-dimension is the x-component of the global wavenumber and of the time t is the frequency. By the result of the process, the choice of the power of the backscatter and the minimum and maximum bin, where the energy lays, take place. These parameters are imported for the next step of the analysis, an example at the figure 4-6.

4.2.3.2 Spectral decomposition and the inverse 2D FFT

The next step is the spectral decomposition of the spectral signal of the inhomogeneous wave field. The aim of this step is the division of the signal into one-component images containing seperated and therefore analyzable parts of the wave field. A spectral representation is illustrated in a k_x-k_y wavenumber section.

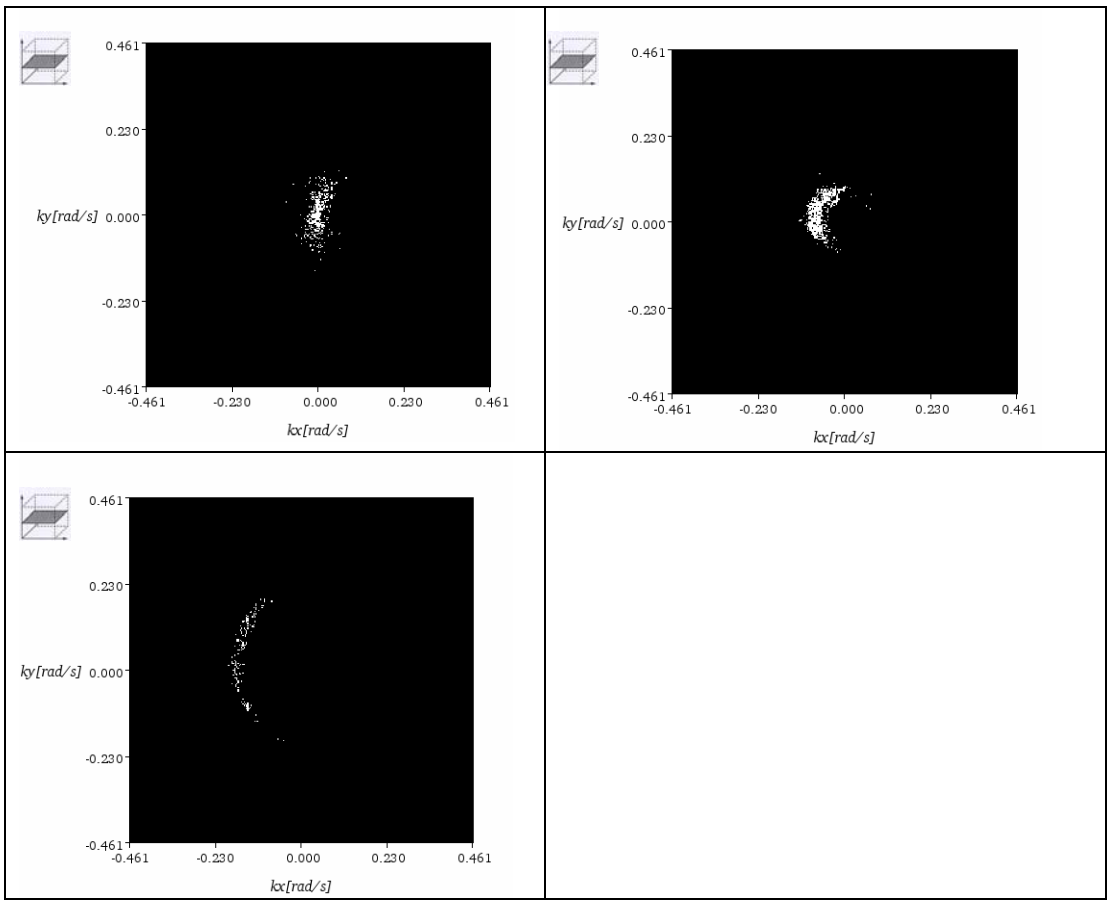

Figure 4-6. Examples of the wavenumber planes at different frequencies from 21st f February at 05.00. The white points show the locations where wave power could be detected within the "global" spectrum. Upper left: ω slide 10, upper right: ω slide 52, lower : ω slide 82.

The spectral decomposition technique is called Directional Dispersion Frequency-Separation and it is based on the combination of the directional wedge filter with the dispersion-shell filter and the frequency separation, yielding a spectral DDF bin. The result of filtering is the separation of the wave field into the different waves components and at the end the reversing of them. The principle of DDF-S is outlined in figure 4-7.

The spectral decomposition and inverse 2D FFT (called MapDF) yields complex-valued spatial one-component images. These complex-valued one-component images are illustrated as power and phase of a separated part of the wave field. Power and phase are shown in figure 5-4.

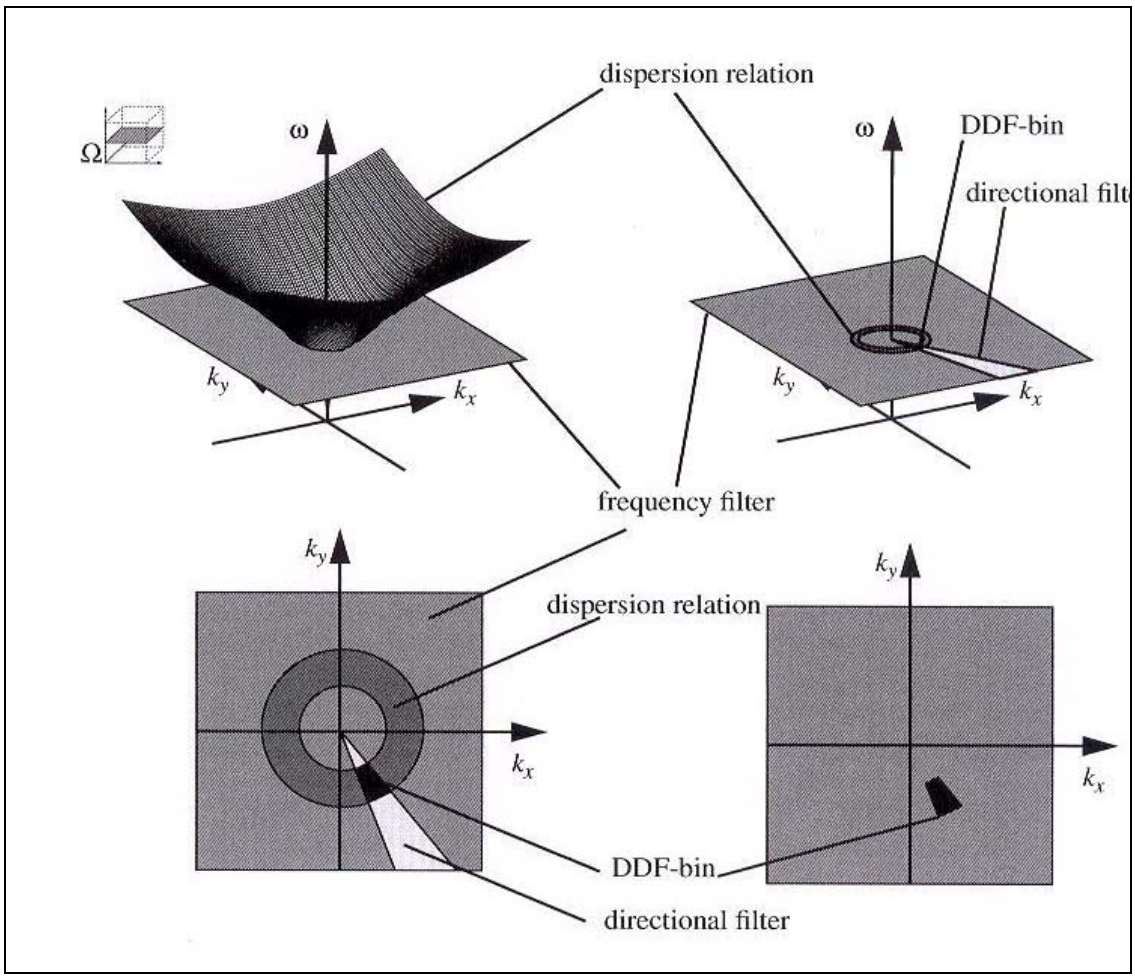

Figure 4-7. These four graphs illustrate the basic concept of the spectral decomposition by filtering and explain the Direction-Dispersive Frequency bin (DDF-bin). Top left: The orientation of the wavenumber by plane with the 3D spectrum. Top right: Definition of the directional bin. Bottom left: Intersected lines of the outer and the inner dispersive shell with the individual plane. The outer and inner dispersion include the wave power from the entire observation area. Bottom right: The DDF bin, which will be defined to cut out the spectrum if significant power could be defined.

4.2.3.3 Calculation of local wavenumbers

In the fourth step, the spatial maps of local-wavenumber vectors from the phase of the complex-valued one-component images are determined, the local-wavenumber estimation method developed by (HAVLICEK et al 1996). For the calculation of the wave numbers, it is necessary to be defined by the user, the number of the pixels that every grid cell take account into the calculation (block size x and y) and three spatial interpolation parameters, the global power, the power of each block and the confi-

dence limit. These three parameters are binominal thresholds which permit or not the use of one frequency for each cell for the calculation of the local wavenumbers. Each of these parameters may be selected optically and checked after the end of the specific step, see section 5.1 where is examined their significance during the optimization analysis. Each of them influence the number of the regression coordinates at the calculation of hydrographic parameter maps, the result is the exclusion of areas where the normal dispersion is not applicable. At the figures 5-6, is shown the control of the spatial parameters.

4.2.3.4 Calculation of hydrographic parameter maps

The final step at the use of the DiSC software is the calculation of the hydrographic parameter maps, this part is absolutely automated and the user does not interfere in the software. This part of the analysis lasts about 40 minutes per data set.
The core of the method has been described at the chapter 3, where is presented the dependency of the dispersion relation on the near currents and the water depth. In the variance spectrum, the linear portion of signal energy of the waves is localized on the dispersion shell of surface waves. Therefore the pilling up, the instant depth, of the water mass could be calculated for each grid cell. The only parameter that has to be defined is the minimum number of the regression coordinates that is by default 10.
The results of DiSC are bathymetry, figure 5-5 and current-vector maps, which are out of the scope of the thesis. (In the given case DiSC has been calculated on boxes of 6 pixel x 6 pixel. Each of these boxes contains one water depth value and on current vector).

4.3 Post – DiSC

At this section, is presented the after DiSC processing. The post-DiSC processing is illustrated at the figure 4-8. The first step was the optimization of the reliability of the results according to the number of the regression coordinates, see section 5.1. The second step is the identification of the tidal cycle from the calculated sea level; the next step is the averaging of each of the periods of analysis for the amelioration of the accuracy of the results. The fourth step is the calculation of the difference be-

tween the beginning and the end of the storm, the final step is the visualization of the results.

4.3.1 Export of data

The final result of the DiSC software is a text file, in which are stored the coordinates of every cell for which has been calculated the instantaneous water depth, the number of the regression coordinates, the calculated depth and the current vector. For the further processing of the data, it was necessary to export the data and to create a new file which includes all the results. For this reason, a program in the PV-Wave has been developed, Appendix VI. The program is consisted by 6 subroutines, the basic concept is that the complete grid of the area of analysis is created, the coordinates of the grid are compared with the coordinates of each of the results and the output is one file where are stored the results at the whole grid. For the cells that has not been calculated any depth, an extreme value is matched.

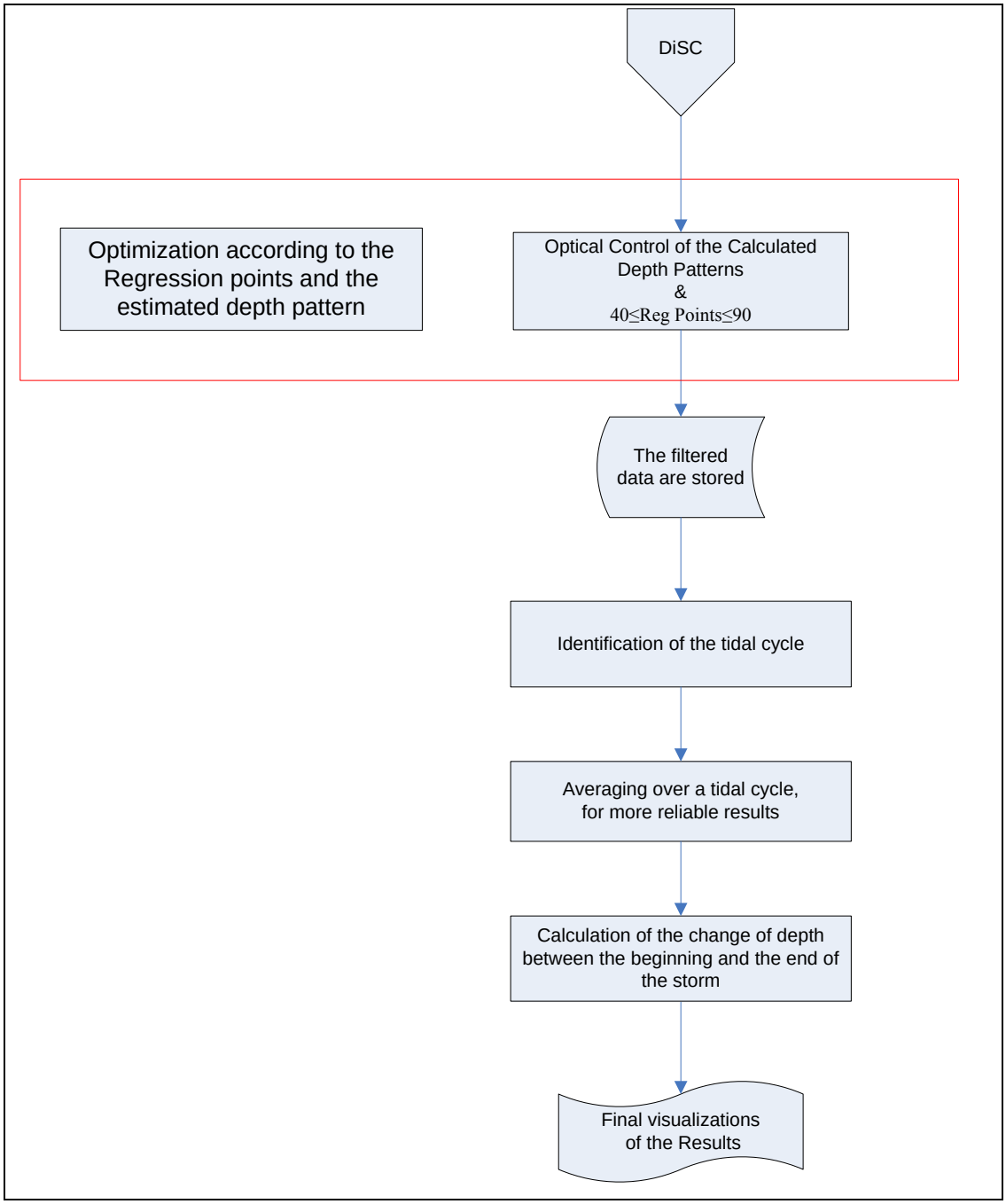

Figure 4-8. Flow chart of the Post-DiSC processing. The first step was the optimization of the reliability of the results according to the number of the regression coordinates. The second step is the identification of the tidal cycle from the calculated sea level, the next step is the averaging of each of the periods of analysis for the amelioration of the accuracy of the results. The fourth step is the calculation of the difference between the beginning and the end of the storm, the final step is the visualization of the results.

The structure of the program permits to the user to define the check of the number of coordinates and to export any of the calculated variables, number of regression coordinates depth or current vectors. The calculation time for a grid of 2304 cells and for 60 files is approximately 4 minutes. The advantages of the process are the grouping of the results according to the requirements of the user and the easy manipulation of the results by using any commercial program, for data analysis, e.g. Microsoft Excel, Golden Software Surfer.

4.3.2 Identification of the tidal signal

The identification of the tidal cycle consist a common (BELL 1999), (ROBINSON et al 2000) way to control the whole series of the image sequence analysis and the comparison with gauge measurements consist strong evidence about the reliability of the results. In this case, for the estimation of the tidal cycle were averaged the calculated sea levels of 9 neighboring cells around the point (3460230.85 m, 6103070.81 m), which cover an area of 3800m^2, and they have been plotted for the twelve hours of each period of analysis, see chapter 6.

4.3.3 Calculation of the difference between two grids

In the current paragraph, is describing the methodology for the calculation of the difference between the beginning and the end of the storm.

For the determination of the volume are used four methods: the rule of Parallelogram, the rule the Extended Trapezoidal Rule, the Extended Simpson's Rule and the Extended Simpson's 3/8 Rule. The reason for this is that the difference in the volume calculations by the four different methods estimates the accuracy of the volume calculations. If the four volume calculations are reasonably close together, the true volume is close to these values. The net volume can be reported as the average of the three values.

Mathematically, the volume under a function $f(x,y)$ is defined by the double integral

$$Vol = \int_{x_{\min}}^{x_{\max}} \int_{y_{\min}}^{y_{\max}} f(x,y)dxdy \quad 4.1)$$

Numerically, this is computed by first integrating over x (x-coordinate) to get the areas under the individual rows, and then integrating over y (y-coordinate) to get the final volume (PRESS et al. 1988). In the next paragraphs are some details about the four methods.

4.3.3.1 Rule of Parallelogram

This is the easiest way to calculate the volume between two surfaces. Each cell of the initial grid is subtracted by the same cell of the final grid and the result is multiplied by the area of the cell.

4.3.3.2 Extended Trapezoidal Rule

The pattern of the coefficients is {1,2,2,2,...,2,2,1}:

$$A_i = \frac{\Delta x}{2}(G_{i,1} + 2G_{i,2} + 2G_{i,3} + \ldots + 2G_{i,n-1} + G_{i,n})$$
$$Volume \approx \frac{\Delta y}{2}(A_1 + 2A_2 + 2A_3 + \ldots + 2A_{n-1} + A_n \quad (4.2)$$

Where Δx is the grid column spacing, Δy is the grid row spacing and $G_{i,j}$ is the grid node value in row *i* and column *j*.

4.3.3.3 Extended Simpson's Rule

The pattern of the coefficients is {1,4,2,4,2,4,2,...,4,2,1}:

$$A_i = \frac{\Delta x}{3}(G_{i,1} + 4G_{i,2} + 2G_{i,3} + 4G_{i,4} + \ldots + 2G_{i,n-1} + G_{i,n})$$
$$Volume \approx \frac{\Delta y}{3}(A_1 + 4A_2 + 2A_3 + 4A_3 + \ldots + 2A_{n-1} + A_n \quad (4.3)$$

where Δx is the grid column spacing, Δy is the grid row spacing and $G_{i,j}$ is the grid node value in row *i* and column *j*.

4.3.3.4 Extended Simpson's 3/8 Rule

The pattern of the coefficients is {1,3,3,2,3,3,2,...,3,3,2,1}:

$$A_i = \frac{3\Delta x}{8}(G_{i,1} + 3G_{i,2} + 3G_{i,3} + 2G_{i,4} + \ldots + 2G_{i,n-1} + G_{i,n})$$
$$Volume \approx \frac{3\Delta y}{8}(A_1 + 3A_2 + 3A_3 + 2A_3 + \ldots + 2A_{n-1} + A_n \quad (4.4)$$

where Δx is the grid column spacing, Δy is the grid row spacing and $G_{i,j}$ is the grid node value in row *i* and column *j*.

Volume results are provided in cubic meters based on the units of the input grid file.

4.3.4 Creation of Maps

The visualization of the results consist the final product of the thesis. The created maps are the mean depth of each point for the twelve hours, one tidal cycle, of the beginning and the end of the storm. The assumption of averaging over one tidal cycle is that the mean value of the depth is constant. Hence the number of the values referred to each grid cell varies between none and twelve, the mean and the standard deviation for each cell have been calculated. The criteria for the use of the calculated mean value were the number of the available data for each cell and the value of the standard deviation should not exceed the 1.5 m. To be possible the comparison between the two periods at the end used only the common cells that there was available depth.

The grid size of the maps is the same with the grid size of the DiSC result, so it is the highest possible resolution and the number of the cells is 46×46. Several methods of interpolation are tested for basis function, linear interpolation, inverse distance, nearest neighbor. The main problem to be confronted was the open boundaries; the tests confirmed the theory (KENNEDY & KOPP 2000) that for this case the appropriate interpolation method is the triangulation.

The final result, see chapter 6, is consisted by the overlay of two different maps, direct visualization and contour map of the calculated depth. The reason of the direct visualization is the avoidance of the distortions due to the interpolation method, common problem of the remote sensing.

The contour map is a two-dimensional representation of three-dimensional data. The first two dimensions are the x and y coordinates, and the third dimension, depth, is represented by lines of equal value. The relative spacing of the contour lines indicates the relative slope of the surface. The area between two contour lines contains only grid nodes having depth values within the limits defined by the two enclosing contours. The difference between two contour lines is defined as the contour interval.

The combination of the two above representations permits at the same time the visualization of the real values and the compact information of the contours about the gradient and makes the comparison of the two periods easier.

5 Optimization

The current chapter presents the influence of each of the parameters of the DiSC to the final result. One aim of the thesis is the investigation of the operational use of this specific method, it is obliged to be determined those parameter and parameter values which minimize the predefined objective function (WAREWEN et al 1999). The DiSC method and the input parameters are presented at the previous chapter; at this one are presented and discussed the effects of the parameters. Therefore, the Chapter 5 is separated into 2 sections, according to the steps of DiSC. The main result, of the optimization process is the development of DiSC new version.

5.1 Calculation of MapDF

The 3D Fast Fourier Transformation transferred the image sequence from the spatial and temporal domain to the energy domain $G(x, y, t) \rightarrow \hat{G}(k_x, k_y, \omega)$. For the calculation of the MapDF, the spectral decomposition and the inverse 2D FFT, have to be defined, the power and the minimum and maximum of the frequency bins that this power lay. These parameters are the anchors for the filtering.

For this reason, the DiSC software provides visualizations of each bin, figure 4-6, as vertical intersections of the k_x, k_y plane with the frequency axis. The dispersion is not planoconvex, as it is visualized usually, but it has volume. Therefore, the user defined interactively the power level and after the minimum and maximum of the bins. As it is expected from the theory, see chapter 3, at the low frequencies, the real signal is not distinguished from the noise, at the intermediate frequencies, there is a distinct signal and at the high frequency bins, the power tends to zero.

The main difficulty at this step is the choice of the frequency bandwidth. For the choice of the $\omega_{\min}$ and $\omega_{\max}$, the user has to consider initially that the long waves are mainly influenced by the bottom that means those waves which belong at the low frequencies. From the other side, at the low frequencies the signal that has the information is full of noise and nonlinear effects as produced by wave grouping (SMITH et al 1996). In addition to that the same scientists show by their experiments and as it is proved by the wave theory, when the $\lambda \gg 20d$, low frequencies, the dispersion

relation does not model the waves, figure 5-1. The third important point is that at the high frequencies, there is an essential influence by the currents, which the DiSC takes account.

Table 5-1. Validity of the Dispersion Relation, the DiSC is used only for the transient water.

Deep Water	$\omega = \sqrt{gk}$	Non-Dispersive
Transient Water	$\omega = \pm\sqrt{gk\tanh(kd)}$	Dispersive
Shallow Water	$\omega = k\sqrt{gd}$	Non-Dispersive

Running the above analysis it became clear that by the empirical choice of the $\omega_{\min}$ and $\omega_{\max}$ (figure 5-1), the results were not reliable and the variance of the calculated depths for the same data in some cases was more than 35m, when the real maximum depth of the area is approximately 10m. So a new module had to be added at the DiSC, with which, the impact of the parameters became visible.

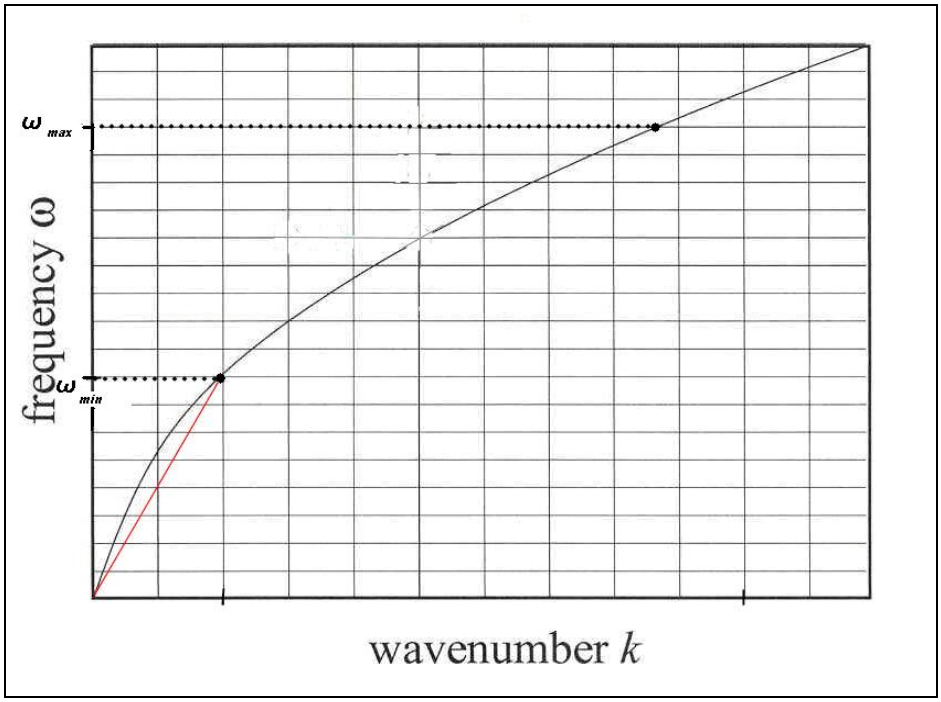

Figure 5-1. The bandwidth of the frequency in which the DiSC may be applied.

The new module, *Check MapDF*, visualizes the centers of the filters and it shows the area where the power values are high enough to be taken account into the inverse

2D-FFT, figure 5-2. The investigation by the *Check MapDF*, revealed the importance of the correct choice of those parameters. The main question that occurred from the results was the existence of grid cells that the calculated depth was at different scale from the adjacent cells, so by using the *Check MapDF* and having visualized the anchors of the filtering, the reason became understandable. During the spectral decomposition and the inverse 2D FFT, was taken account low frequencies which have no or little wave induced power.

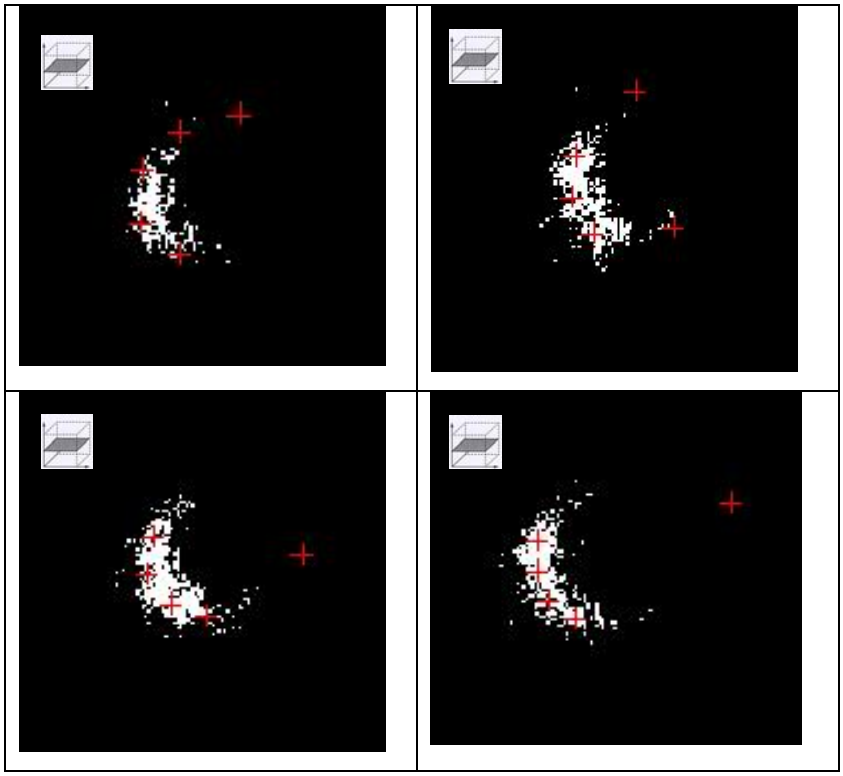

Figure 5-2. Four wavenumber planes cutting at different frequencies the global spectrum. The red crosses give the local solution achieved by the inverting technique. The crosses out of the area of power are erroneous results due to not dispersion waves at low frequencies, that could not be isolated by the DiSC algorithm so far. The axis of the figure are k_x-ky (21st of February 2002, at 02:00).

Therefore, the achievement, by following the sequence of the frequency slices and increasing the ω_{min} is that the final results are ameliorated, figure 5-3, the ω_{min} at the 1st is 33, at the 2nd is 37, at the 3rd is 38 and at the 4th is 44, clockwise. It could be increased more, but at this case, real information is lost. The choice of the ω_{min} should be in such way, to keep the equilibrium between the excluded frequencies and

the useful information; this part is still subjective and depends on the experience of the analyst.

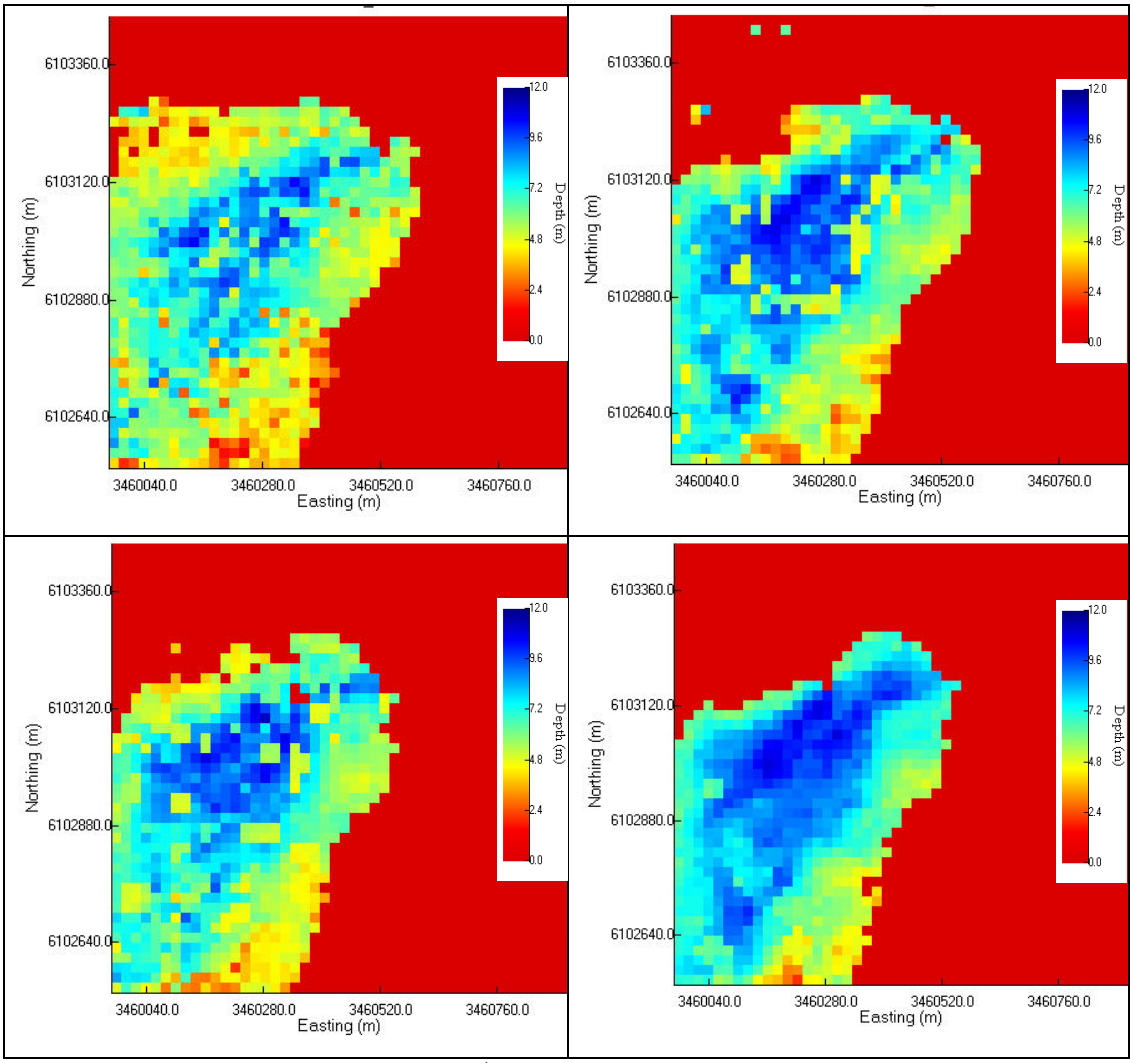

Figure 5-3. Four maps of the depth (21st of February 2002, at 02:00) as they have been calculated by the DiSC. Upper left: The best result of the old version of DiSC, upper right and lower left: Intermediate results and lower right: The best result with the new version of the DiSC, where the pattern of the depth is uniform and similar with the nautical maps.

5.2 Calculation of Local Wavenumbers

For the calculation of the local wavenumbers, it is obligatory to define the block size x and y and three spatial interpolation parameters, the global power, the power of each block and the confidence limit.

In this thesis, the block size is kept constant and has been defined according to the spatial resolution of the radar. Thus the optimization of this step is concerning the interpolation parameters. The choice of those parameters is interactive by visual con-

trol. The power is the main steering parameter into the algorithm, and influences the other two. So firstly, the power is optimized, secondly the block power and at last the confidence.

The result of the inverse 2 Dimensional Fast Fourrier Transformation is spatial visualizations of the wave components, magnitude and phase, which have been extracted during the previous steps, for each frequency; the threshold level of the power that has to be chosen by increasing the magnitude in such way that there are not crossings of the local wavelengths in each frequency, figure 5-4.

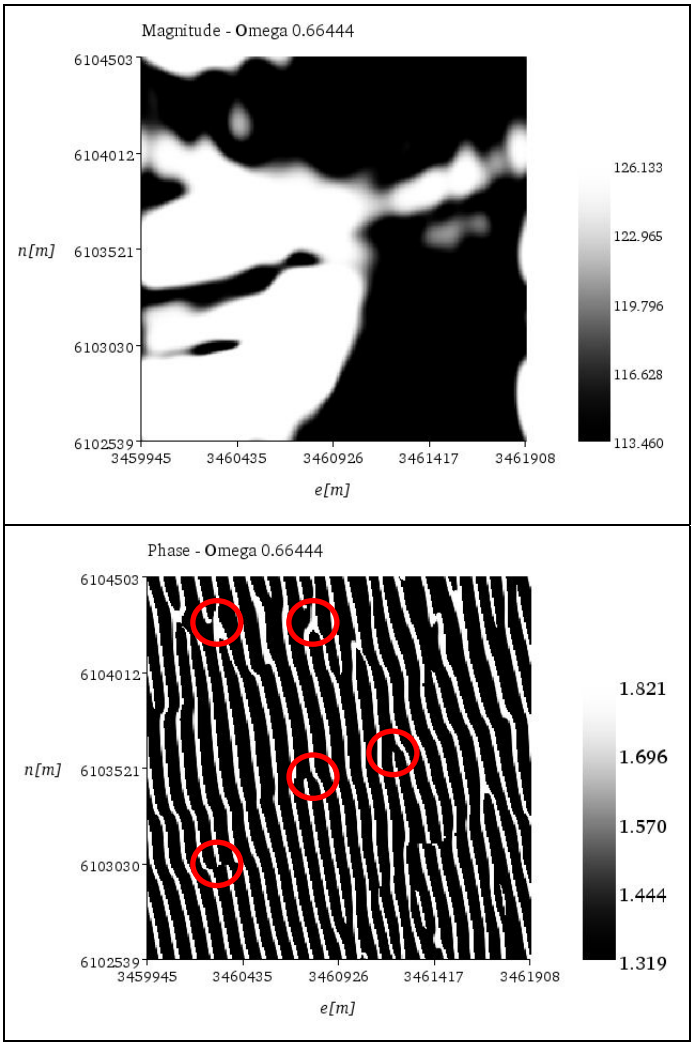

Figure 5-4. The magnitude and the phase at the 0.66444 frequency. The scale of the magnitude laying between 113.4 and 126.1 and it has been arranged such a way that there are no forkings at the phase visualization (red circles). The dataset is from 27th of February 2002 at 12.00.

At the example, it is shown the magnitude and the phase of the 0.66444 frequency. The scale of the magnitude varying between 113.4 and 126.1 and it has been arranged such a way that there are no forkings at the phase visualization.

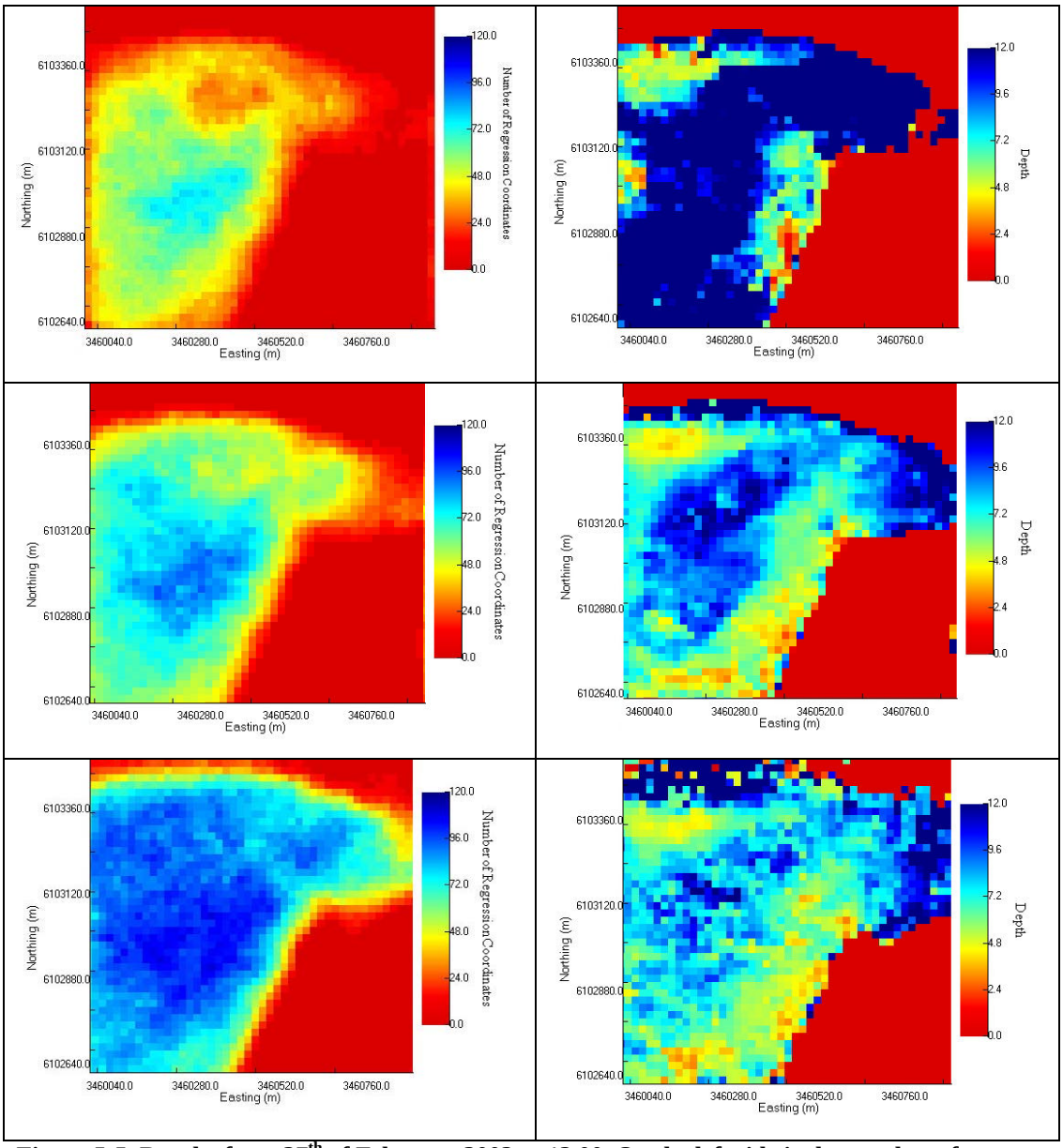

Figure 5-5. Results from 27th of February 2002 at 12.00. On the left side is the number of regression coordinates (red is 0 and blue is 120) and on the right side is the estimated depth (red is 0 m and blue is 12 m depth). First row: the low number (40) of regression coordinates overestimates the depth. Second row: the number of the regression coordinates is about 70 and the pattern of the depth is uniform. Third row: the high number of the regression coordinates (120) underestimates the depth.

Within the first version of the DiSC software, there were not any check module about those three parameters, hence the choice was subjective and was depending on the experience of the user and on the replicates of the analysis. Therefore from the first part of the analysis, the result was the definition of the minimum and maximum power in combination with the fact that the number of the regression coordinates should be “more than 30 and not too high”, personal contact with (SEEMANN), and comparison with the nautical maps. The figure 5-5 shows that the high number (about 120) of the regression coordinates underestimate the depth, the opposite effect was the low number (50) of the regression coordinates. The optimal number of regression coordinates varies around 70 and the pattern of the depth is uniform. The reason of this is an open question but the observation of this is one more of the achievements of the thesis. The other two parameters could be checked at the end of the local wavenumbers calculation.

Thus at the process is described above, the evaluation of the parameters was influenced by the analyst. For this reason a set of modules for the control of the parameters was developed.

Therefore, at the new version of the DiSC software, the evaluation of the parameters is taking place by visualizing the three parameters at the spatial domain where they effect, figure 5-6.

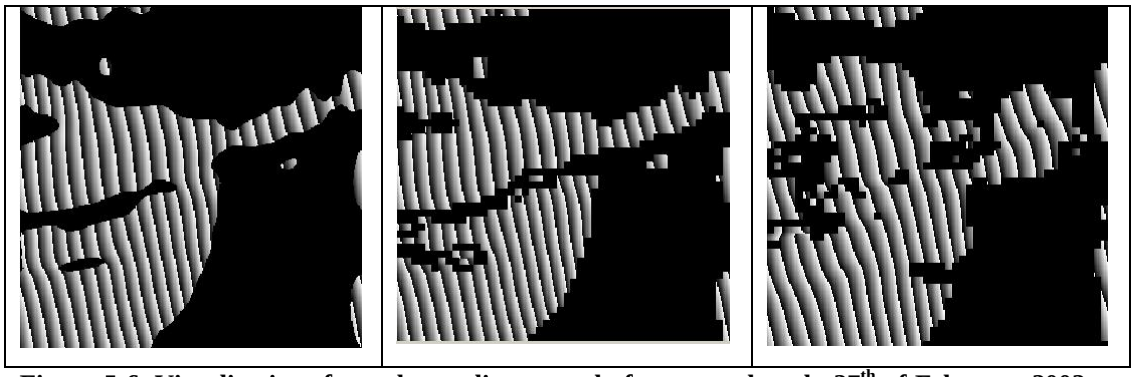

Figure 5-6. Visualizations from the quality control of one wavelength, 27th of February 2002 at 12.00. Left: Visualization of the wavelength according to the defined power threshold, center: Visualization of the wavelength according to the defined block power threshold, right: Visualization of the wavelength according to the defined confidence threshold. At the black areas has not calculated any wavelength as the threshold is high enough. The pattern of the wavelength has no forking, which is proved that the threshold is the correct to exclude the non-linear effects. The wave patterns on the top and on the left of the visualizations are artifacts by the filtering. The x-coordinate is form west to south and the y-coordinate from south to north.

The last step of the optimization is for the Block Power and the Confidence level, for both of them several datasets were processed with different parameters, their effect is not essential and only in extreme values, it was obvious their influence. The optimization of the parameters for the calculation of the local wavenumbers proved that the significant one is the global power and the other two are trivial or at least they are important in case of validation of the result.

6 Results

The analysis described at the previous chapters has been used to process 2 periods of 12 hours, during the storm of February 2002, see section 4.1. The area of common results covers 385353 m^2.

An interesting result is the tidal cycle, the twelve hours permits the investigation of the tidal cycle. At the figure 6-1, the red line represents the 10 min average per hour of the time series of water level in Westerland, closest gauge, shifted by 1 h lag due to distance, 20th and 21st of February 2002. The gauge measurements are used to show the general trend of the water level, during the same period. The blue line represents the mean sea water level of an area, 3800m^2, around the point, GK coordinates (3460230.85 m, 6103070.81 m).

According to the tide calendar, (BUNDESAMT FUER SEESCHIFFAHRT UND HYDORGRAPHIE 2002) the high water is at 18:00, the low water at 23:00 and again at 5:00 there is high water, the floods patterns are obvious also by the DiSC results. The ebb is not obvious and seems that the slack water last for 6 h, this result could be explained as the result of the wind influence on the water mass.

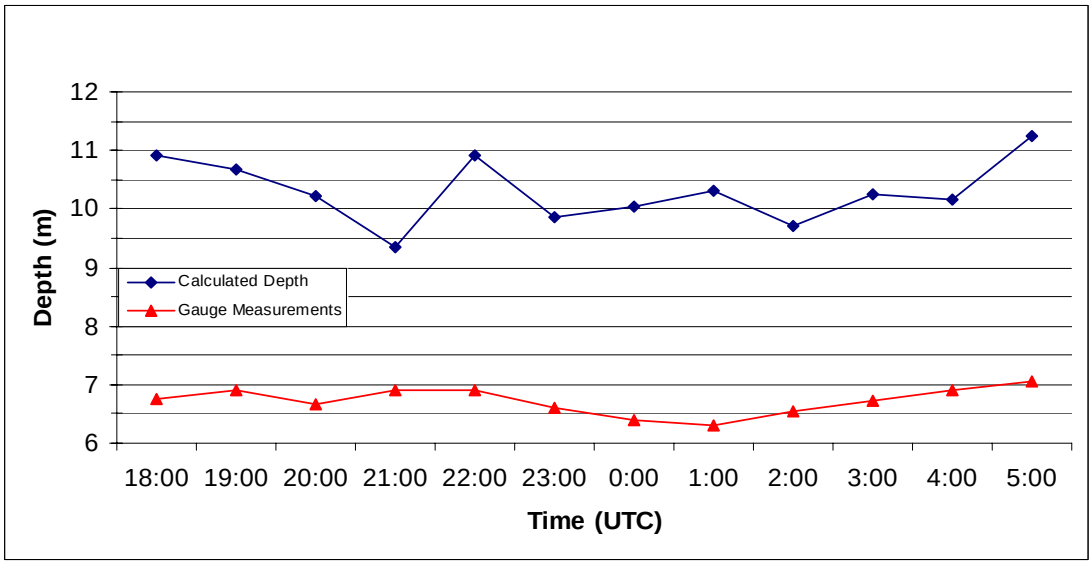

Figure 6-1. Graph of the tidal cycle, the blue line is the estimated tidal cycle by the DiSC results and the red line is the tidal cycle as measured by a gauge in Westerland.

The extreme value from the DiSC at 22.00 is an open question, which cannot be explained by the nature or even from the DiSC algorithm. The results are similar for the

rest of the area of research and most of the cases the influence of the morphology of the seabed is obvious.

For both periods, the time series of the calculated depths for each cell has been averaged; hence there is one mean depth map in the beginning and one mean depth map in the ending phase of the storm. The figures 6-2 and 6-3 present the results of the depth calculation.

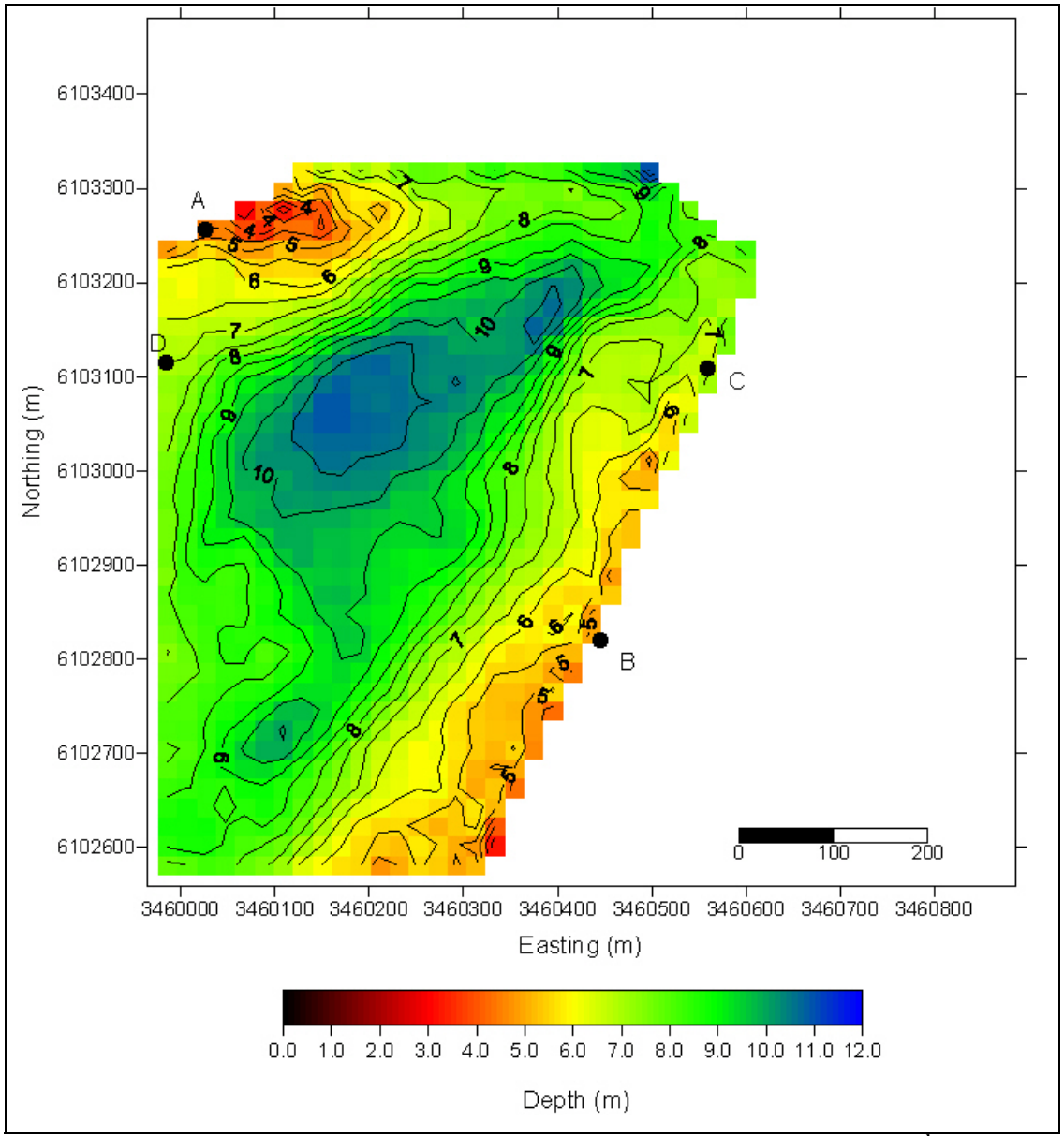

Figure 6-2. Depth of the area of investigation during the beginning of the storm, 20th of February 2002, as result of averaging the calculated depths for 12 hours.

Depth contours are given at 1 m intervals (see section 4.3.4). The deeper transverse channel in the centre of the image is thought to be a real feature that is shown also at the nautical maps. The results per hour are given at the Appendix VIII and IX.

Both of the two results illustrate the mean depth for the twelve hours of the analysis. They do not have a common reference so the direct comparison is not possible. A general and not so accurate method is to transfer them to the same reference level is by using the measurements from the tide gauge.

The difference of the average sea level between the 2 periods is approximately 0.4 m, at the beginning of the storm the sea level is higher 0.4 m than at the ending phase of the storm, Appendix X. Therefore, the assumption is that the 0.4 difference transfer them at a common reference level.

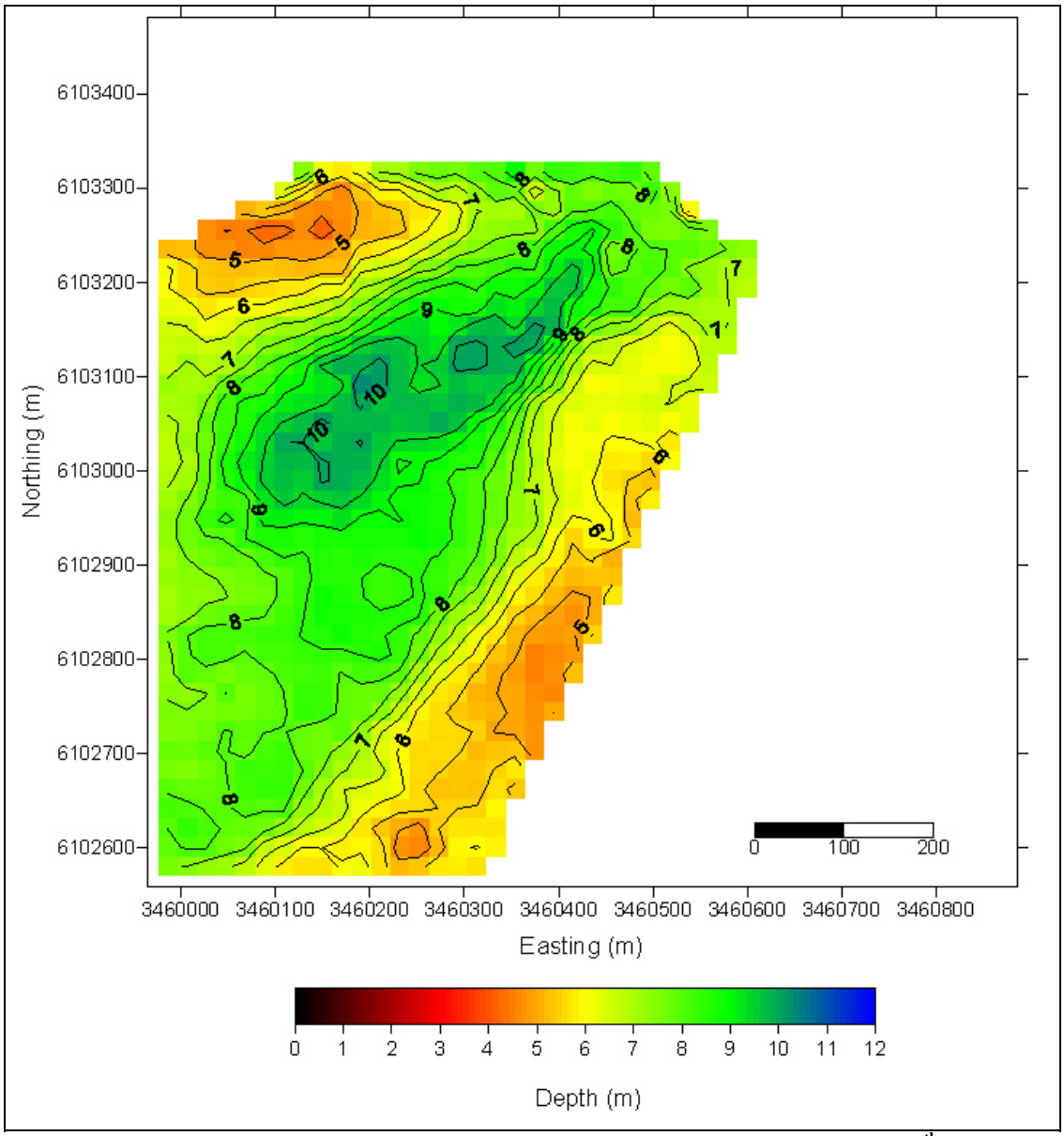

Figure 6-3. Depth of the area of investigation during the final phase of the storm, 28th of February 2002, as result of averaging the calculated depths for 12 hours.

The difference of the bathymetry between the two periods, having common reference level, is illustrated in figure 6-5, shows that at the beginning of the storm, the channel is estimated 0.5 m deeper (maximum depth appproximately 11 m) than at the end of the storm (maximum depth approximately 10 m). At the first period the spatial pattern of the depth seems to be uniform and well formed. At the second period, the influence of the storm is obvious and there is accumulation of sediment almost everywhere.

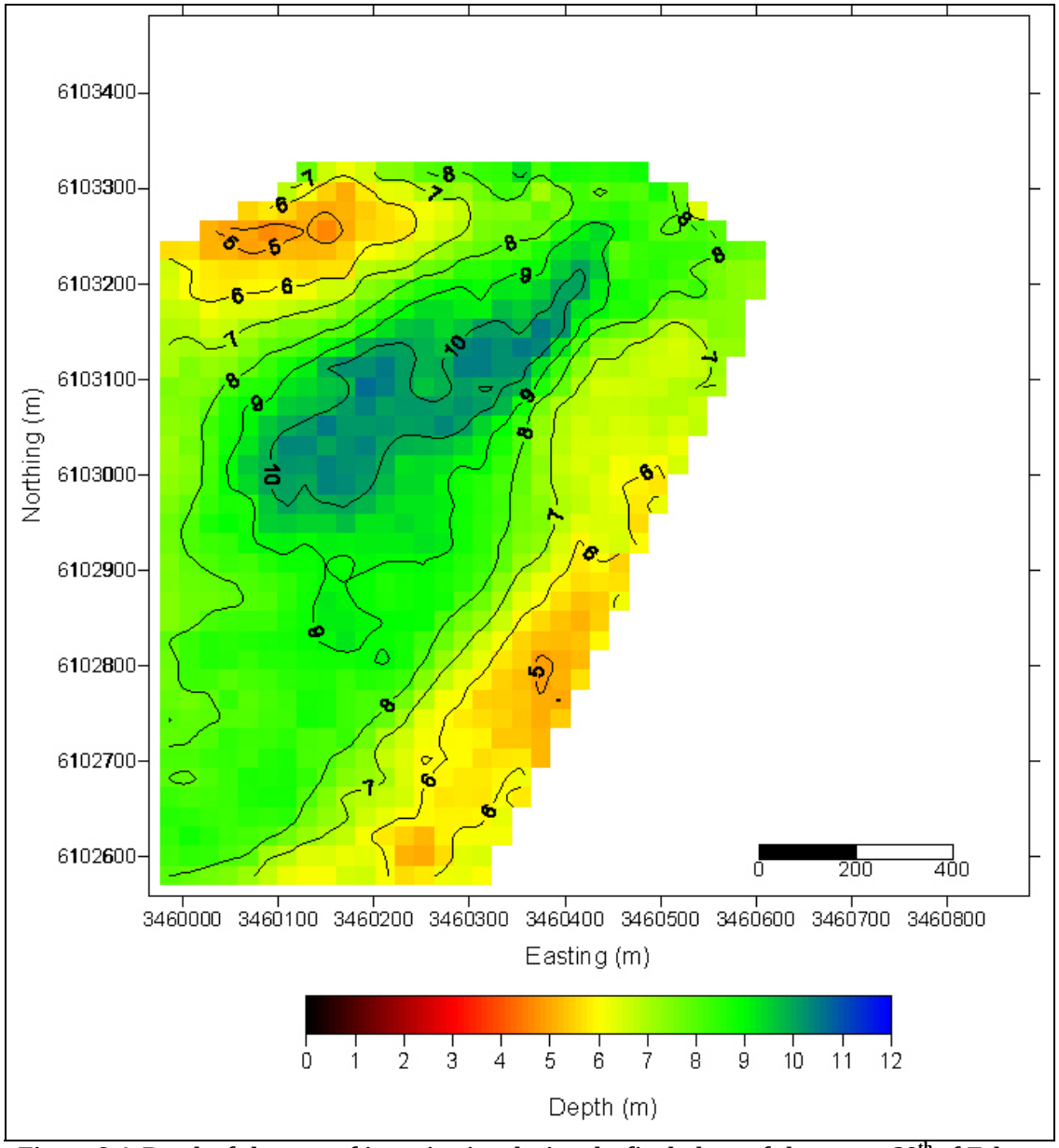

Figure 6-4. Depth of the area of investigation during the final phase of the storm, 28th of February 2002, as result of averaging the calculated depths for 12 hours, corrected by a factor of 04 m, according to the gauge measurements.

At the North West part of the map, at the first period there is a swallow area, the same feature there is also at the end of the storm. But at the end of the storm the area is deeper, therefore this area may be considered as source of sediment, but certainly the main part of the sand has been imported from outside the observation frame.

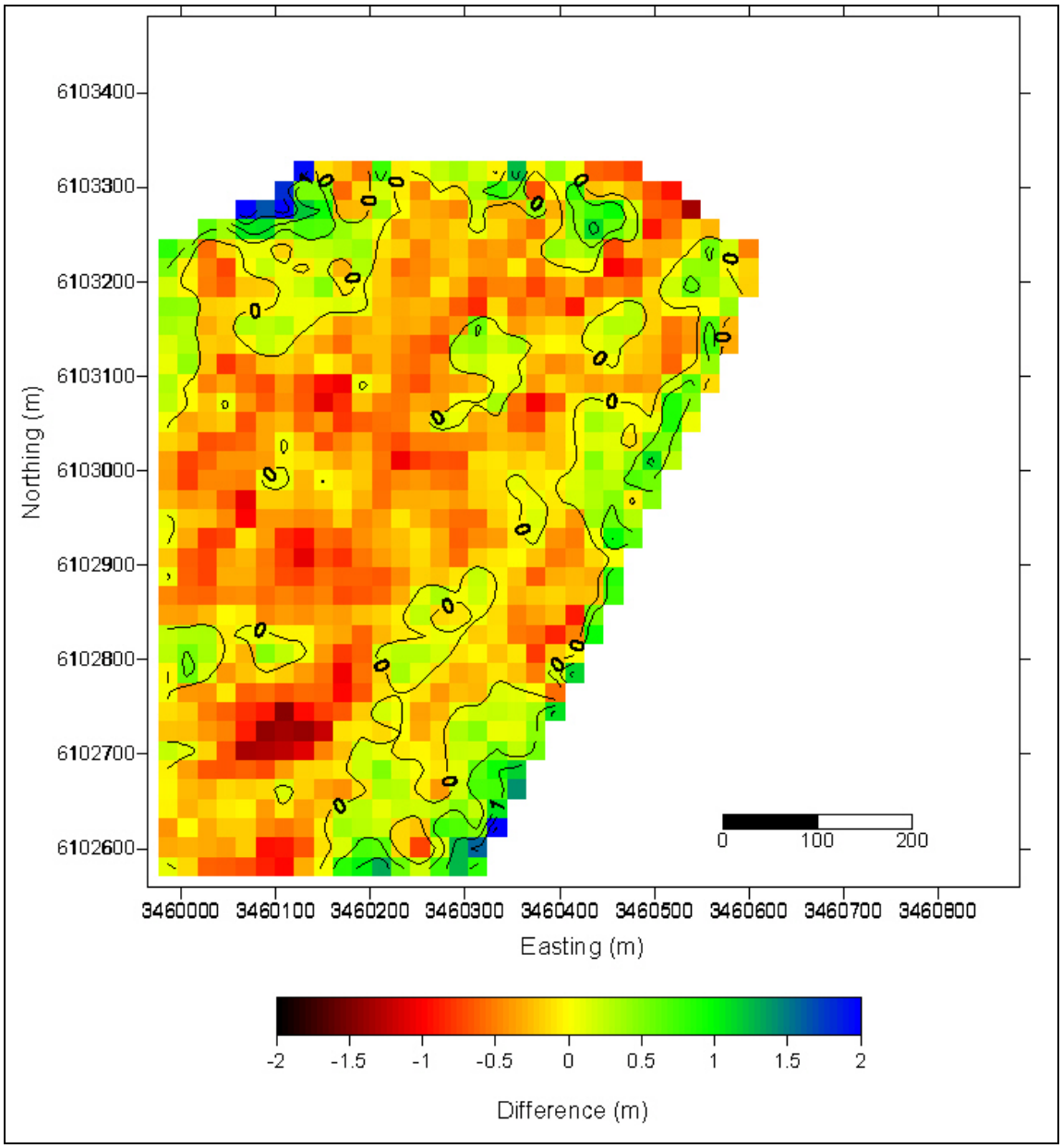

Figure 6-5. The Difference between the ending phase of the storm and the beginning of the storm.

Near the shore, the east side of the result maps the gradient of isodepth lines have similar distribution; more specific, the feature at the north east side, that is embayed by the isoline of the 7 m has been propagated during the storm. The above results are better shown at the figure 6-5, the difference of the mean calculated depths between

the end of the storm and the beginning of the storm is presented. The isolines of the change in depth are shown that in the area there is erosion, approximately 0.5 m in the deep areas and sediment deposition at the shallow areas.

For the qualitative investigation of the sediment deposition or erosion during the storm, are taken few cross sections, see figure 6-1, from B to A (Appendix XI) and from C to D, figure 6-6, which cross the channel at the deepest area. Both of the figures are shown sediment mainly accumulation of sediment during the storm.

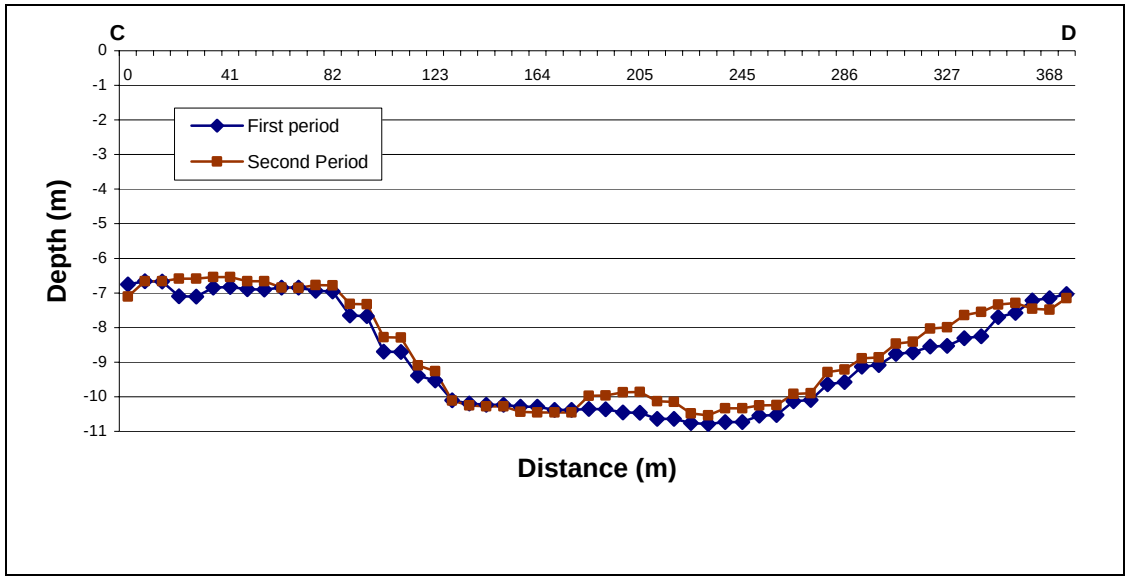

Figure 6-6. Cross section of the two estimated see depth, from C(3460558, 6103109) to D (3459985, 6103109) (see figure 6-2). There is deposition of sediment almost across all the cross section during the storm.

As it is described at the methodology, section 4.3.3, there is the effort for numerical estimation of the sediment equilibrium due to the storm. The difference of the mean depth and the results could be subtracted because the calculated sea level have been corrected according to the mean measured sea level by the gauge in Westerland. Hence it is reasonable to consider the same reference level. The results of the four methods that have used are summarized at the table 6-1.

Table 6-1. Calculation of the volume between the grids before and after the storm, which under conditions could be considered as the sediment net loss of the frame of investigation.

Numerical Method	Difference of sediment volume (m^3)
Parallelogram Rule	-52190
Trapezoidal Rule	-50971
Simpson's Rule	-49345
Simpson's 3/8 Rule	-51390
Mean Value	-50974

For the estimation of the accuracy on the above results, is used the accuracy of the method, (SENET & SEEMANN 2000b), ±0.25 m per cell, so the accuracy is estimated ±20% or 10000 m^3, but in general the assumption of the constant difference between two periods, of the mean sea level is not strong enough and decreases the accuracy of the calculation.

7 Discussion

The work presented here is a complete approach of the nearshore depth estimation by the use of radar image sequences and the linear wave theory. The comprehension and the interpretation of the results consist a query that should be answered.

7.1 The exertion of the DiSC

The optimization of the Dispersive Surface Classificator had elevated from the obscurity, the importance and the strong influence of three different features at the processing of the radar image sequence and at the quality of the final result. These three features are the correct choice of the minimum and maximum frequency for the decomposition of the global spectrum, the modules for the control of the selection of the regression parameters and the number of the regression coordinates according to the reliability of the results.

The set of figures 5-4 presents the final result of the same dataset, processed with the same parameters, except the minimum and maximum frequency bin for the decomposition of the global spectrum. Even this visual comparison of the final product of the method, shows that there are some cells that the estimated instantaneous depth varies in neighboring cells more than 6 m. Due to the continuity of the mass and in general the common experience that in one area when the sediment is fine, this phenomenon cannot happen. Therefore the existence of these features could be explained as artifacts of the image processing. Also the observation that the processing of data with different values for the minimum and maximum frequency bin at the same power influences the final result lead to the development of a module for the quality check of the parameters.

The upper left figure 5-4 is the best result of the old version, after several replicates. The development of the quality control module, visualization of the used bins and in which direction for the decomposition of the spectrum, ameliorated the results. The sources of the problem was that in the most of the cases the decomposition and the inverse 2D FFT, were taken account areas of zero energy and because of the sinusoidal transformation were created these “shallow” areas. The lower right figure 5-4, result of the new version of DiSC, has none of this kind of features.

The second conclusion from the exertion of DiSC is the clarification of the regression parameters for the calculation of the local wavenumbers. These three parameters, the global power, the block power and the confidence are binominal thresholds; their impact is on the number of the regression coordinates at the calculation of the hydrographic parameters.

The result of the inverse 2D FFT is the creation of maps of wave components which they have the same energy as the monitored wave field. Within this process, in same cases at one point, there is more than one wavelength, this phenomenon exists in the nature but it is not possible to be modeled by the linear wave theory. This is limitation of the physical model that is used in DiSC. Therefore the aim of the new module, which has been developed for each of these three parameters, is to avoid the areas that the linear theory is not valid.

By using the module of the new version, it is proved that if the choice of the global power is accurate the two other regression parameters have minor influence on the results, except in extreme selections of values of the parameters.

This fact is a brave step for the operationalisation of the DiSC. The number of the regression parameters could be reduced. Therefore the process could be faster in respect of the duration of calculations and the user interaction with the individual parts of the method.

The last result of the DiSC optimization is the impact of the number of the regression coordinates on the final result. As it is shown at the figures 5-4, the number of the regression coordinates consist an indicator about the reliability of the calculated instantaneous depth. When there is a high number of the regression coordinates, the depth is underestimated and when the number of the regression coordinates is low, the depth is overestimated. This observation is useful for the control of the final result and also it is possible to be adopted in the DiSC software, as one more step at the automation of the calculations.

7.2 Geophysical interpretation

The main product of the present investigation is the visualization of the estimated depths at the beginning and at the end of the storm of 20th to 28th February 2002. The maps that have been produced illustrate geomorphological features of the seabed and offer strong evidences for the mechanisms of the sentiment motion in the area, more specific:

The results shown at the figures 6.2 and 6.4 could be separated into three different areas, near the shore, the channel and the shallow area at the North-West.

Near the shore there are not results, the isoline of the 5 m in both cases is the limit up to which the method has results. As it is presented at the section 4.2, the core of DiSC method is the dispersion relation as part of the linear theory; there are limitations due to the fact that the propagation of the waves at the shallow areas is not linear. In this case that the Sylt Tief is the East border of the North Sea, the fetch for the development of the waves is enough large for the creation of long waves which have the additional effect of the strong

wind during the same period, therefore the dispersion relation near the shore is not valid and the DiSC is not applicable.

The reason that there are not results at the northern part of the research area is similar. According to the Admiralty Charts, 2002, there is a slope of a deep channel, approximately 20 m and the area is protected by the island of Romo. The existence of the Romo Island prevents the development of enough long waves for the application of DiSC. Moreover, as it is proved by the validation scatter plot of the method, figure 7-1, (ZIEMER et al 2004) the DiSC underestimates the depths over 20 m, when the method is able to separate the dispersive from the not dispersive waves. In this case due to the slope the dispersion relation is not applicable.

The comparison between the North-East areas of the results indicates shore increase. The area that is embayed by the isoline of 7 m has the tendency to expand, and the shape of this underwater spit follows the shape of the coast. The foregone conclusion from the figure 6-6 is similar; the isolines shifted towards the sea, the effective wavelength transfers the nearshore bar crest in the deeper areas, the same effect has been described also in other publications (TAKEWAKA 2005).

The shallow area, at the North West part, lies near the limits of the method. The minimum estimated depth at the beginning of the storm is approximately 3.5 m and at the end of storm the minimum depth is about 4.5 m. According to the validation curve, figure 7-1, and also the dispersion relation, these depths tend to the limits of the method. But the step by step control of the method and the filtering of the results at the end, according to the number of the regression coordinates proved that those data are valid. The map of the difference shows that in this area there is erosion, maximum difference in depth is approximately 2 m. This fact could convince that the shallow North-West area of the results is a limited source of sediment for this period.

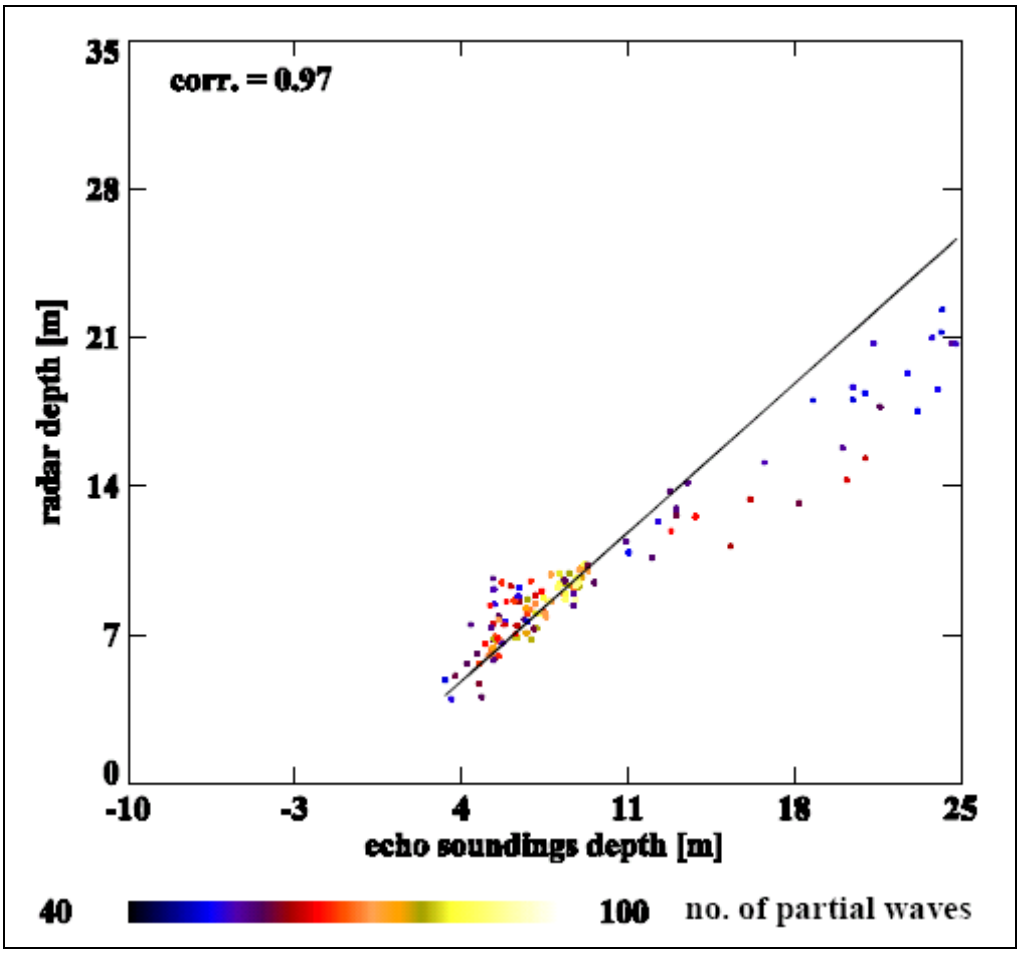

Figure 7-1. Scatter diagram produced by the comparison between radar-deduced water depths with echo sounding depths. The dot's colours qualify the radar depth by representing the number of partial wave components used for the estimate. The deviation for deeper water cases is due to the asymptotic character of the dispersion for increasing values of λ / d , (SENET et al 2003).

The chart of the differences, figure 6-5 and the cross section visualization, figure 6-6, show that in the area of investigation, the sentiment is deposited during this storm almost everywhere, but the source of the sediment cannot be defined. There are not available data about the coast equilibrium of sediment for the same period and also the small erosion that is mentioned at the North West part is not sufficient to refill the area. At the publications of (AHRENDT 1994) and (AHRENDT 2001), it is proved that the motion of sediment is northwards at the North-West side of the Sylt Island; and also the visualization by the Admiral Charts of the channel system of the area indicates that transfer of sediment from the North (Rømo Island) to the South (Sylt Island) is not possible.

The estimation of the quantity of the sediment which has been exchanged during the storm, by the exertion of several numerical methods, proved that 50000 m^3 ($\pm$10000 m^3) has been

deposited in seven days. Have been used 4 numerical methods to prevent the possibility of any systematic error and to check the variability of the estimated quantity according to the numerical method of integration. According to (AHRENDT 1994) the loss of the sediment at the north part of the Sylt Island is about 850000 m^3 per year. Hence the estimated quantity that is deposited is approximately the 5% of the annual sediment loss of the Coast of Sylt Island. This result is reasonable if it is consider that the wind intensity and the direction during the first days of the storm is south west and at the end of the storm is west, Appendix XII, it is proved that the storm of the present investigation is the longest of the 6 year and has the highest wind velocities.

These four evidences lead at the conclusion that there is longshore sediment transport, but cannot be defined the source of the sediment, by the present investigation, which shows only the accumulation of sediment in the area of List Tief during this specific storm. The origin of the sediment probably is the erosion of the coast and the longshore transport from the rest of Frisian Islands.

The figure 6.6 shows a known but impressive phenomenon about the tidal cycle during a storm, the wind setup. According to the tide calendar, at 18.00 of 22nd of 2002, there is high water at the List West, at 21.00 is slack water, at 23.00 the low water, at 02.00 again slack water and at 05.00 high water. The average of water level of 9 cells which is presented at the figure 6.6 shows the 2 high water conditions and the slack water, there is not low water. Probably, the reason is the wind setup; the surface wind stress on the water mass is enough to eliminate the sun and moon gravity forces. Therefore, it seems as there is not low water level. There is not obvious reason for the extreme value at 22.00, but similar anomaly is also obvious at the gauge measurements of the sea level.

8 Conclusions

The Dispersive Surface Classificator DiSC is a remote sensing method which allows the determination of spatial maps of the hydrographic parameters water depth and near surface currents, but till now was under experimental use and continuous development, even thought that is a commercial product. There was not a stable methodology for the monitoring of the local depths and the existence of many parameters was transforming it into an unfriendly method and software. The present thesis answers all the above queries about the DiSC through the example of the determination of the difference in the depth during the period of an extreme storm.

The methodology that developed and presented analytically, consist a complete approach for the operationalisation of the DiSC. Before the implementation of the thesis, there were 9 different parameters that had to been defined, without having the possibility of quality control; now after the optimization and the development of the control quality modules, the 7 most important parameters (minimum and maximum frequency bin, the power of global spectrum, the regression parameters, power, block power, confidence limits the size of the cell) could be selected and checked easily; and for one more (minimum number of regression coordinates), is known the bandwidth of its variation for reliable results, an open question is only the number of the frequency bins for the decomposition of the global spectrum.

As it proved by the new module which visualizes the bins of the global spectrum, the use of low frequencies, which include the noise, was a trap during the analysis and was creating false and unreliable depth components. Moreover the choice of the regression parameters was based on the visual interpretation of the power and phase of the decomposed global spectrum and the importance, for the reliability of the regression coordinates was not cleared. It is essential to be mentioned that even the standardization of the method, the development of a concrete methodology and the development of the quality control modules, the user of the method has to be trained.

The simplification of some components of the DiSC made it more “users friendly” but the core of the method is based on the combination of the remote sensing and the image processing with the wave theory, three scientific domains which are complicated and under constant investigation; each step of the DiSC is the interaction of all

of them and the use of the DiSC requires long training and deep understanding of all the processes.

Sea state and tides are inhomogeneous in areas close to the coast due to the spatial variations in the sea-bottom's bathymetry. The dynamical processes result, in long-term or in extreme weather conditions, sand transport. This transport can endanger coastal structures and shorelines. This phenomenon occurs around the Sylt Island where tremendous sand transport occurs due to the sea state and strong tidal currents.

The aim of this thesis was the estimation of depth at the area of Salzsand. Radar-image sequences acquired during a tidal cycle at the beginning and the ending phase of an extreme storm, used for the determination of the depth at these two periods. The comparison of them, under specific assumptions about the accuracy of the method and the influence of the tidal cycle, proved that the results of DiSC are reasonable. Also other investigations, more expensive, by side-scan sonar (SENET & SEEMANN 2002b) and time consuming (AHRENDT 1994) of the same area of research have similar results. The calculated volume of the sediment that has been deposited is close to the bibliographic estimations for the sediment losses of the Sylt's coasts. In addition to that the identification of the tidal signal is one strong and indisputable indicator that the method could be used broadly for the monitoring of the coastal areas. The achievements of this thesis clarified all the obscured points of the DiSC method and transformed it from one experimental into an operational, reliable and low cost tool for the monitoring of the coastal zone.

The DiSC method and the implemented software consist a stable base for further development of the method. Till now, the method has been used for the analysis of radar image sequences and video from experimental tank (SENET 2004). It is proposed that a similar investigation with this one has to been implemented for the operationalisation of the method for image sequences captured by video cameras under real conditions. As the cost of the acquisition, installation and maintenance of this kind of equipment is much lower than the cost of the radar systems, the method could broadly distributed and used as part of the monitoring routine. In addition to that, the spatial and temporal cover of one area by the radar radius and the results from the DiSC could be combined with models for coastal areas, as input files or correction factors during the simulation process.

Moreover, the theory, the results and previous investigations for the validation of the method (SENET & SEEMANN 2002a, SENET & SEEMANN 2002b) have proved that the minimum depth that the method may be used is approximately 4 m. The reason is that the waves are not anymore dispersive and other phenomena, such as the wave breaking, current influence, are dominant in very shallow areas. Therefore, it is proposed the extension of the DiSC to non-linear theories for the modeling of those phenomena.

The DiSC is based on the dispersion relation, a common accepted physical approach of the sea-waves. It is proposed the use of the refraction laws, which describe the refraction paths as a function of the bathymetric patterns and the currents, to estimate the refraction patterns from the different local 3D spectra and to examine the wave field approaching shallow-water areas.

The Dispersive Surface Classificator consist a general method of remote sensing analysis, as it is an approach of the dynamics of dispersive boundaries. Therefore, it is proposed to transfer DiSC from the hydrographic application of analyzing water waves to other disciplines, by the replacement of the dispersion relation of the sea surface with the dispersion relation for other dispersive surfaces. There is a broad range of activities for extension of DiSC but the further development of the algorithm and the applications depend on the specific problems that have to been solved.

References

AHRENDT, K. (2001): Expected effect of climate change on Sylt island: results from a multidisciplinary German project, *Clim. Res.* 18: 141–146.

BARRICK, D. E. (1977): Ocean surface current mapped by radar. *Science* 198, 138-144.

BELL, P. S. (1999): Shallow water bathymetry derived from an analysis of X-band marine radar images of waves. *Coastal Engineering* 37: 513–527.

CROMBIE, D.D. (1955): Doppler spectrum of sea echo at 13.56 Mc/s, *Nature* 175, 681-682.

DOONG, D.-J. (2003): Uncertainty assessment of wave remote sensing, PhD thesis, Department of Hydraulic and Ocean Engineering, National Cheng Kung University, Tainan, Taiwan, Republic of China.

GANGESKAR, R., GRONLIE, O. (2000): Wave Height Measurement with a Standard Navigation Ship Radar -Results from Field Trials. – In: Proceedings of the Sixth International Conference on Remote Sensing for Marine and Costal Environments, Charleston, South Carolina.

GODA, Y. (1970): Numerical experiments on wave statistics with spectral simulation. *Rep. Port and Harbour Res. Inst*., Japan 9: 3–57.

GRONLIE, O. (1995): Microwave Radar Directional Wave Measurements - MIROS Results. – In: Proceedings of the WMO/IOC Workshop on Operational Ocean Monitoring using Surface Based Radars, WMO report no 32, WMO/TD-No.694, Geneva.

HASSELMANN, K. (1962): On the non-linear energy transfer in a gravity wave spectrum, 1: general theory. *J. Fluid Mech*. 15, pp 273.

HAVLICEK, J.P., HARDING, D.S. & BOVIK, A.C. (1996): The multicomponent AM-FM image representation. –In: IEEE Transactions on image processing, 5(6): 1094-1100.

ITO, K. (Ed.). "Turing Machines." §31B in *Encyclopedic Dictionary of Mathematics, 2nd ed., Vol. 1*. Cambridge, MA: MIT Press, pp. 136-137, 1987.

KENNEDY M. & KOPP S. (1996): Understanding Map projections. 110pp.;Rendlands, USA (Enviromenta Systems Research Institute Inc.).

LILLESAND, T.M., KIEFER, R.W. (1994): Remote Sensing and Image Interpretation. New York (John Wiley and Sons).

LONG, M., W. (1983): Radar reflectivity of Land and Sea (Second Edition), Dedham (Artech House, Inc).

LONGUET-HIGGINS, M. S. (1952): On the Statistical Distribution of the Heights of Sea Waves. *J. Mar. Res.*: 11, 245–266.

LONGUET-HIGGINS, M.S., CARTWRIGHT, D.E. & SMITH, N.D. (1963): Observations of the directional spectrum of sea waves using the motions of a floating buoy.- In: Ocean wave spectra: 111. (Prentice Hall).

MARSDEN, J.E. & CHORIN, A.J. (2004): Mathematical introduction to fluid mechanics. 169pp.; Berlin (Springer).

MILES, J.W (1957): On the generation of sea-surface waves by shear flows. *J. Fluid Mech*. 3.

MOON, F.C. (1992): Chaotic and Fractal Dynamics: An Introduction for Applied Scientists and Engineers; New York (John Wiley and Sons).

NIETO, J.C., REICHERT, K., DITTMER, J. (1999): Use of nautical radar as a wave monitoring instrument. Coastal Engineering 37: 331–342.

NOVAK, P., NALLURI, C. (Editor), NARAYANAN, R. (Editor), MOFFAT A.I.B. (Editor) (2001): Hydraulic Structure (3rd Edition); London, New York, Oslo, Philadelphia, Singapore, Stockholm (Taylor & Francis).

OPPENHEIM, A.V. & LIM, J.S. (1981): The importance of phase in signals. –In: Proceedings of the IEEE, 69: 529-541.

OUTZEN, O., (1998): Bestimmung der Wassertiefe und der oberflaechennahen Stroemung mit einem nautischen Radar, diploma thesis, GKSS Research Center, University of Hamburg, (GKSS report number: GKSS 98/E/60).

PHILLIPS, O.M. (1966): The dynamics of the upper ocean; Cambridge (University Press).

PRESS, W.H., TEUKOLSKY, S.A., VETTERLING, W.T. & FLANNERY, B.P. (1992): Numerical Recipes in C: The Art of Scientific Computing, Second Edition, 994. New York (Cambridge University Press).

PRINS, J. (1996): Statistical Methods Group. – In: NIST/SEMATECH e-Handbook of Statistical Methods. (http://www.nist.gov/stat.handbook).

REICHERT, K., HESSNER, K., NIETO, J.C., DITTMER, J. (1999): WaMoSII: A Radar based Wave and Current Monitoring System. Proceedings of ISOPE'99, Brest.

ROBINSON I. S., WARD N. P., GOMMENGINGER C. P., & TENORIO-GONZALES M. A. (2000): Coastal Oceanography Applications of Digital Image Data from Marine Radar. *American Meteorological Society* : 721-735.

SEEMANN, J. (1997): Interpretation der Struktur des Wellenzahl-Frequenzspektrums von Radar-Bildsequenzen des Seegangs, PhD thesis, GKSS Research Center, University of Hamburg, (GKSS report number: 97/E/68).

SEEMANN, J., SENET, C.M., and F. ZIEMER (2000): Local Analysis of Inhomogeneous Sea Surfaces in Coastal Waters Using Nautical Radar Image Sequences, Mustererkennung 2000, Springer, Berlin, Informatik aktuell, pp. 179-186.

SEEMANN, J., SENET, C.M., WOLFF, U., and F. ZIEMER (2000): Nautical X-Band Radar Image Processing: Monitoring of Morphodynamic Processes in Coastal Waters, Oceans"2000, Conference Proceedings, Rhode Island, USA.

SEEMANN, J., SENET, C.M., WOLFF, U., HATTEN, H., and F. ZIEMER (2000): Hydrographic Parameter Maps Retrieved from Nautical Radar Image Sequences of Inhomogeneous Water Surfaces, IGARSS"2000, Conference Proceedings, Volume V, pp. 1898-1900, Honolulu, Hawaii.

SENET, C.M. (2004): Dynamics of Dispersive Boundaries: The determination of Spatial Hydrographic-Parameter Maps from Optical Sea-Surface Image Sequences, PhD thesis, GKSS Research Center, University of Hamburg.

SENET, C.M., SEEMANN J. & Ziemer F. (2001): The Near-Surface Current Velocity Determined from Image Sequences of the Sea Surface, *IEEE Transactions on Geoscience and Remote Sensing* 39 No. 3: pp. 492-505.

SENET, C.M., SEEMANN, J. & ZIEMER, F. (2003): Determination of Bathymetric and Current Maps by the Method DiSC Based on the Analysis of Nautical X-Band Radar-Image Sequences of the Sea Surface, (Elsevier Science).

SENET, C.M., SEEMANN, J. (2002a): Studie I: "State of the Art". Technical report, GKSS Research Center GmbH, Geesthacht, Germany.

SENET, C.M., SEEMANN, J. (2002b): Studie II: "Validation". Technical report, GKSS Research Center GmbH, Geesthacht, Germany.

SKOLNIK, M. (1970): Radar Hanbook (First Edition), New York, St. Louis, San Francisco, Auckland, Bogota, Caracas, Lisbon, London, Madrid, Mexico, Milan, Montreal, New Delhi, Paris, San Juan, Sao Paulo, Singapore, Sydney, Tokyo, Toronto (McGraw- Hill, Inc.).

SKOLNIK, M. (1990): Radar Hanbook (Second Edition); New York, St. Louis, San Francisco, Auckland, Bogota, Caracas, Lisbon, London, Madrid, Mexico, Milan, Montreal, New Delhi, Paris, San Juan, Sao Paulo, Singapore, Sydney, Tokyo, Toronto (McGraw- Hill, Inc.).

SMITH, M.J., POULTER, E,M. & McGregor J.A. (1996): Doppler Radar Measurements of Wave groups and breaking waves. *J. Geophys. Res,*101, 14269-14282.

SOUKISSIAN, T. (2003): Lecture Notes at coastal engineering. School of Environmental Sciences, Marine Science Department, University of Aegean, Mytilene.

TAKEWAKA, S. (2005): Measurements of shoreline positions and intertidal foreshore slopes with X-band marine radar systems. *Coastal Engineering Journal* 47: 91-107.

TOMCZAK, M. (2005): An introduction to physical oceanography (lecture notes). Marine Sciences Deprtment, Flinders University of South Australia, Adelaide.

VALEJO, S.M. (2000): International perspectives in integrated coastal zone management, Course notes of ICZM, Kiel.

VOGELZANG, J. (2000): Motto für ein EU-Antrag.

WAVEREN, R.H., GROOT, S., SCHOLTEN, H., GEER, F.C., WOESTEN, J.H.M., KOEZE, R.D., NOORT, J.J. (1999): STOWA/RIZA, 1999, Smooth Modelling in Water Management, Good Modelling Practice Handbook; STOWA report 99-05, Dutch Dept. of Public Works, Institute for Inland Water Management and Waste Water Treatment report 99.036.

WINKEL N. (1994): Modellierung von Seegang in extremen Flachwasser PhD thesis, University of Hamburg, Faculty of Geosciences, GKSS Research Center, Geesthacht, Hamburg, Germany.

ZIEMER, F. (1991): Directional spectra from shipboard navigation radar during LEWEX. Directional Ocean Wave Spectra, edited by R.C. Beal, The Johns Hopkins University Press, Baltimore U.S.A., 80-84.

ZIEMER, F., DITTMER, J. (1994): A System to Monitor Ocean Wave Fields. – In: Proceedings of the OCEANS'94 October 13 - 16: 28 - 31.

- (1989): FURUNO - Operators manual for FR 1201; Nishimomiya, Japan (FURUNO ELECTRIC CO., LTD)

- (2000): Meßsysteme für Meteorologie und Umweltschuty; Hamburg, Germany (Siggelkow Gerätebau GmbH)

- (2001), Generalplan Küstenschutz: Integriertes Küstenschutzmanagement in Schleswig-Holstein.

- (2002): Gezeitenkalendar, Hoch- und Niedrigwasserzeiten für die Deutsche Bucht und deren Flussgebiete, (BUNDESAMT FUER SEESCHIFFAHRT UND HYDORGRAPHIE).

- (2003): Fundamentals of the remote sensing – Remote Sensing Tutorial, Canada Centre for Remote Sensing.

I. Appendix

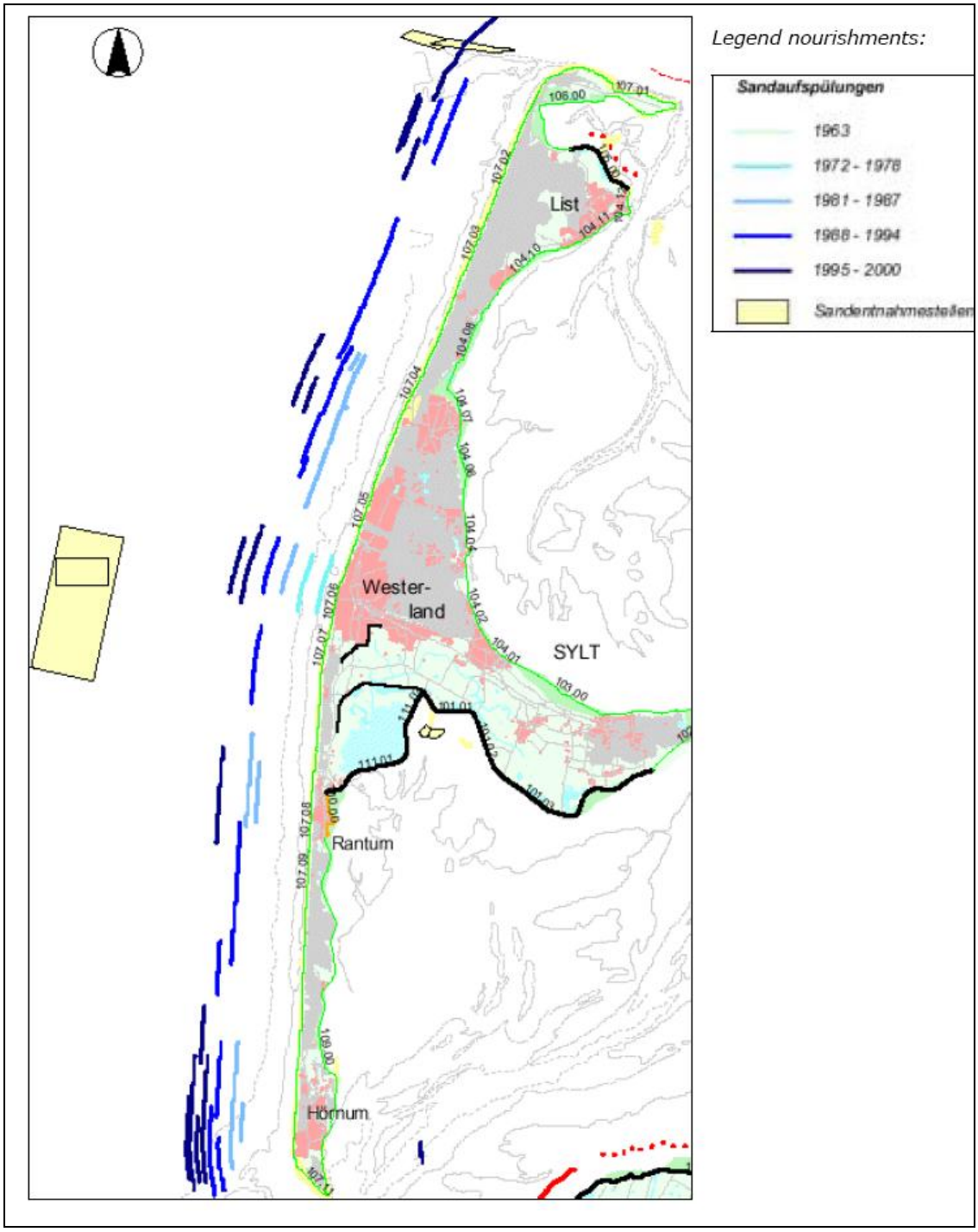

Figure I-1. Sand nourishments at Sylt (GENERALPLAN KUSTENSCHUTZ 2001).

II. Appendix

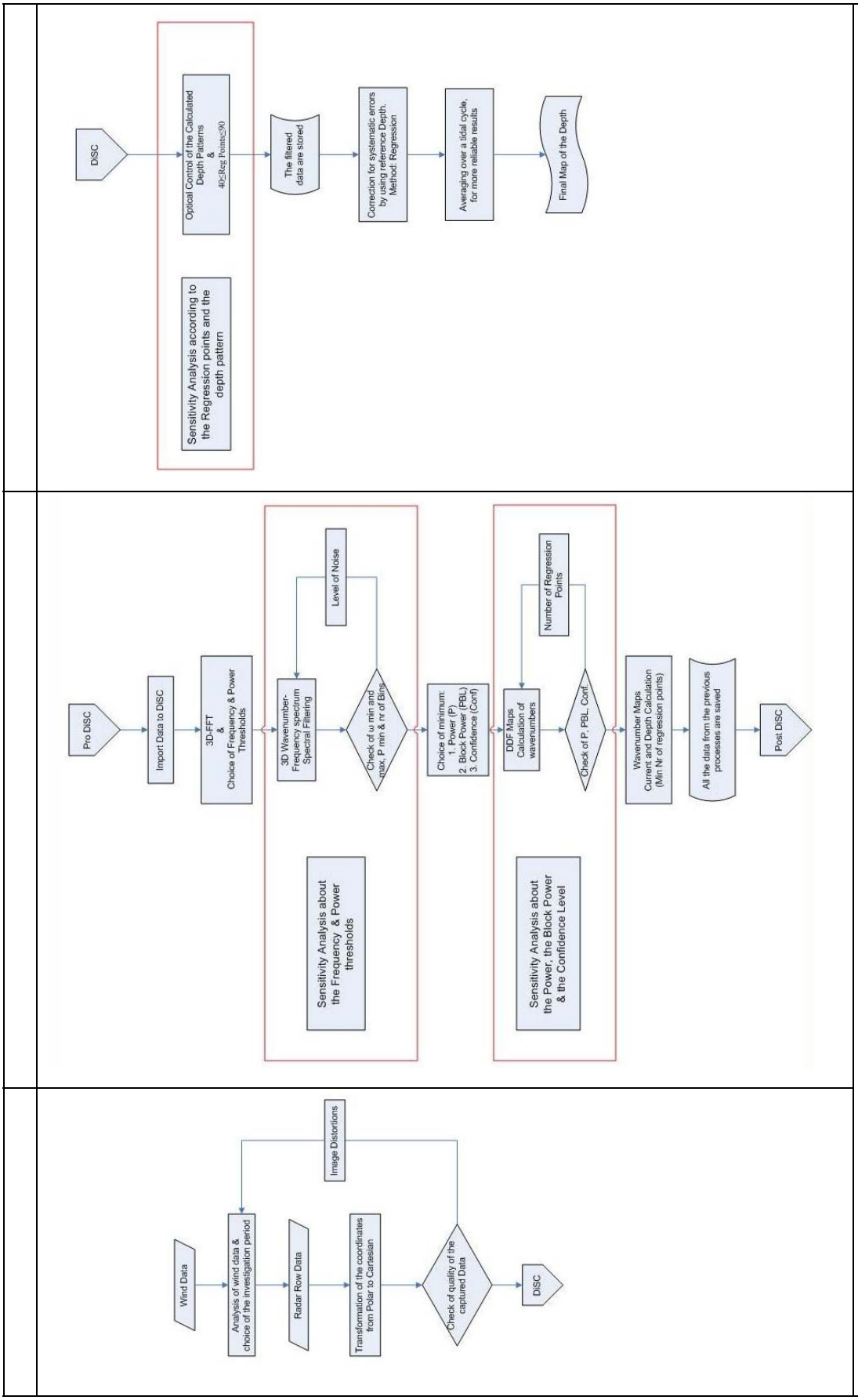

Figure II-1. The complete flow chart of the methodology of the present investigation. Pro-DiSC includes the necessary preparations for the exertion of the Dispersive Surface Classificator (DiSC) and at the Post-DiSC are included the post process analysis and investigation of the results of DiSC.

III. Appendix

Table III-1. The storm events 2000-2005 and duration.

Date	Time	Hours
2000 1 17	18	13
2000 1 18	7	
2000 1 29	21	10
2000 1 30	7	
2000 1 31	4	6
2000 1 31	10	
2000 2 9	3	8
2000 2 9	11	
2000 3 3	12	4
2000 3 3	16	
2000 3 15	1	3
2000 3 15	4	
2000 5 27	10	
2000 5 27	13	3
2000 10 30	1	30
2000 10 31	6	
2000 12 13	7	6
2000 12 13	13	
2001 2 5	0	5
2001 2 5	5	
2001 6 3	8	7
2001 6 3	15	
2001 10 31	11	22
2001 11 1	9	
2002 1 28	14	10
2002 1 29	0	
Date	Time	Hours
2002 2 20	19	6
2002 2 21	1	
2002 2 22	0	6
2002 2 22	6	
2002 2 22	16	12
2002 2 23	4	
2002 2 26	13	7
2002 2 26	20	
2002 10 27	20	7
2002 10 28	3	
2003 10 9	1	5
2003 10 9	6	
2003 12 6	1	2
2003 12 6	3	
2003 12 14	12	15
2003 12 15	3	
2003 12 15	13	8
2003 12 15	21	
2003 12 21	15	2
2003 12 21	17	
2004 3 19	16	9
With Gaps		
2004 3 20	0	

2004 3 21	0	11
2004 3 21	11	
2004 5 22	16	4
2004 5 22	20	
Date	Time	Hours
2004 9 12	14	4
2004 9 12	16	
2004 9 21	14	
Gaps		9
2004 9 21	23	
2004 10 25	12	2
2004 10 25	14	
2004 11 18	0	9
2004 11 18	9	
2004 12 22	9	3

2004 12 22	12	
Date	Time	Hours
2005 1 1	23	
Gaps		24
2005 1 2	23	
2005 1 8	5	19
2005 1 9	0	
2005 1 20	1	
Gaps		25
2005 1 21	2	
2005 2 12	18	6
2005 2 13	0	

IV. Appendix

Table IV-1. Input file to DiSC, are defined the number of dimension, the number of pixels in each direction, the number of images, the coordinates in meters of the lower left corner of the image, the length at x and y dimension of each pixel the rotation of the antenna, the units of the 3 dimensions and the name of the image sequence.

comment // Benutzerkommentar
3 // Dimension
288 // n1
288 // n2
256 // n3
3459944.4792 // o1
6102538.9792 // o2
0 // o3
6.8182 // s1
6.8182 // s2
1.73000000000 // s3
m // unit1
m // unit2
s // unit3
02202200_small.carth // filename

V. Appedix

Table V-1. All the processing data and the different parameters of the begining of the storm, 20th February of 2002

	MapDf				Wave Number			
	Shoot	Omega Min	Omega Max	Power	Nr of Bins	Power	Confidence	Block Power
02201800_0	1	33	82	220	130	130	0,985	130
	2	33	82	220	130	120	0,985	130
	3	33	82	220	130	125	0,985	130
	4	33	82	220	130	115	0,985	130
	5	33	82	220	130	117	0,985	130
	6	33	82	220	130	113	0,985	130
	7	35	65	218	130	115	0,985	130
	8	35	80	218	130			
	9	41	70	218	130	117	0,985	130
	10	41	70	218	130	121	0,985	130
	11	41	70	218	130	123	0,985	130
02201900_0	1	33	83	219	130	125	0,985	130
	2	33	83	219	130	120	0,985	130
	3	33	83	219	130	115	0,985	130
	4	33	83	219	130	118	0,985	130
	5	33	83	219	130			
	6	43	70	219	130	118	0,985	130
	7	41	67	217	130	123	0,985	130
	8	43	70	219	130	123	0,985	130
	9	43	70	219	130	123	0,99	130
02202000_0	1	33	82	217	130	?125	0,985	130
	2	33	82	217	130	120	0,985	130
	3	33	82	217	130	115	0,985	130
	4	33	82	217	130	110	0,985	130
	5	33	82	217	130	125	0,985	130
	6	33	82	217	130	113	0,985	130
	7	41	67	217	130	119	0,985	130
	8	41	67	217	130	123	0,985	130
	9	46	67	217	130	122	0,985	130
	10	46	67	217	130	120	0,985	130
02202100_0	1	32	81	218	130	125	0,985	130
	2	32	81	218	130	120	0,985	130
	3	32	81	218	130	115	0,985	130
	4	32	81	218	130	113	0,985	130
	5	32	81	218	130			
	6	38	70	218	130	117	0,985	130
	7	38	70	218	130	123	0,985	130
	8	38	70	218	130	123	0,992	130
02202200_0	1	33	82	217	130	125	0,985	130
	2	33	82	217	130	120	0,985	130

	3	33	82	217	130	115	0,985	130
	4	33	82	217	130	113	0,985	130
	5	33	82	217	130			
	6	41	70	217	130	117	0,985	130
	7	41	70	217	130	121	0,985	130
	8	41	70	217	130	123	0,99	130
02202300_0	1	32	82	220	130	125	0,985	130
	2	32	82	220	130	120	0,985	130
	3	32	82	220	130	115	0,985	130
	4	32	82	220	130	118	0,985	130
	5	32	82	220	130		0,985	130
	6	38	82	220	130	118	0,985	130
	7	38	82	220	130	121	0,985	130
	8	38	82	220	130	121	0,99	130
02210000_0	1	32	79	218	130	125	0,985	130
	2	32	79	218	130	120	0,985	130
	3	32	79	218	130	115	0,985	130
	4	32	79	218	130	118	0,985	130
	5	32	79	218	130		0,985	130
	6	37	70	218	130	118	0,985	130
	7	37	70	218	130	121	0,985	130
	8	37	70	218	130	121	0,992	130
02210100_0	1	33	81	217	130	125	0,985	130
	2	33	81	217	130	120	0,985	130
	3	33	81	217	130	115	0,985	130
	4	33	81	217	130	117	0,985	130
	5	33	81	217	130			
	6	39	75	217	130	117	0,985	130
	7	45	75	217	130	120	0,985	130
	8	45	75	217	130	120	0,992	130
02210200_0	1	31	81	217	130	125	0,985	130
	2	31	81	217	130	120	0,985	130
	3	31	81	217	130	115	0,985	130
	4	31	81	217	130	117	0,985	130
	5	31	81	217	130			
	6	40	72	217	130	117	0,985	130
	7	40	72	217	130	119	0,985	130
	8	40	72	217	130	119	0,992	125
02210300_0	1	31	83	216	130	115	0,985	130
	2	31	83	216	130	120	0,985	130
	3	31	83	216	130	117	0,985	130
	4	31	83	216	130	112	0,985	130
	5	31	83	216	130			
	6	36	75	216	130	117	0,985	130
	7	36	75	216	130	120	0,985	130
	8	40	72	216	130	120	0,985	130
	9	40	72	216	130	122	0,985	130
	10	40	72	216	130	122	0,99	130
	11	48	72	216	130	122	0,99	130

	12	48	72	216	130	121	0,985	130
	13	48	72	216	130	120	0,985	130
02210400_0	1	32	80	215	130	115	0,985	130
	2	32	80	215	130	118	0,985	130
	3	32	80	215	130	121	0,985	130
	4	32	80	215	130	114	0,985	130
	5	37	80	215	130	118	0,985	130
	6	37	75	215	130	118	0,985	130
	7	38	70	215	130	122	0,985	130
	8	38	70	215	130	122	0,985	125
	9	38	70	215	130	122	0,99	125
	10	32	80	218	130			
	11	40	74	218	130	122	0,985	125
	12	40	74	218	130	122	0,985	130
	13	40	74	218	130	122	0,99	130
	14	40	74	218	130	122	0,985	120
02210500_0	1	31	79	216	130	116	0,985	130
	2	31	79	216	130	120	0,985	130
	3	31	79	216	130	125	0,985	130
	4	31	79	216	130	119	0,985	130
	5	31	79	216	130			
	6	36	65	216	130	119	0,985	130
	7	36	65	216	130	119	0,99	130
	8	36	65	216	130	119	0,999	130
	9	36	65	216	130	119	0,992	130
	10	36	65	216	130	119	0,992	130
	11	32	65	216	130	119	0,992	125
	12	41	65	216	130	119	0,992	130
	13	41	65	216	130	119	0,992	125

VI. Appendix

	MapDf				Wave Number			
	Shoot	Omega Min	Omega Max	Power	Nr of Bins	Power	Confidence	Block Power
02271000_0	1	35	84	215	130	115	0,985	130
	2	35	84	215	130	118	0,985	130
	3	35	84	215	130	120	0,985	130
	4	35	84	217	130	122	0,985	130
	5	35	84	217	130	120	0,985	130
	6	35	84	217	130	126	0,985	130
	7	35	84	217	130	124	0,985	130
	8	35	84	217	130			
	9	44	70	217	130	124	0,985	130
	10	44	70	217	130	122	0,985	130
	11	44	70	217	130	124	0,985	125
	12	48	75	217	130	124	0,985	125
02271100_0	1	35	81	217	130	119	0,985	130
	2	35	81	217	130	121	0,985	130
	3	35	81	217	130	123	0,985	130
	4	35	90	217	130	123	0,985	130
	5	35	84	217	130	124	0,985	130
	6	32	90	217	130			
	7	42	65	217	130	124	0,985	130
	8	42	70	217	130	119	0,985	130
	9	45	68	217	130	121	0,985	130
	10	45	68	217	130	120	0,98	130
	11 (12)	45	68	217	130	120	0,985	130
					130			
2271200_0	1	34	83	217	130	119	0,985	130
	2	34	90	217	130	119	0,985	130
	3	34	87	217	130	123	0,985	130
	4	34	95	217	130	123	0,985	130
	5	34	95	217	130	125	0,985	130
	6	34	90	217	130	125	0,985	130
	7	34	90	217	130			
	8	42	70	217	130	125	0,985	130
	9	42	70	217	130	120	0,985	130
	10	42	70	217	130	115	0,985	130
2271300_0	1	33	82	219	130	118	0,985	130
	2	33	82	219	130	115	0,985	130
	3	33	82	219	130	121	0,985	130
	4	40	80	219	130	120	0,985	130
2271400_0	1	33	83	217	130	117	0,985	130
	2	33	83	217	130	120	0,985	130
	3	33	83	217	130	122	0,985	130
	4	33	83	217	130	125	0,985	130
	5	33	83	217	130			
	6	44	75	217	130	122	0,985	130
	7	44	75	217	130	125	0,985	130
2271500_Phil_0	1	32	83	217	130			130
	2	32	83	217	130	112		130
	3	32	83	217	130	115		130
	4	32	83	217	130	120		130

	5	32	83	217	130	118		130
	6	32	83	217	130	122		130
	7	32	83	217	130			
	8	46	75	217	130	118		130
	9	46	75	217	130	122		130
2271500_0	1	32	83	217	130	115		130
	2	32	83	217	130	118		130
	3	32	90	217	130	118		130
	4	32	83	215	130	118		130
2271600_0	1	31	76	216	130	112	0,985	130
	2	31	76	216	130	115	0,985	130
	3	31	76	216	130	108	0,985	130
	4	30	85	216	130			
	5	40	75	216	130	108	0,985	130
								130
2271700_0	1	30	77	218	130	104	0,985	130
	2	30	77	218	130	110	0,985	130
	3	30	85	218	130		0,985	130
	4	33	75	218	130	110	0,985	130
	5	33	75	218	130	114	0,985	130
2271800_0	1	32	76	218	130	106	0,985	130
	2	32	85	218	130		0,985	130
	3	35	75	218	130	112	0,985	130
	4	35	75	218	130	115	0,985	130
2271900_0	1	32	80	215	130	109	0,985	130
	2	32	80	215	130	105	0,985	130
	3	32	80	215	130			
	4	46	72	215	130	121	0,985	130
	5	46	75	215	130	11	0,985	130
	6	57	75	215	130	113	0,985	130
	7	57	75	215	130	115	0,985	130
	8	57	75	215	130	113	0,985	130
2272000_0	1	34	79	216	130	105	0,985	130
	2	34	79	216	130	115	0,985	130
	3	34	79	216	130	120	0,985	130
	4	34	73	216	130			
	5	42	73	216	130	120	0,985	130
	6	42	73	216	130	120	0,992	130
	7	52	73	216	130	120	0,992	130
	8	46	73	216	130	120	0,985	130
								130
2272100_0	1	37	76	216	130	105	0,985	130
	2	35	80	216	130			130
	3	41	73	216	130	117	0,985	130
	4	41	73	216	130	119	0,985	130
	5	41	73	216	130	120	0,985	130
	6	41	73	216	130	120	0,99	130
2280100_0	1	34	81	214	130	114	0,985	130
	2	34	81	214	130	120	0,985	130
	3	34	81	214	130	118	0,985	130
	4	34	81	214	130	115	0,985	130
	5	34	81	214	130	122	0,985	130
	6	34	81	214	130	117	0,985	130

7	34	79	217	130	118	0,985	130
8	34	81	217	130			
9	41	78	217	130	122	0,985	130
10	32	85	214	130			
11	41	65	214	130	120	0,985	130
12	41	65	214	130	117	0,985	130
13	45	75	214	130	117	0,985	130
14	50	80	214	130	117	0,98	130
15	50	80	214	130	117	0,992	130

VII. Appendix

```
;*****************************************************************************
; PV WAVE Header
;-----------------------------------------------------------------------------
; File name        :   start
; Residency        :
; Programe name    :   After_DiSC_Processing
; Module name      :            Bathymetry
; Version nr                    :         1.0
; Date             :      05.11.2005
; Place            :      GKSS / Geesthacht
; Author           :      Stelios F.
; Email                                                                  :
            stylianos.flampouris@gkss.de
;-----------------------------------------------------------------------------
; Description              :   Initializing the compiling of all the routines
;-----------------------------------------------------------------------------
;
;*****************************************************************************

RETALL
.LOCALS
DELVAR, /ALL
CLOSE, /ALL
DEVICE, /CLOSE

set_plot,'win32'
@stat_startup
@math_startup
;@sigpro_startup
;@ip_startup

.run coordinates
.run datarr_creation
.run filenamed
.run comparison
.run output
surfer_main
```

```
;*******************************************************************************
;
;-------------------------------------------------------------------------------
; Description               :   The main of the After_DiSC_Processing
;-------------------------------------------------------------------------------
;
;*******************************************************************************

PRO surfer_main

Print, '--------------------------------------
Print, 'The surfer_main is running'
Print, 'By stelios f.
Print, 'GKSS Research Center
Print, '--------------------------------------

WAIT,1

;The subroutine 'coordinates' reads the coordinates of the result
;from DiSC. The coordinates are in meters
            coordinates, linenr
;The subroutine 'datarr_creation' reads the data and creates an array
            datarr_creation, data_arr, linenr
; The subroutine 'filenamed' checks for the existence of the input
; data file and calls two more subroutines the 'comparison' and the
; 'output'
            filenamed, lookfor, data_arr
END
```

```
;*****************************************************************************
;-----------------------------------------------------------------------------
; Description           :   The subroutine 'coordinates' is reading the coordinates
;
        of the result from DiSC. The coordinates are in meters
;-----------------------------------------------------------------------------
;*****************************************************************************

PRO coordinates, linenr

        Print, '-------------------------------------
        Print, 'The coordinates is running'
        Print, '-------------------------------------


        OPENW,1, 'coordinates.txt'
                FOR xcoordinate = DOUBLE(3459944.47920), DOUBLE(3461867.21160),
DOUBLE(40.9092) DO BEGIN
                        FOR ycoordinate = DOUBLE(6102538.97920), DOUBLE(6104462.71160),
DOUBLE(40.9092) DO BEGIN
                                xcoordinate1 = STRING(xcoordinate - 0.0208,format="(D12.2)")
                                ycoordinate1 = STRING(ycoordinate - 0.0208,format="(D12.2)")
                                        coordinates = xcoordinate1+' '+ ycoordinate1
                                        PRINTF,1, coordinates
                        ENDFOR ;ycoordinate
                ENDFOR ;xcoordinate
        CLOSE,1
;Counting the lines
        linenr = LONG(0)
        OPENR,1, 'coordinates.txt'
                WHILE (NOT EOF(1)) DO BEGIN
                        READF,1,line
                                linenr = linenr+1
                ENDWHILE
        CLOSE,1
END
```

```
;*****************************************************************************
;
;-----------------------------------------------------------------------------
; Description           :   The datarr_creation reads the data and creates an array
;-----------------------------------------------------------------------------
;*****************************************************************************

PRO datarr_creation, data_arr, linenr

        Print, '--------------------------------------
        Print, 'The datarr_creation is running'
        Print, '--------------------------------------

;Creation of data array
        data_arr=DBLARR(120,linenr)
        lincnt = 0l
        line = STRARR(1)
        OPENU, 1, 'C:\surfer\coordinates.txt'
                WHILE (NOT EOF(1)) DO BEGIN
                        READF,1,line
                ; To define the x_coordinate, have to find the position of the
                ;first point ".", so search for it
                        pos_firstpoint = STRPOS(line,'.')
                        x_coordinate = DOUBLE(STRMID(line,pos_firstpoint(0)-7,10))
                data_arr(0,lincnt) = x_coordinate
                ;print,'x = ',x_coordinate
                ; To define the x_coordinate, have to find the position of the
                ;second point ".", so search for it
                        pos_secondpoint =STRPOS(line,'.',pos_firstpoint(0)+1)
                        ;print,'pos_secondpoint=',pos_secondpoint
                y_coordinate = DOUBLE(STRMID(line,pos_secondpoint(0)-7,pos_secondpoint(0)-
pos_firstpoint(0)-1))
                data_arr(1,lincnt) = y_coordinate
                ;print,'y_coordinate=',data_arr(1,lincnt)
                lincnt = lincnt+1
                ENDWHILE
        CLOSE,1
END
```

```
;*****************************************************************************
;-----------------------------------------------------------------------------
; Description          :  The subroutine 'filenamed' checks for the existence of
;
        the input data file and calls two more subroutines the
;
        'comparison' and the 'output'
;-----------------------------------------------------------------------------
;*****************************************************************************

PRO filenamed, lookfor, data_arr
        Print, '-------------------------------------
        Print, 'The filenamed is running'
        Print, '-------------------------------------
        fn=LONG(2)
existfiles_strvec = STRARR(1)
;definition of the variables
        FOR day = 28, 28, 1 DO BEGIN
                FOR hour = 0, 23, 1 DO BEGIN
                        FOR shoot = 0, 20, 1 DO BEGIN
                                day1 = STRCOMPRESS(STRING(day),/Remove_all)
                                daylen = STRLEN(day1)
                                IF daylen LT 2 THEN BEGIN
                                        day1 = '0'+ day1
                                ENDIF ELSE BEGIN
                                        day1 = day1
                                        ENDELSE
                        hour1 = STRCOMPRESS(STRING(hour),/Remove_all)
                                hourlen = STRLEN(hour1)
                                IF hourlen LT 2 THEN BEGIN
                                        hour1 = '0'+hour1
                                ENDIF ELSE BEGIN
                                        hour1 = hour1
                                        ENDELSE
                        shoot1 = STRCOMPRESS(STRING(shoot),/Remove_all)
                                shootlen = STRLEN(shoot1)
                                IF shootlen LT 2 THEN BEGIN
                                shoot1 = '0'+shoot1
                                        ENDIF ELSE BEGIN
                                shoot1 = shoot1
                                        ENDELSE
                        fname = '02'+day1+hour1+'00_'+shoot1+'_result_6x6.txt'

;Existence of file
                f_path = 'C:/project_b_results_fin/'
                        lookfor = f_path+fname
                        file_exist=FINDFILE(lookfor, count = fe_counter)
                        IF fe_counter EQ 1 THEN BEGIN
                                existfiles_strvec = [existfiles_strvec,file_exist]
                        PRINT, lookfor
                        ;PRINT,existfiles_strvec
                                comparison, lookfor, data_arr, fn
        fn=fn+1
                        ENDIF
                                ENDFOR ;shoot
                        ENDFOR ;hour
                ENDFOR ;day
output, data_arr

END
```

```
;*****************************************************************************
;
;-----------------------------------------------------------------------------
; Description          :  The subroutine 'comparison' creates an index which matches the 'coordinates' with the
                          coordinates of the result from DiSC and simultunuously the results are filtered but the number
                          of regression points (GT 40)
;-----------------------------------------------------------------------------
;*****************************************************************************

PRO comparison, lookfor, data_arr, fn

        Print, '--------------------------------------
        Print, 'The comparison number
        Print, fn
        Print, '--------------------------------------

;Creation of the full data array with the correct coordinates..!
        lincnt = 0l
        line = STRARR(1)
        OPENR, 1, lookfor
         WHILE (NOT EOF(1)) DO BEGIN
                        READF,1,line
                                ;print,     line
                ; To define the x_coordinate of the data, have to find the position of the
                ;first point ".", so search for it
                        pos_firstpoint = STRPOS(line,'.')
                                ;print,'pos_firstpoint = ',pos_firstpoint
                        x_coordinate = DOUBLE(STRMID(line,pos_firstpoint(0)-7,9))
                                ;print, x_coordinate
                ; To define the y_coordinate of the data, have to find the position of the
                ;second point ".", so search for it
                        pos_secondpoint = STRPOS(line,'.',pos_firstpoint(0)+1)
                                ;print,'pos_secondpoint = ',pos_secondpoint
                y_coordinate = STRMID(line,pos_secondpoint(0)-7,9)
                        ;print, y_coordinate
        ;For qualifying reasons the regression points of each "depth" must be more than 40
        ;So first read the regression points anf if greater than 40,we accept the calculated depth

                pos_secondtab = STRPOS(line,' ',pos_secondpoint(0)+1)
                        ;print,'pos_secondtab = ',pos_secondtab

                pos_thirdtab = STRPOS(line,' ',pos_secondtab(0)+1)
                        ;print,'pos_thirdtab = ',pos_thirdtab

                nr_reg_point = DOUBLE(STRMID(line,pos_secondtab(0),pos_thirdtab(0)-
pos_secondtab(0)))
                        ;print, 'nr_reg_point', nr_reg_point

                IF nr_reg_point(0) GT 40 THEN BEGIN

                                ;To define the depth, have to find the position of the third point "."

                                pos_thirdpoint = STRPOS(line,'.',pos_secondpoint(0)+1)
                                        ;print,'pos_thirdpoint = ',pos_thirdpoint

                        ;pos_fourthpoint = STRPOS(line,'.',pos_thirdpoint(0)+1)
  ;print,'pos_fourthpoint = ',pos_fourthpoint
                        ;pos_fifthpoint = STRPOS(line,'.',pos_fourthpoint(0)+1)
  ;print,'pos_fifthpoint = ',pos_fifthpoint

                        depth = DOUBLE(STRMID(line,pos_thirdpoint(0)-2,5))

                                        print, 'depth', depth

                ENDIF ELSE BEGIN
```

```
                depth = 0

        ;print, 'depth', depth

        ENDELSE

        ;Index

            a=LONG(data_arr(0,*))
            b=LONG(x_coordinate)
                x_index = WHERE(a EQ b(0))
                        ;PRINT,'x_index', x_index

                y_index = WHERE(LONG(data_arr(1,x_index)) EQ LONG (y_coordinate(0)))
                        ;PRINT, y_index

                right_line = x_index(y_index)
                        ;PRINT, right_line

                data_arr(fn,right_line) = depth(0)
                        ;PRINT,'Z=', data_arr(fn,right_line)

        lincnt = lincnt+1

        ENDWHILE

    CLOSE,1

END
```

```
;*****************************************************************************
;
;-----------------------------------------------------------------------------
; Description        :   The subroutine 'comparison' creates an index which matches the 'coordinates' with the
coordinates of the result from DiSC and simultunuously the results are filtered but the number of regression
points (GT 40)
;-----------------------------------------------------------------------------
;
;*****************************************************************************

PRO comparison, lookfor, data_arr, fn

        Print, '--------------------------------------
        Print, 'The comparison number
        Print, fn
        Print, '--------------------------------------


;Creation of the full data array with the correct coordinates..!
        lincnt = 0l
        line = STRARR(1)
        OPENR, 1, lookfor
         WHILE (NOT EOF(1)) DO BEGIN

                        READF,1,line
                                ;print,     line
                ; To define the x_coordinate of the data, have to find the position of the
                ;first point ".", so search for it
                                pos_firstpoint = STRPOS(line,'.')
                                ;print,'pos_firstpoint = ',pos_firstpoint
                                        x_coordinate = DOUBLE(STRMID(line,pos_firstpoint(0)-7,9))
                                ;print, x_coordinate
                ; To define the y_coordinate of the data, have to find the position of the
                ;second point ".", so search for it
                        pos_secondpoint = STRPOS(line,'.',pos_firstpoint(0)+1)
                                ;print,'pos_secondpoint = ',pos_secondpoint
                y_coordinate = STRMID(line,pos_secondpoint(0)-7,9)
                        ;print, y_coordinate
        ;For qualifying reasons the regression points of each "depth" must be more than 40
        ;So first read the regression points anf if greater than 40,we accept the calculated depth
                                pos_secondtab = STRPOS(line,' ',pos_secondpoint(0)+1)
                        ;print,'pos_secondtab = ',pos_secondtab
                                pos_thirdtab = STRPOS(line,' ',pos_secondtab(0)+1)
                        ;print,'pos_thirdtab = ',pos_thirdtab
                        nr_reg_point = DOUBLE(STRMID(line,pos_secondtab(0),pos_thirdtab(0)-
pos_secondtab(0)))
                        ;print, 'nr_reg_point', nr_reg_point
                                IF nr_reg_point(0) GT 40 THEN BEGIN
                                ;To define the depth, have to find the position of the third point "."
                                        pos_thirdpoint = STRPOS(line,'.',pos_secondpoint(0)+1)
                                        ;print,'pos_thirdpoint = ',pos_thirdpoint

                        ;pos_fourthpoint = STRPOS(line,'.',pos_thirdpoint(0)+1)
  ;print,'pos_fourthpoint = ',pos_fourthpoint
                        ;pos_fifthpoint = STRPOS(line,'.',pos_fourthpoint(0)+1)
  ;print,'pos_fifthpoint = ',pos_fifthpoint
                                                depth = DOUBLE(STRMID(line,pos_thirdpoint(0)-2,5))
                                                        print, 'depth', depth
                                ENDIF ELSE BEGIN
                                        depth = 0
                                ;print, 'depth', depth
                        ENDELSE
                                ;Index
                    a=LONG(data_arr(0,*))
                    b=LONG(x_coordinate)
```

```
                        x_index = WHERE(a EQ b(0))
                                ;PRINT,'x_index', x_index
                        y_index = WHERE(LONG(data_arr(1,x_index)) EQ LONG (y_coordinate(0)))
                                ;PRINT, y_index
                                right_line = x_index(y_index)
                                ;PRINT, right_line
                                data_arr(fn,right_line) = depth(0)
                                ;PRINT,'Z=', data_arr(fn,right_line)
                        lincnt = lincnt+1
                        ENDWHILE
        CLOSE,1
END

;*****************************************************************************
; Description           :   The subroutine 'output' extracts the data into two different files. The coordinates:
coor_result.txt                 The data: data_result.txt
;*****************************************************************************

PRO output, data_arr
        Print, '--------------------------------------
        Print, 'The output is running'
        Print, '--------------------------------------

;Output subroutine
;Coordinates Output
        OPENW,1, 'C:/surfer/coor_result.txt'
                for j=0l,2302 do begin
                str_dum1='  '
                        for i=0l,1 do begin
                                str_line1 = STRING(data_arr(i,j), format="(D12.2)")
                                str_dum1=str_dum1 + str_line1
                        endfor ;column
                                        PRINTF,1,str_dum1
                endfor ; lines
CLOSE,1
;Data Output
        OPENW,1, 'C:\surfer/data_result.txt'
                for j=0l,2302 do begin
                                        str_dum='  '
                                        for i=2,55 do begin
                                str_line = STRING(data_arr(i,j), format="(D6.2)")
                                                        str_dum=str_dum + str_line
                                        endfor ;column
                        PRINTF,1,str_dum
                endfor ; lines
CLOSE,1
END
```

VIII. Appendix

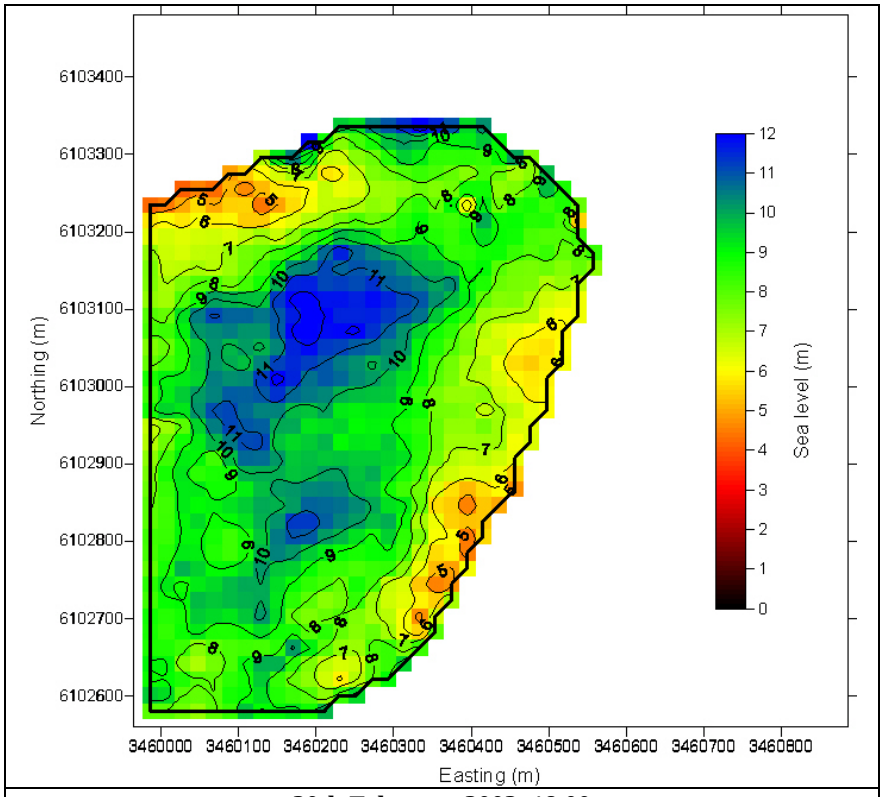

20th February 2002, 18.00

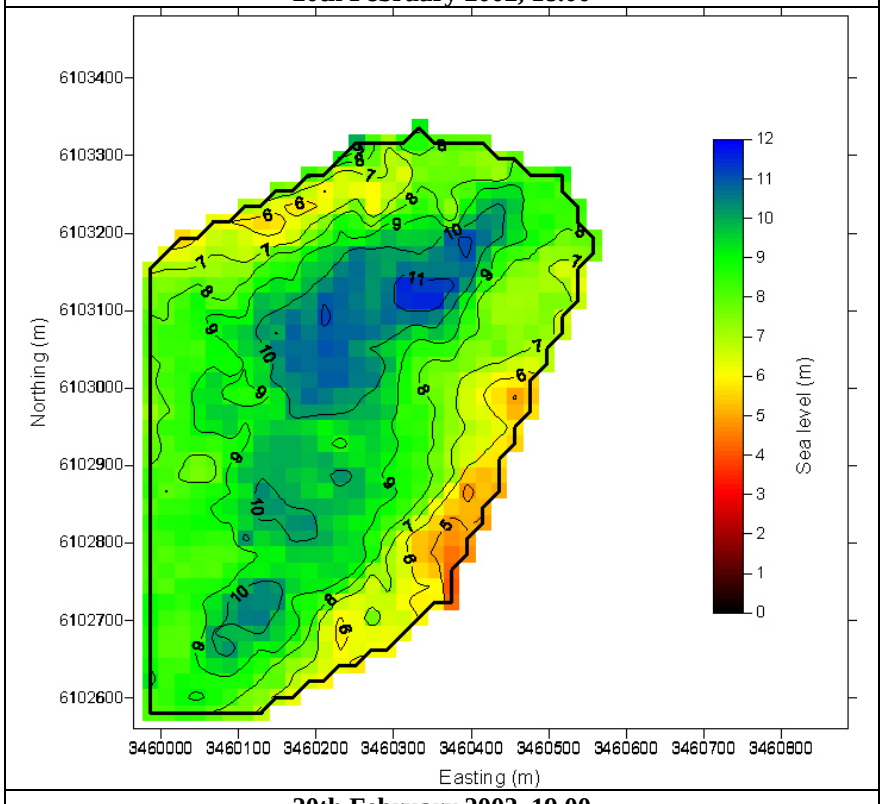

20th February 2002, 19.00

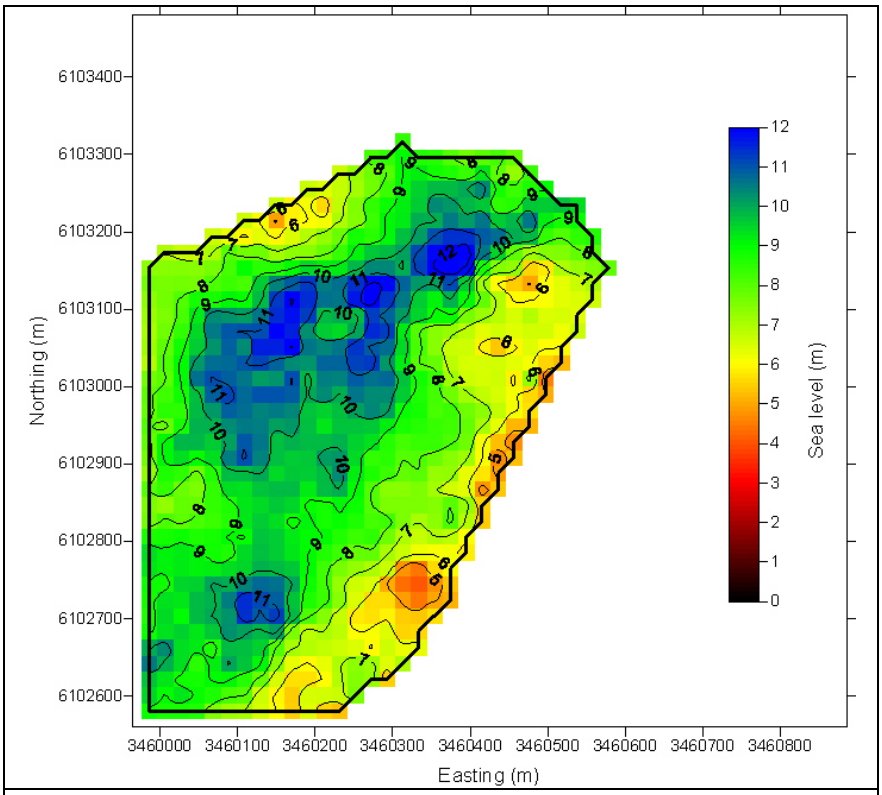

20th February 2002, 20.00

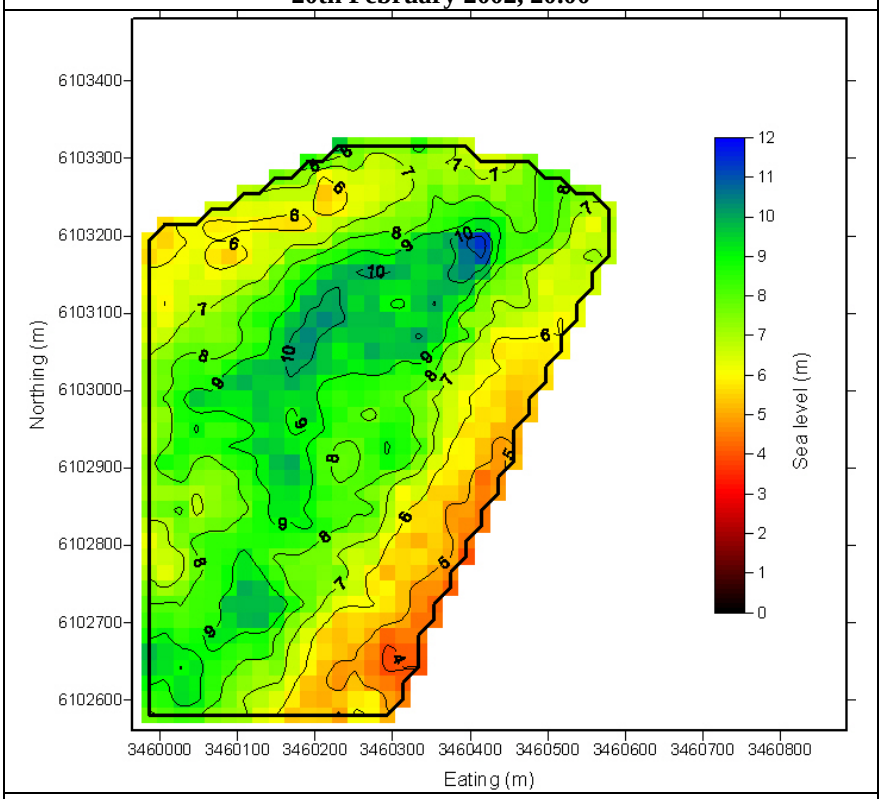

20th February 2002, 21.00

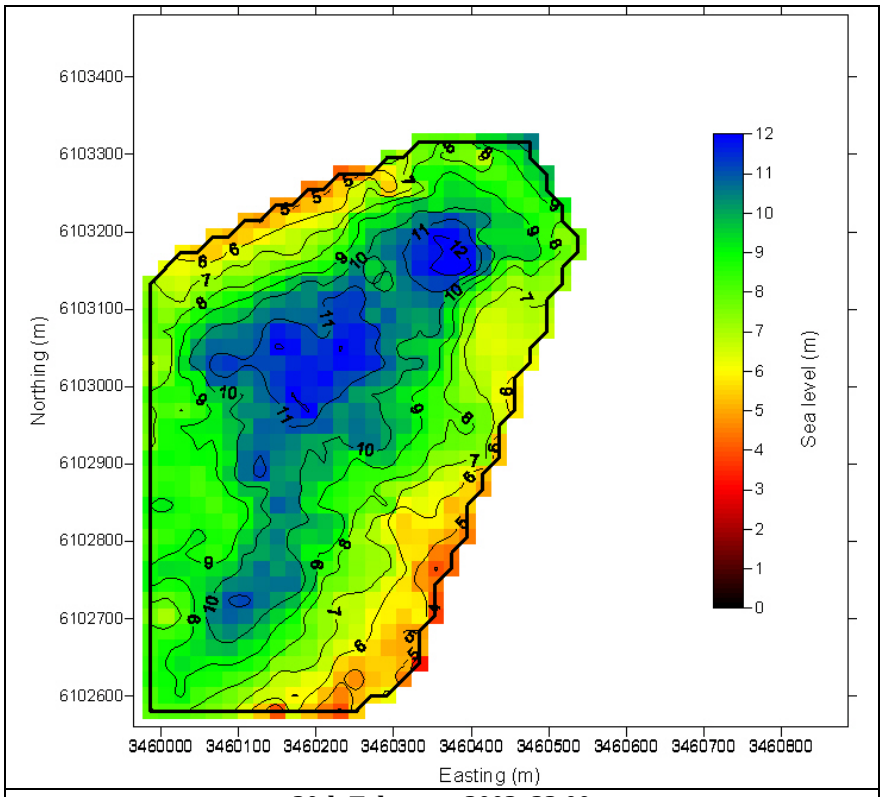

20th February 2002, 22.00

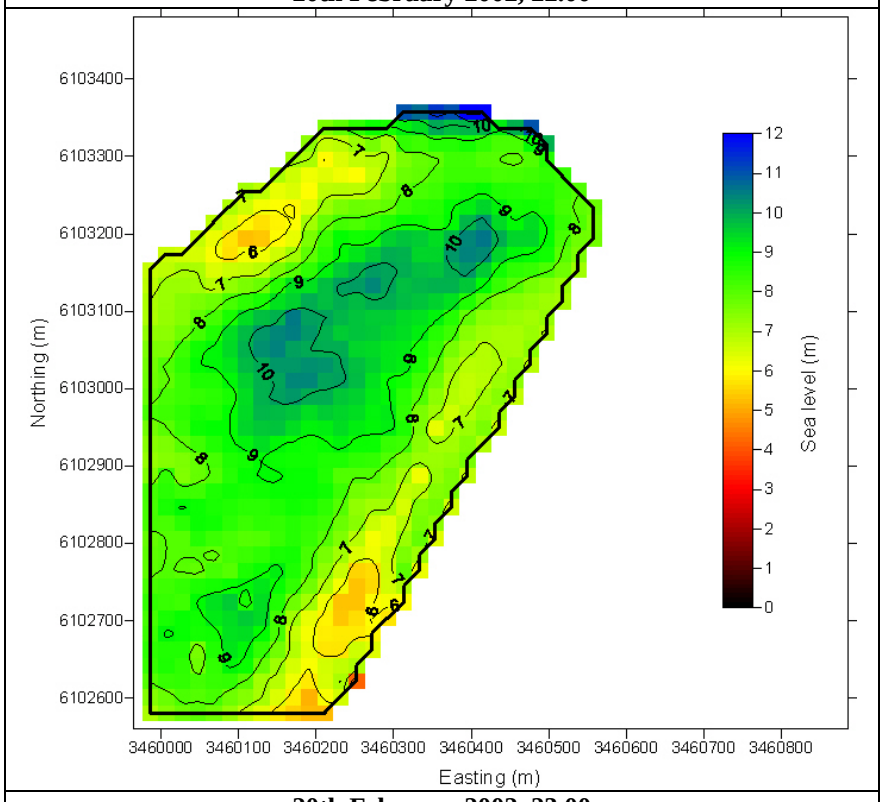

20th February 2002, 23.00

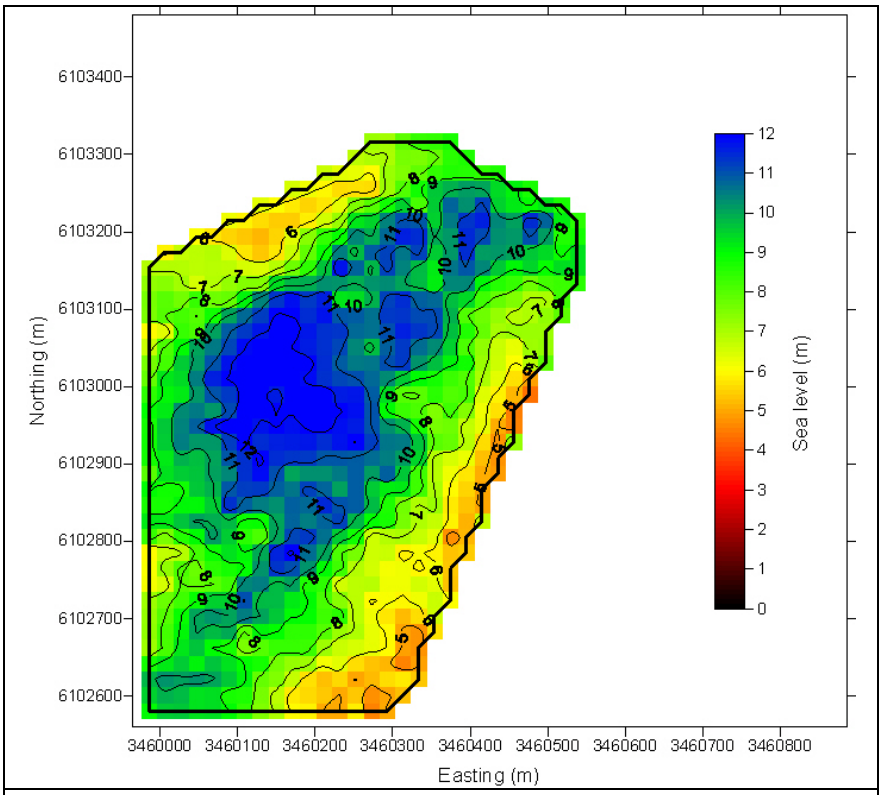

21th February 2002, 00.00

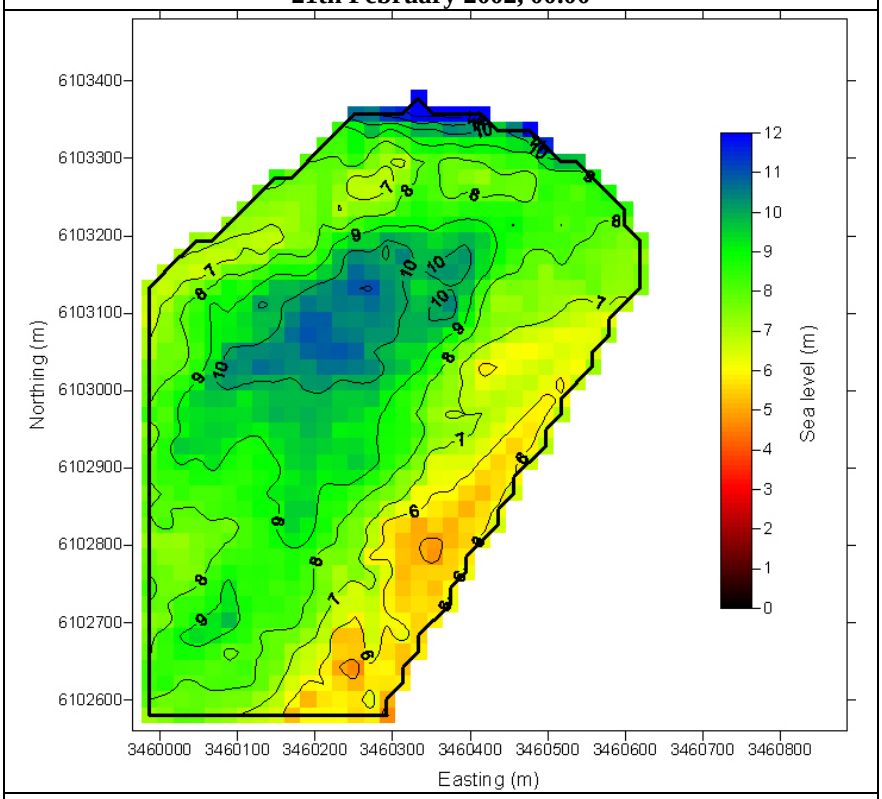

21th February 2002, 01.00

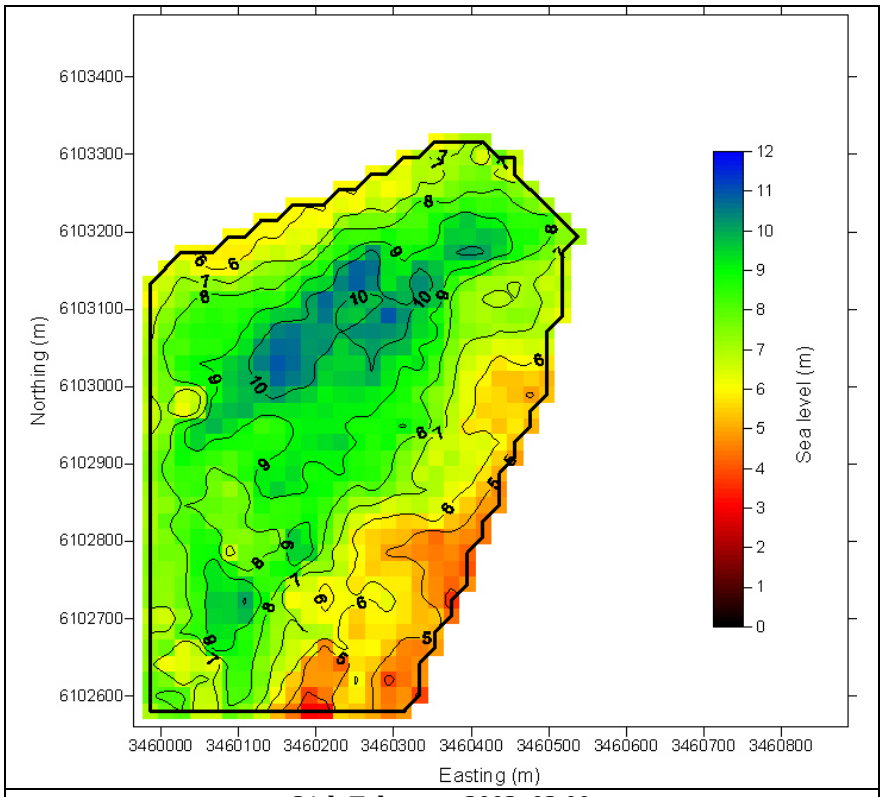

21th February 2002, 02.00

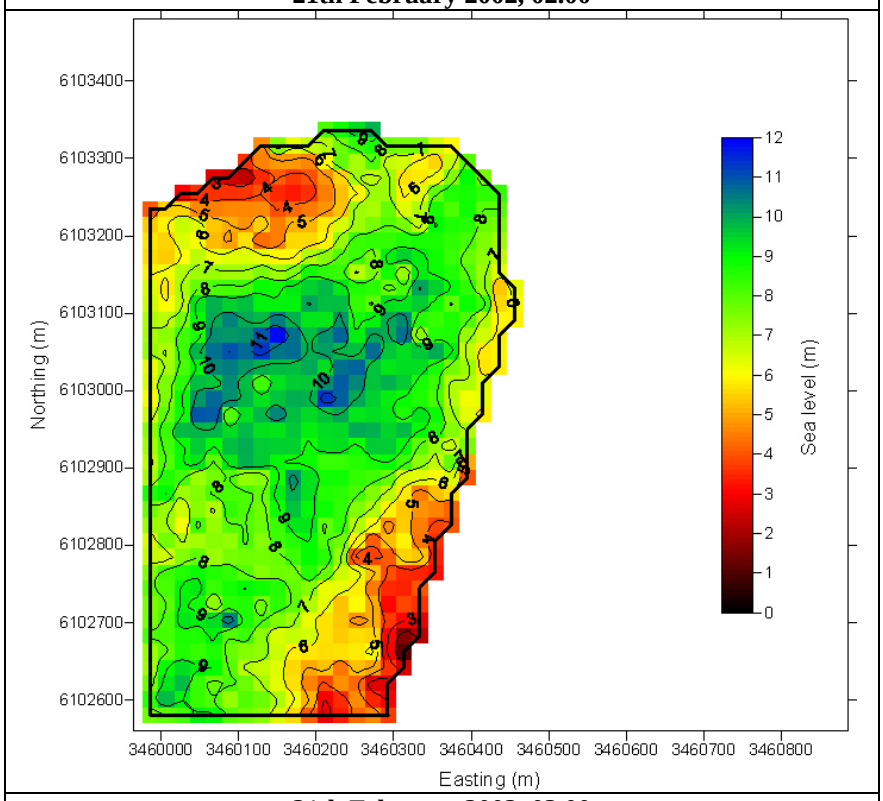

21th February 2002, 03.00

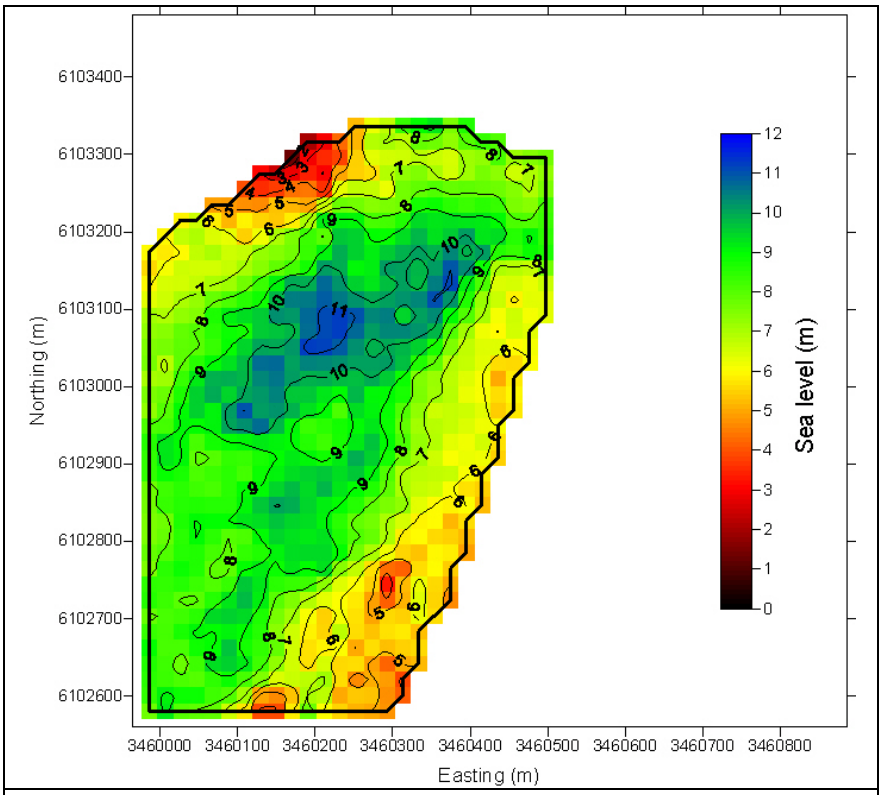

21th February 2002, 04.00

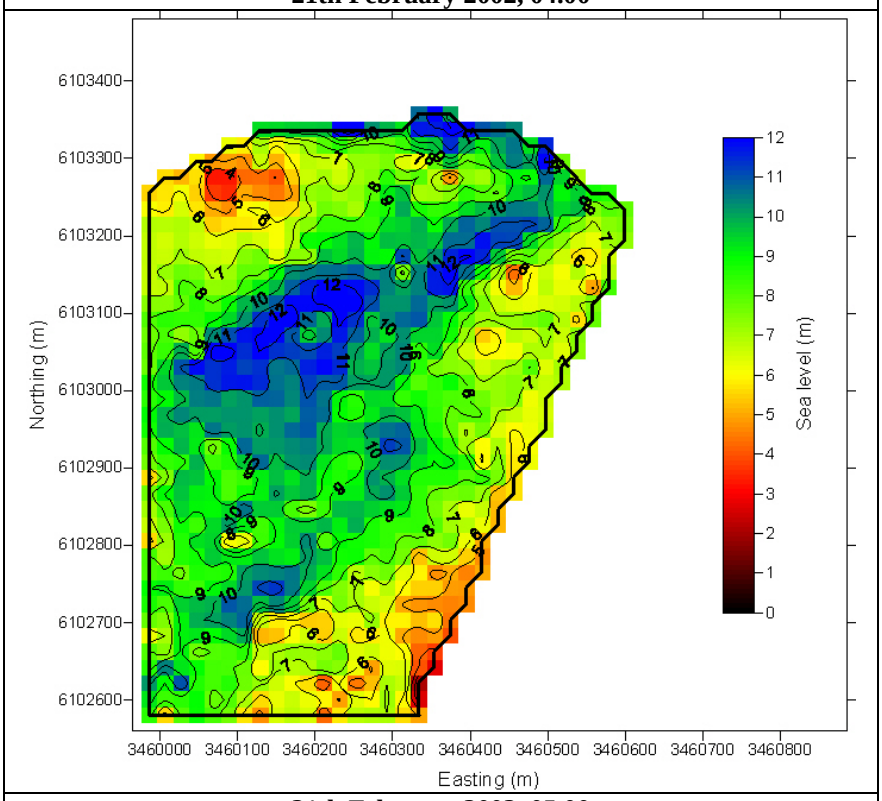

21th February 2002, 05.00

Figure VIII-1. The visualizations of the final results per hour for the beginning of the storm (20th February 2002, 18.00 - 21th February 2002, 05.00).

IX. Appendix

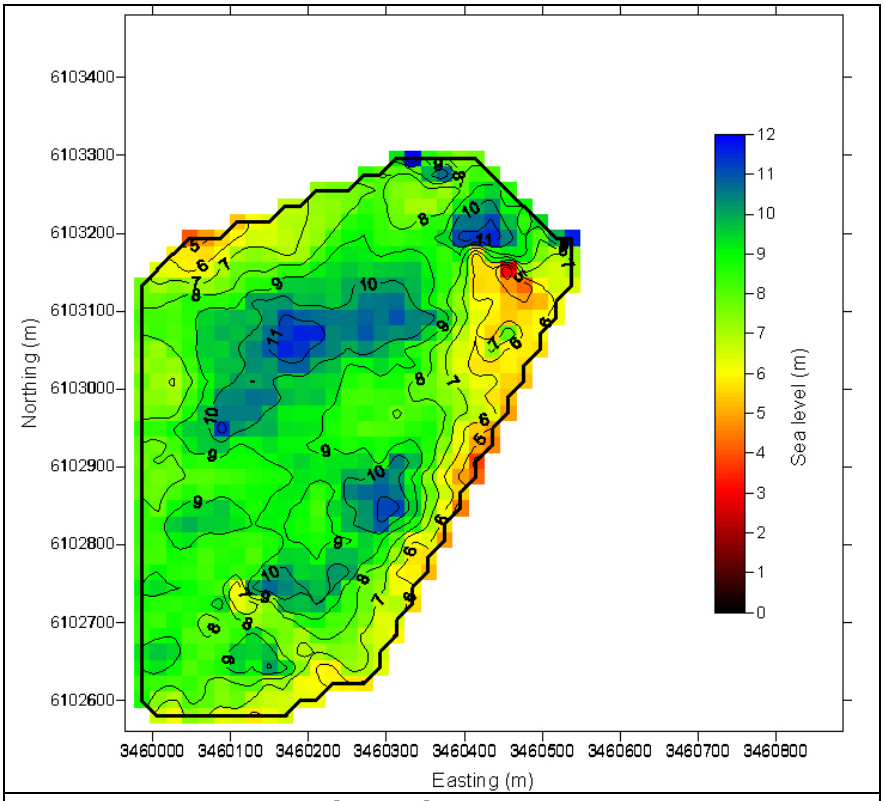

27th Feruaby 2002, 10.00

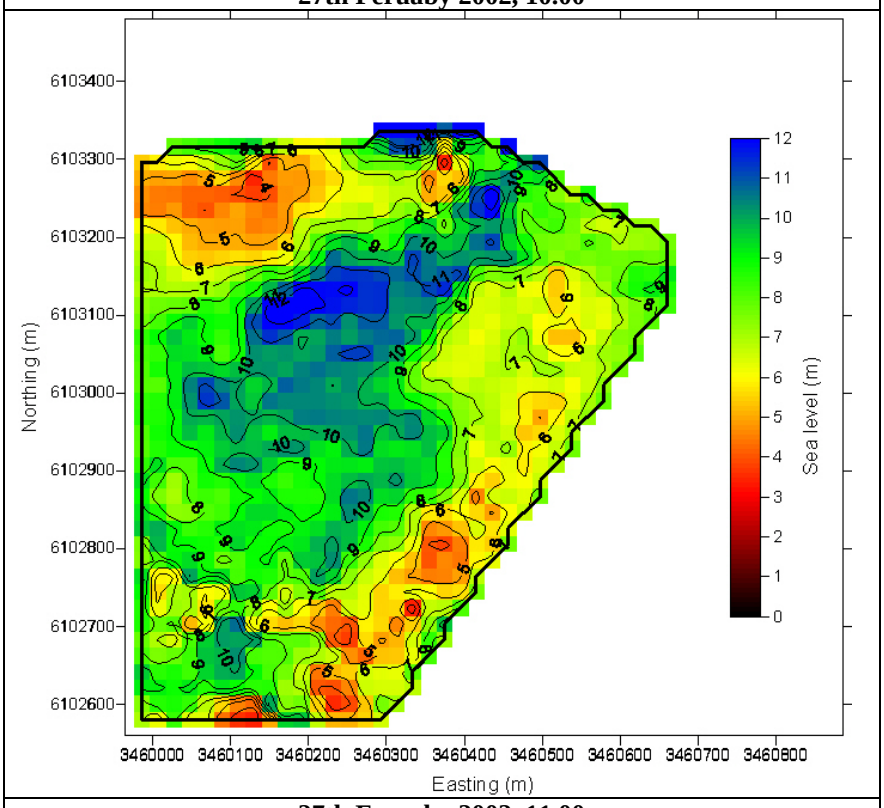

27th Feruaby 2002, 11.00

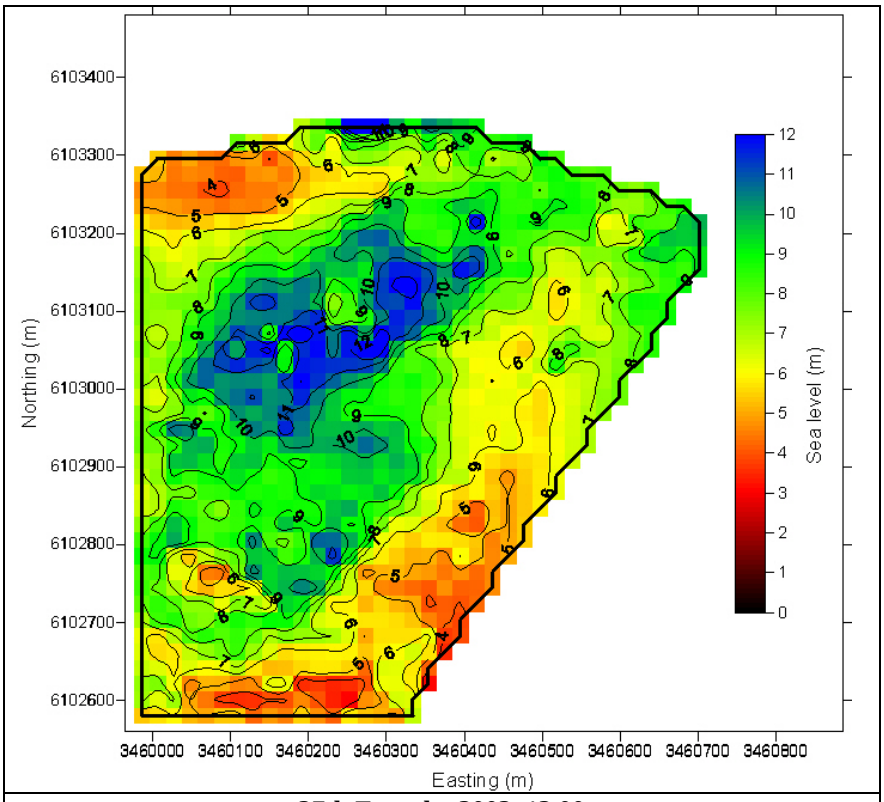

27th Feruaby 2002, 12.00

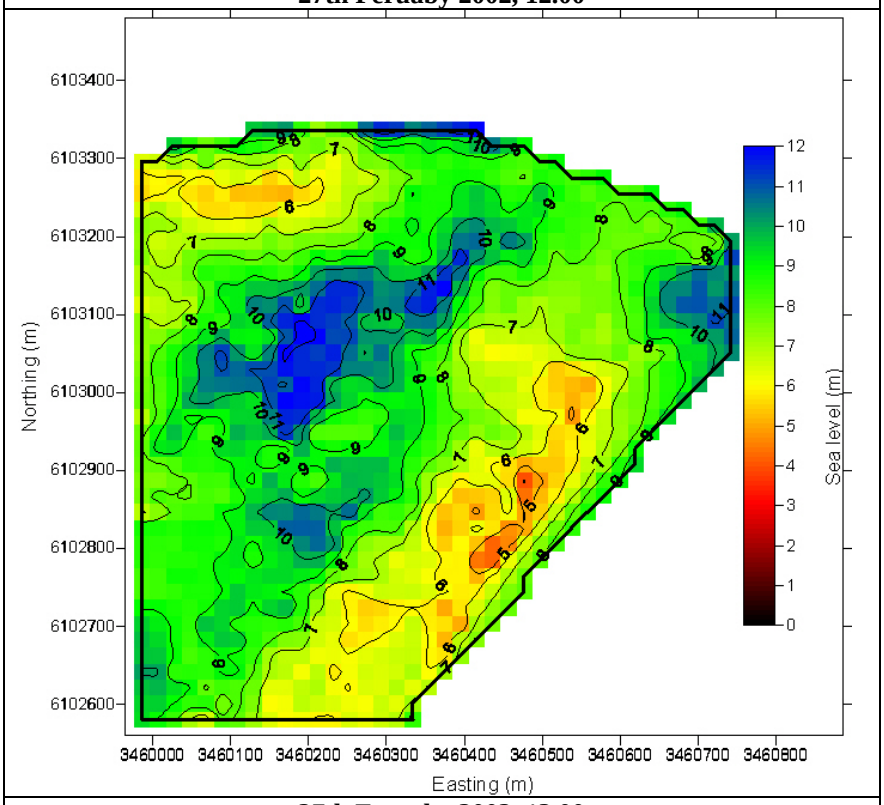

27th Feruaby 2002, 13.00

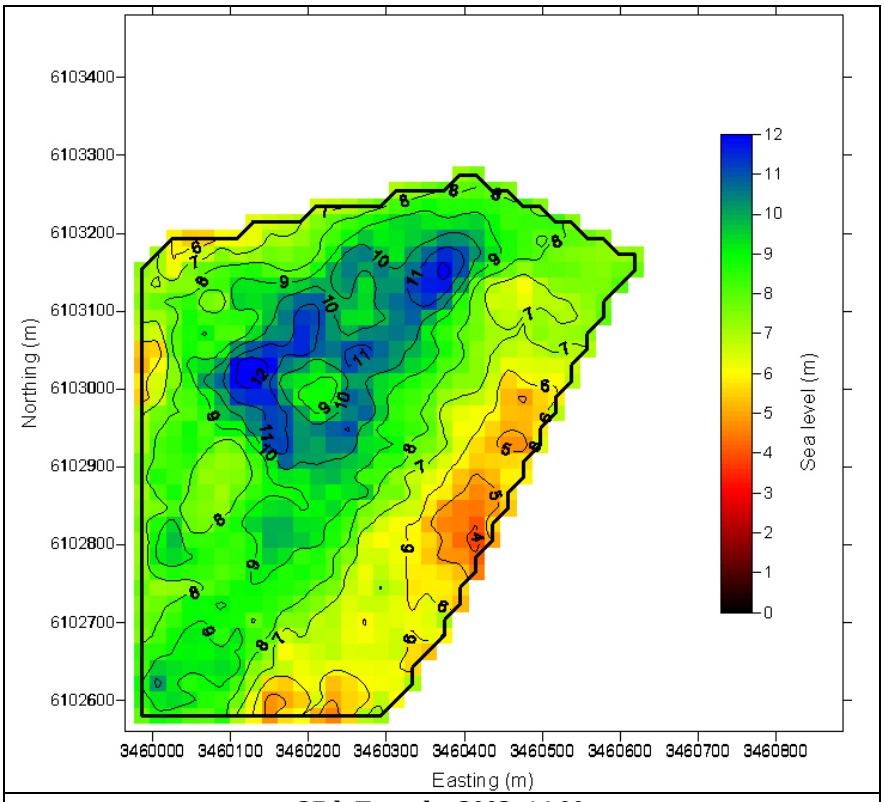

27th Ferуaby 2002, 14.00

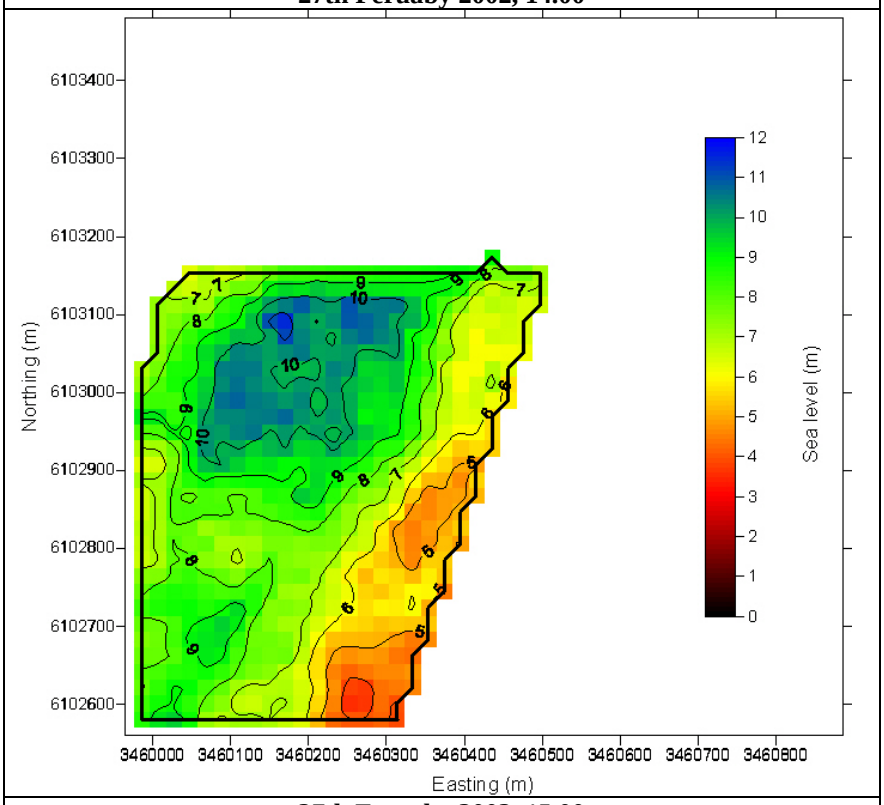

27th Ferуaby 2002, 15.00

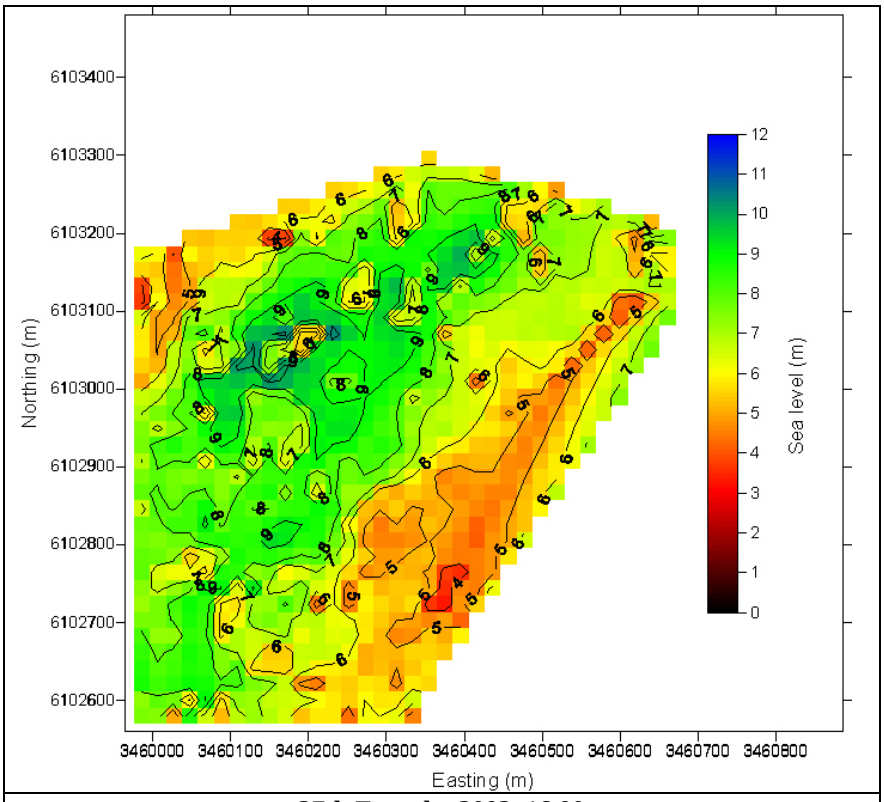

27th Feruaby 2002, 16.00

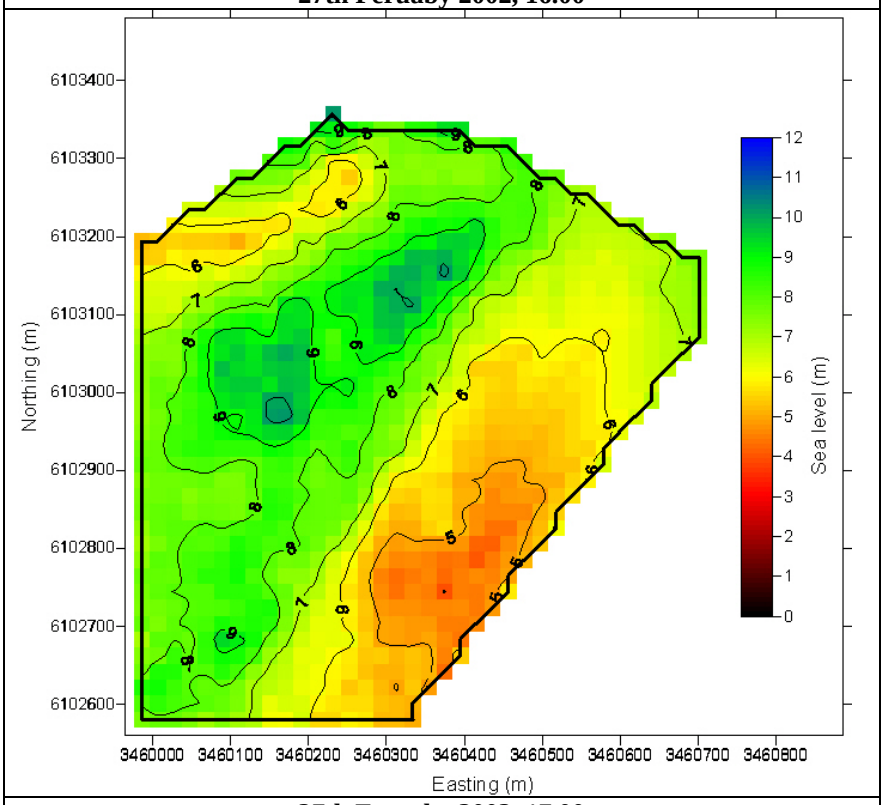

27th Feruaby 2002, 17.00

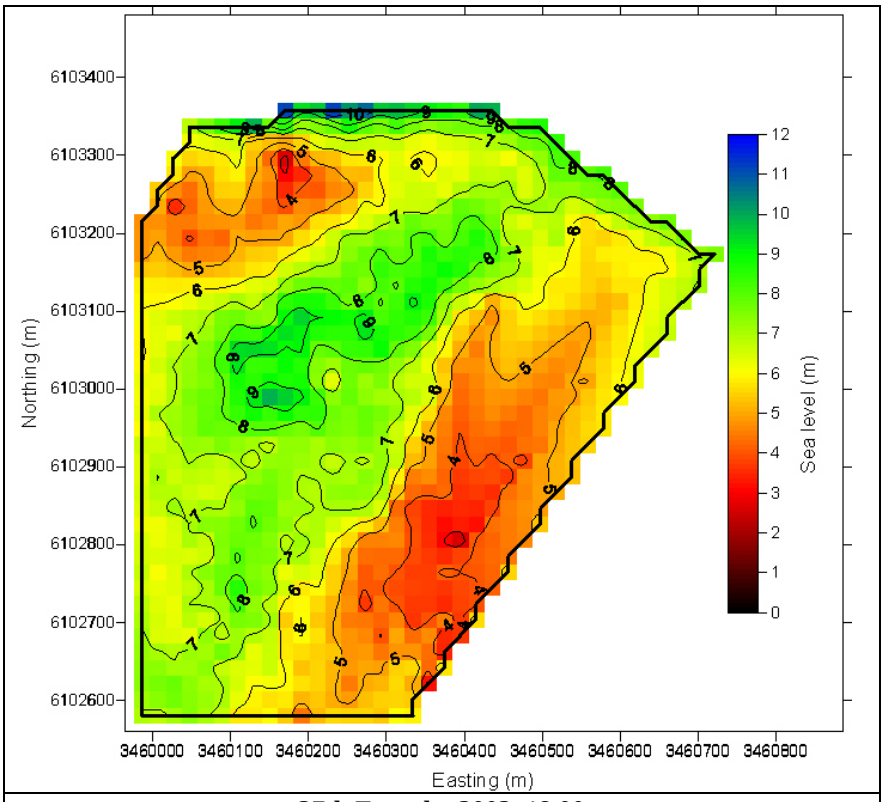

27th Feruaby 2002, 18.00

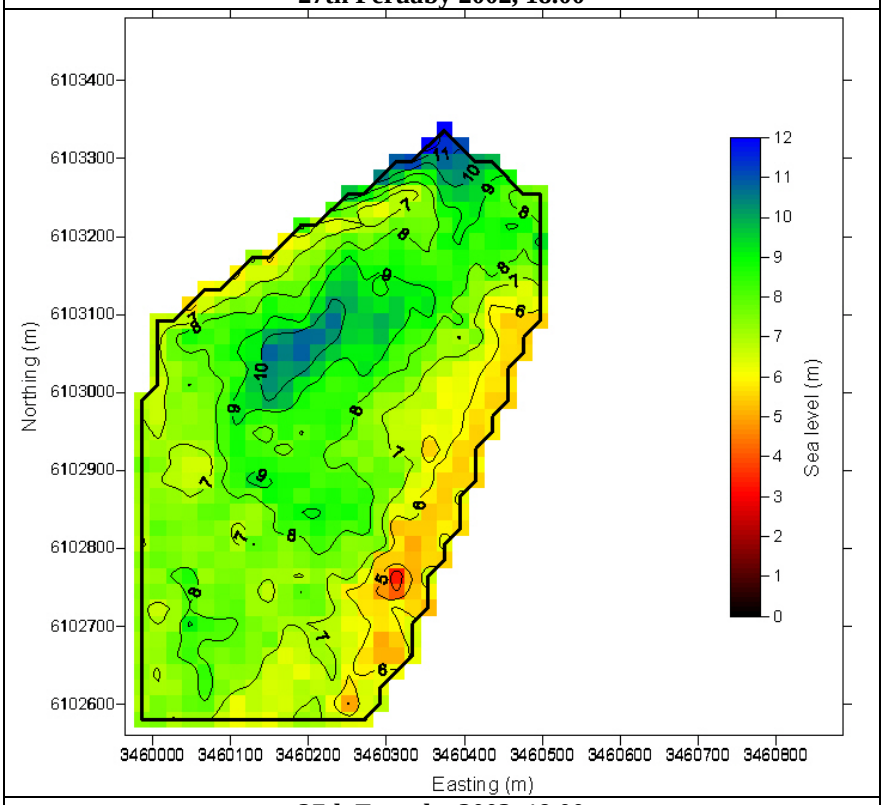

27th Feruaby 2002, 19.00

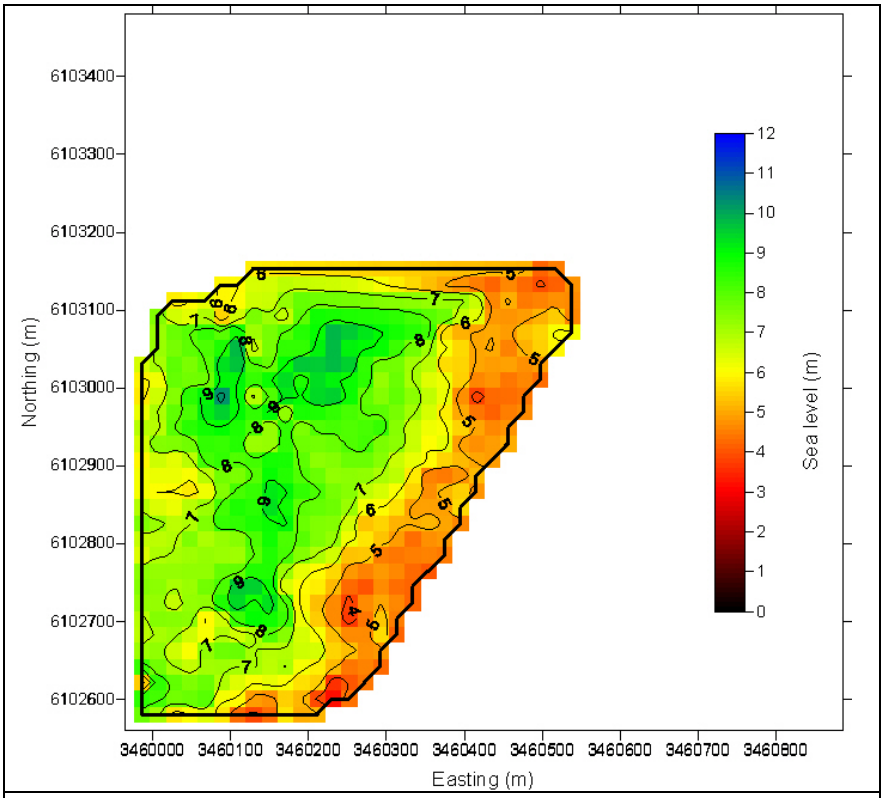

27th Feruaby 2002, 20.00

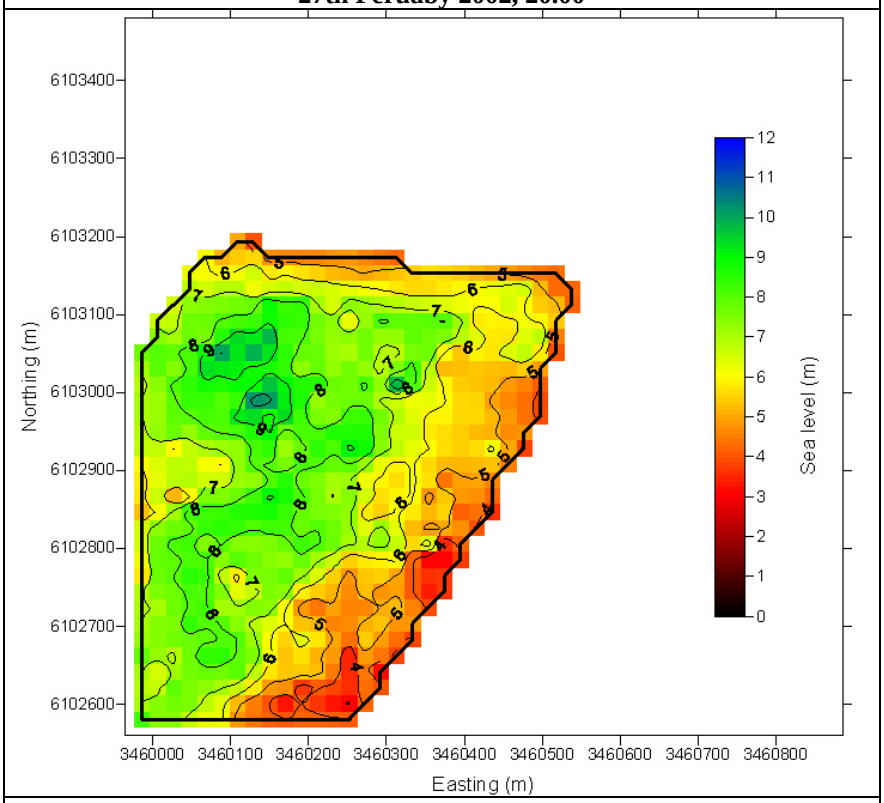

27th Feruaby 2002, 21.00

Figure IX-1. The visualizations of the final results per hour for the ending phase of the storm (27th February 2002, 10.00 - 27th February 2002, 21.00)

X. Appendix

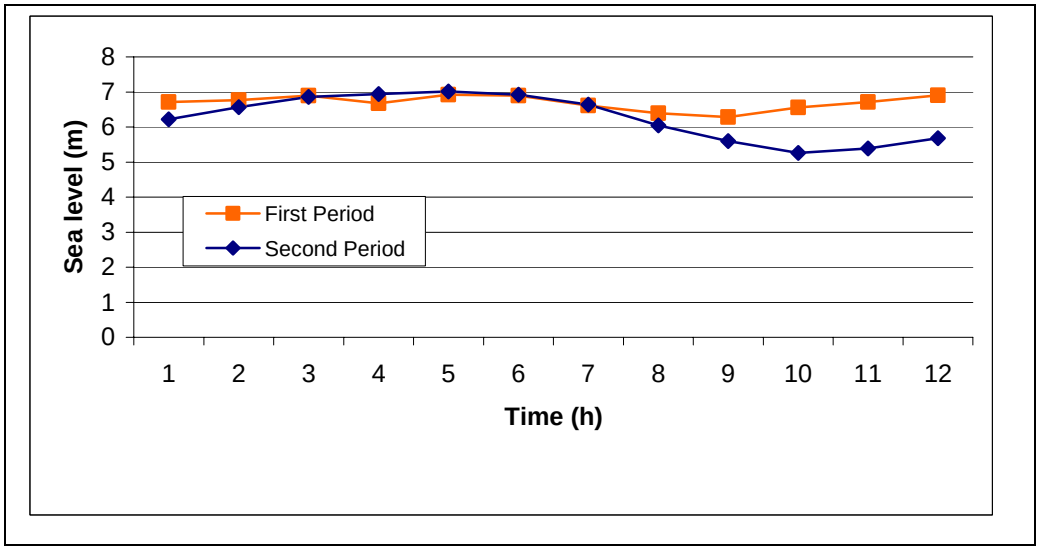

Figure X-1. The tidal measurements in Westerland for the beginning and the ending phase of the storm. The orange line is the measurement during the first period, and an exterior influence (probably from the wind) is obvious. The blue line is the wave measurement durinf the ending of the storm, and the shape tends to be sinusoidal.

XI. Appendix

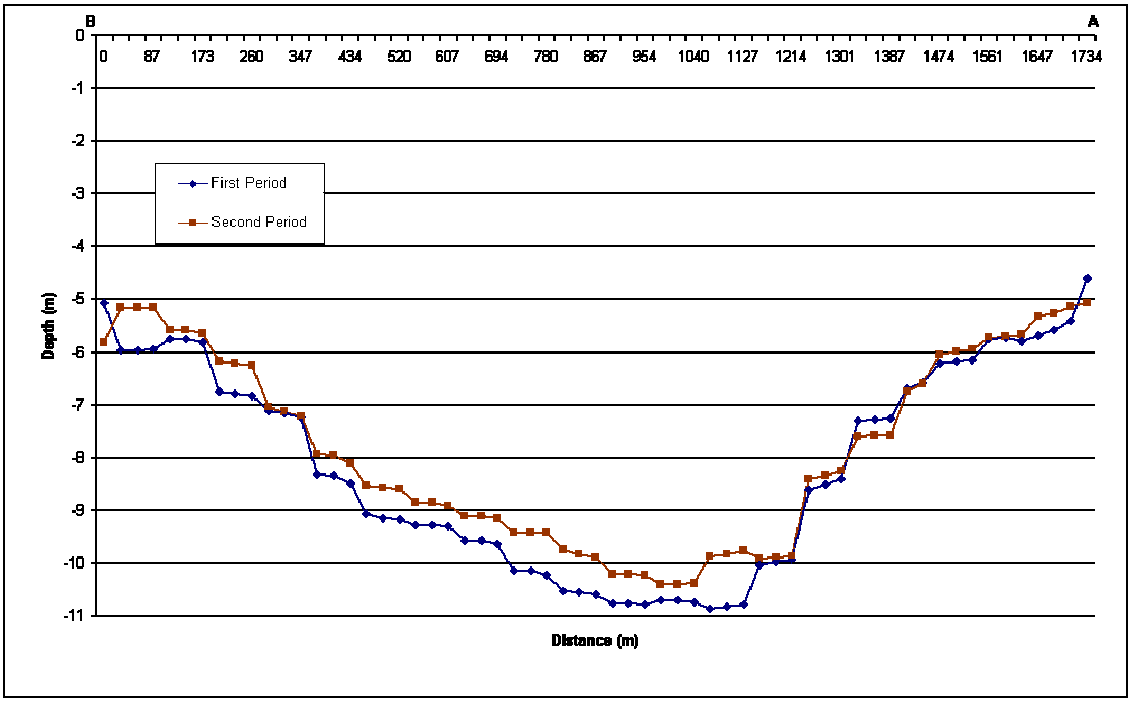

Figure XI-1. Cross section of the two estimated see depth, from B (3460432, 6102825) to A (3460027, 6103252) (see figure 6-2). There is deposition of sediment almost across all the cross section during the storm.

XII. Appendix

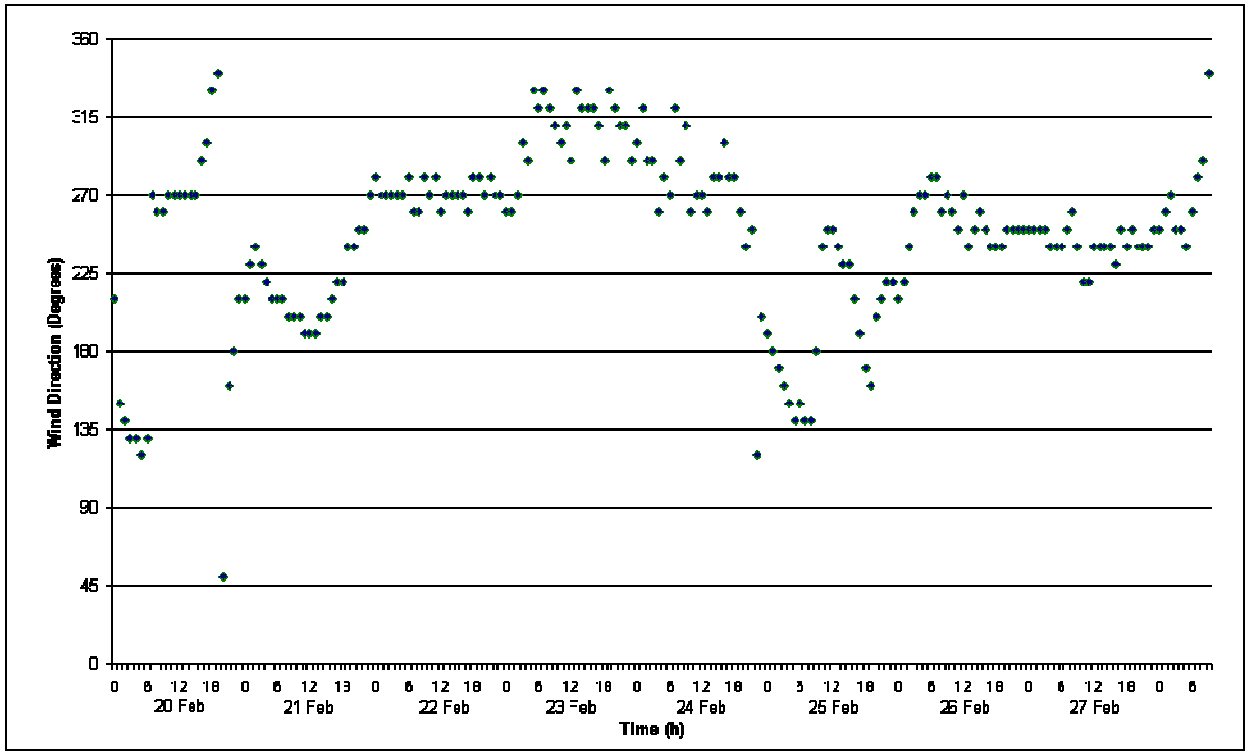

Figure XII-1. Plot of the wind direction from 20th to 28th of February 2002.